Molecular markers of myeloid-derived suppressor cells and their functional role for homing and in disease models in mice

Molekulare Marker von myeloiden Suppressorzellen und ihre funktionelle Rolle für deren zielgerichtete Migration und bei Krankheitsmodellen in Mäusen

Doctoral thesis for a doctoral degree
at the Graduate School of Life Sciences,
Julius-Maximilians-Universität Würzburg,
Section Infection and Immunity

submitted by

Ina-Nathalie Eckert

from

Kitzingen, Germany

Würzburg, 2022

Submitted on:

……..……..

Office stamp

Members of the *Promotionskomitee*:

Chairperson: Prof. Dr. Christian Janzen

Primary Supervisor: Prof. Dr. Manfred Lutz

Supervisor (Second): Prof. Dr. Dr. Andreas Beilhack

Supervisor (Third): Prof. Dr. Georg Gasteiger

Date of Public Defence: ……..

Date of Receipt of Certificates: …….

Inhalt

1 Introduction

1.1 Characteristics of MDSCs

MDSCs are a heterogeneous population of innate immune cells which accumulate during various pathological conditions and conduct immunosuppressive functions (Gabrilovich & Nagaraj 2009b). Particular cytokines, including GM-CSF, induce the expansion of myeloid progenitor cells, which under normal conditions differentiate into macrophages and neutrophils performing immune effector functions (Burgess & Metcalf 1980). During certain pathologies however, like cancer or chronic infections, monocytes and neutrophils can be by activated by inflammatory or microbial signals to become immunosuppressive MDSCs (Ribechini et al 2010, Ribechini et al 2017). MDSCs origin from the bone marrow and can be found in the spleen, tumors and immune-activated tissues, but not in lymph nodes (Gabrilovich & Nagaraj 2009b). MDSCs can be divided into two major subpopulations: the M-MDSCs, which exhibit morphological and phenotypic similarities to monocytes, and the G-MDSCs resembling neutrophils (Movahedi et al 2008a). While G-MDSCs and M-MDSCs exhibit lower phagocytic activities than macrophages and DCs, their production of ROS, NO, arginase as well as immunosuppressive cytokines is increased (Kumar et al 2016).

1.1.1 Development of MDSCs

MDSCs are absent in healthy individuals but are induced during chronic inflammatory conditions as a consequence of prolonged exposure to cytokines (Veglia et al 2021b). The expansion of MDSCs is regulated by GM-CSF (Ribechini et al 2017, Young et al 1991), G-CSF (Sawanobori et al 2008),VEGF (Gabrilovich et al 1998, Kusmartsev et al 2008), S100A8 and S100A9 (Cheng et al 2008, Menetrier-Caux et al 1998, Sinha et al 2008a). After the licensing process resulting in the development of resting MDSCs (R-MDSCs) in the bone marrow, the activation of the MDSCs by infectious or inflammatory stimuli in the tissues is required (A-MDSCs) (Figure 1) (Ribechini et al 2017, Veglia et al 2021b). Licensing of monocytes by GM-CSF induces the activation of the PI3K/AKT/mTOR pathway and modifies the formation of IFN-γ signaling platforms on the cell surface (Ribechini et al 2017). The activation of these R-MDSCs with LPS, a component of the cell wall of gram-negative bacteria, and IFN-γ results in the production of NO in mice and IDO in human. M-MDSCs probably do not develop from a distinct precursor but are monocytes with a different polarization, which can further develop into DCs if no activation takes place (Figure 1) (Ribechini et al 2017, Rössner et al 2005). For *in vitro* generation of A-MDSCs, we culture bone marrow cells for 3 days followed by the activation with LPS and IFN-γ for 16 h, which results in iNOS expression. Other groups showed

that the culture with GM-CSF and IL-6 for 3 days can also yield A-MDSCs, and IL-6 upregulated the expression of Arg1 in a STAT3-dependent manner (Marigo et al 2010, Weber et al 2020).

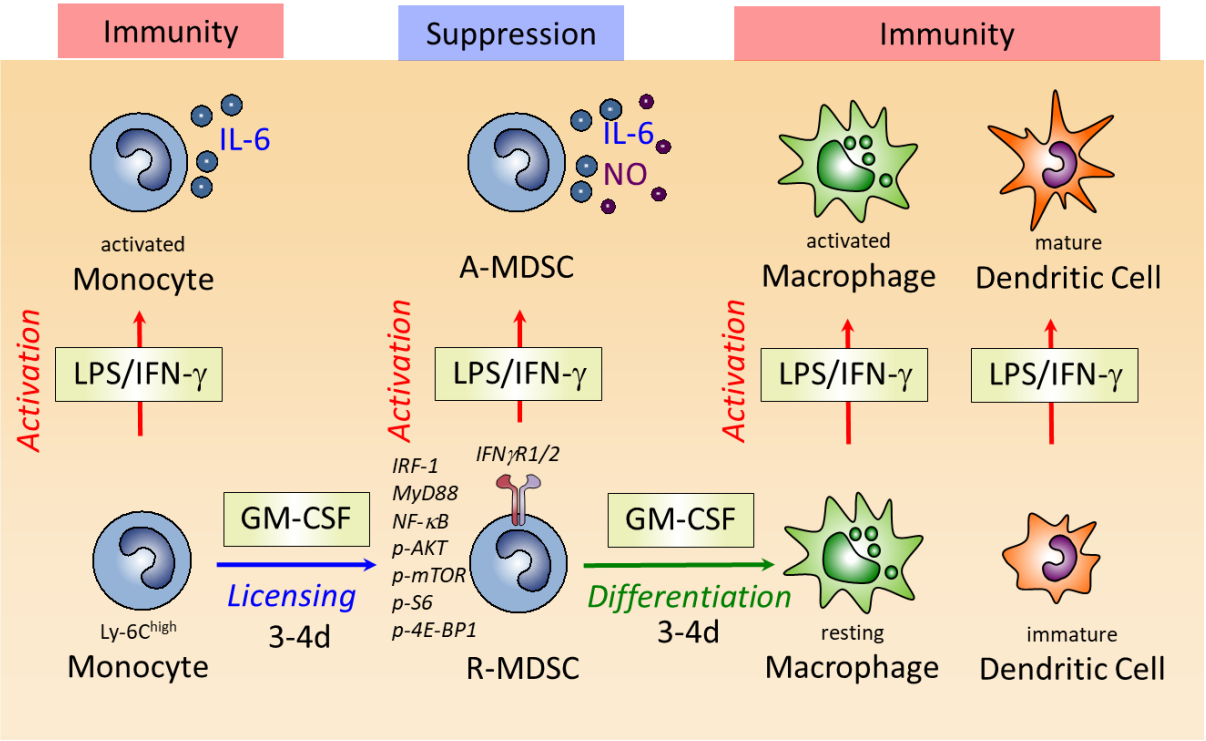

Figure 1: Activation stages of monocytes and monocyte-derived cells. Monocytes can be activated with LPS and IFN-γ to secrete the pro-inflammatory cytokine IL-6. In the presence of GM-CSF for 3-4 days, however, monocytes convert into R-MDSCs, which can then be activated to become immunosuppressive MDSCs. If the R-MDSCs are not activated, the monocytes can differentiate to macrophages and dendritic cells in the presence of GM-CSF, which exert immunostimulatory functions upon activation. Figure credit: Prof. Manfred Lutz.

1.1.2 Suppressive mechanisms of MDSCs

MDSCs suppress T cells by various mechanisms (Figure 2), which partially depend on the MDSC subset. One mechanism of T cell suppression is the deprivation of L-arginine, which leads to the downregulation of CD3 ζ-chain expression (Rodriguez et al 2002) as well as inhibiting the upregulation of the cell cycle regulators cyclin D3 and cyclin-dependent kinase 4 (Rodriguez et al 2007). This results in the inhibition of T cell proliferation. The arginine depletion is achieved by the expression of the enzymes iNOS and arginase, which metabolize L-arginine into NO or urea and ornithine, respectively (Bronte & Zanovello 2005). Another important mechanism of T cell suppression is the induction of oxidative stress by ROS and reactive nitrogen species, which include peroxynitrite ($ONOO^-$) and hydrogen peroxide both emerging from NO. ROS secreted mainly by the G-MDSC subset damage various cellular components such as proteins, lipids, and nucleic acids, which results in increased inflammation

and apoptosis (Ohl & Tenbrock 2018). ROS and peroxynitrite can modify the T cell receptor and CD8 molecules, leading to a deficit in MHC binding (Nagaraj et al 2007). NO, which is mainly secreted by M-MDSCs, inhibits T cell activation by downregulating JAK3/STAT5 signaling on T cells and MHC class II expression on antigen-presenting cells (Bingisser et al 1998, Harari & Liao 2004). Similar to the effect of arginine deprivation, H_2O_2 also reduces the expression of the CD3 ζ-chain of the TCR, followed by T cell unresponsiveness upon stimulation (Schmielau & Finn 2001).

MDSCs can also interfere with T cell migration by nitrosylating CCR2, which is required for the homing to effector organs, and by downregulating the lymph node homing receptor CD62L via interaction with ADAM17 (Hanson et al 2009, Molon et al 2011).

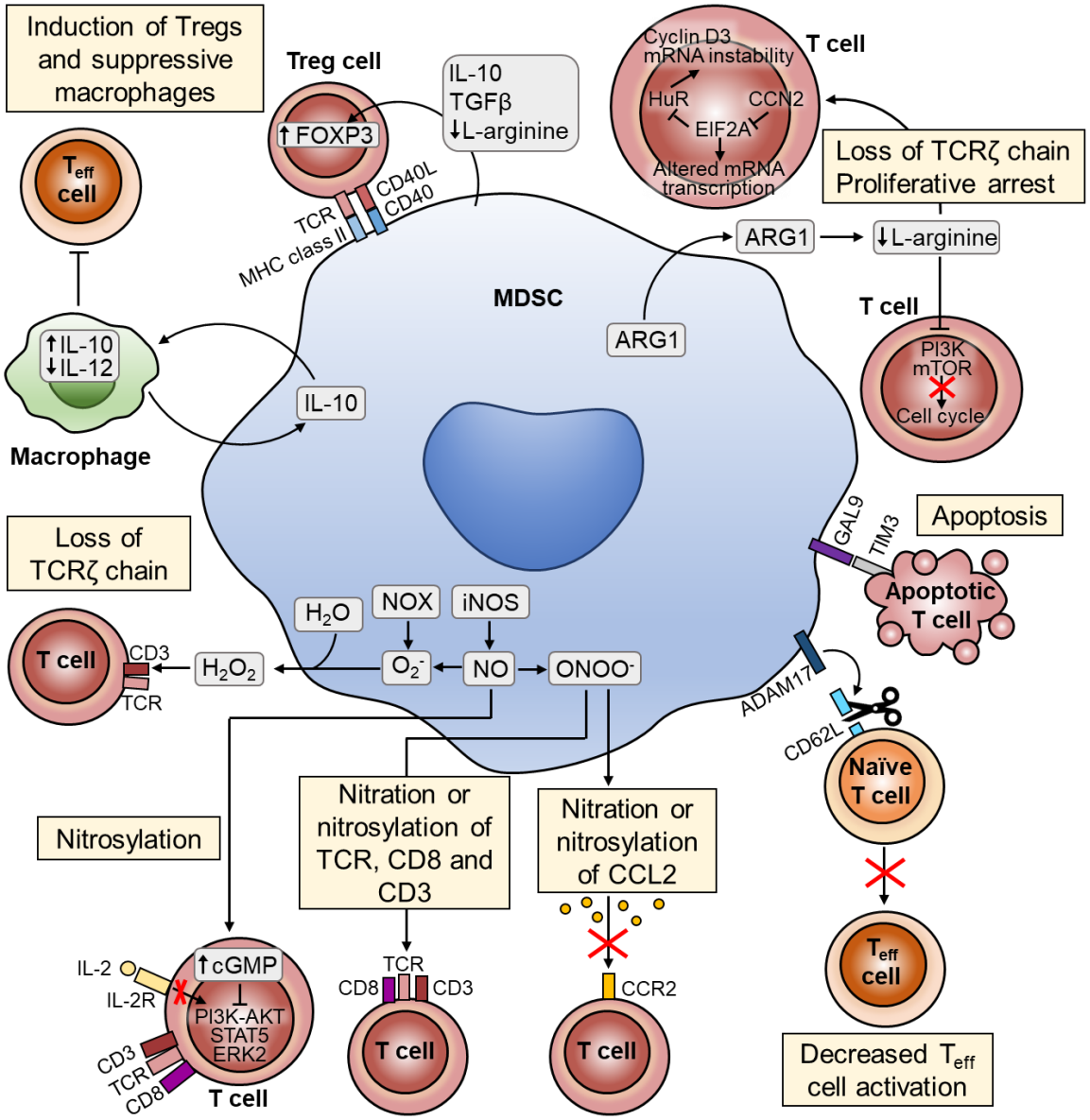

Figure 2: Suppressive mechanisms of MDSCs. MDSCs can suppress T cells by arginine starvation, TCR, CD8, and CD3 nitrosylation, inhibition of T cell homing, apoptosis induction, Treg and suppressive macrophage induction, and decrease of T cell activation. Figure according to (Gabrilovich et al 2012).

MDSCs were furthermore shown to express PD-L1 (Lu et al 2016a, Yamauchi et al 2018), which binds to PD-1 on activated T cells and leads to inhibition of T cell proliferation, effector functions and induces apoptosis (Zitvogel & Kroemer 2012).

Treg generation as well as the conversion of $CD4^+$ T cells into Tregs can be induced by MDSCs. The latter was shown to be dependent on IL-10 and IFN-γ (Huang et al 2006b). Moreover, interaction of CD40 on MDSCs with CD40L on T cells was found to be required to activate Tregs. A role of CTLA-4 (Yang et al 2006) and Arg1 (Serafini et al 2008) was also suggested. Besides suppressing T cells, we also found MDSCs to induce apoptosis in DCs in an *M.tb* prime-boost vaccine model in mice (Ribechini et al 2019). Furthermore, MDSCs were shown to impact macrophages by increasing the IL-10 secretion while reducing the production of IL-12 *in vivo* (Sinha et al 2007).

As mentioned before, the T cell suppressive mechanisms of MDSCs partially vary depending on the MDSC subset. While M-MDSCs express high levels of iNOS, which leads to the production of NO, M-MDSCs hardly produce ROS (Youn et al 2008b). On the other hand, G-MDSCs produce high levels of ROS depending on NADPH, but low levels of NO (Movahedi et al 2008a, Youn et al 2008b).

To validate the suppressive capacity of MDSCs a suppression assay can be performed (Figure 3). Therefore, R-MDSCs from *in vitro* cultures or sorted myeloid cells from *in vivo* models are added to T cells, which are activated with αCD3 and αCD28 antibodies, and co-cultured for several days. Activated T cells secrete cytokines leading to the activation of R-MDSCs, including IL-1β, TNF, IFN-γ, and IL-10 (Janeway et al 2001, Pulugulla et al 2018, Umansky et al 2016). The A-MDSCs then suppress the proliferation of the T cells, which can be measured by flow cytometry.

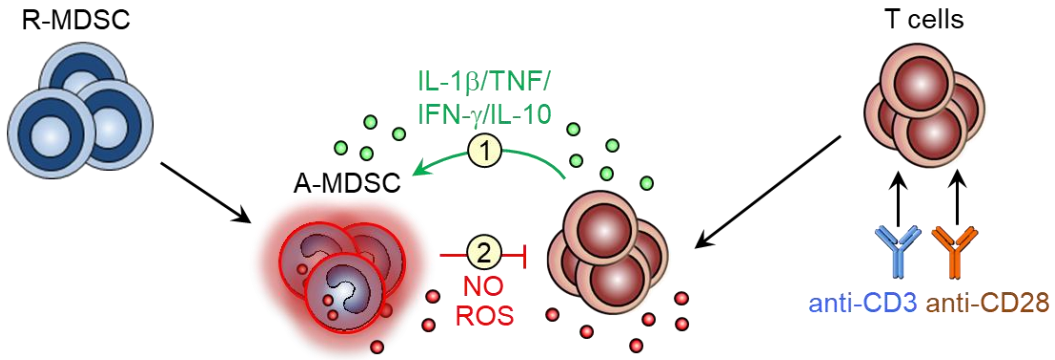

Figure 3: Stages of an *in vitro* suppression assay. Activated T cells and R-MDSCs are co-cultured. 1: Cytokines secreted by T cells activate the MDSCs. 2: A-MDSCs suppress the T cell proliferation.

1.1.3 Phenotypic markers of human and mouse MDSC subsets

Discriminating MDSCs from surface markers is still difficult, since non-suppressive monocytes and neutrophils express the same markers, therefore intracellular staining of effector markers is required. Murine M-MDSCs and G-MDSCs both express CD11b and Gr-1 (Kusmartsev et al 2004). Since Ly-6C and Ly-6G markers were found to be a more specific alternative for Gr-1, this marker should not be used anymore for MDSC identification (Rose et al 2012). M-MDSCs express high levels of Ly-6C but no Ly-6G, whereas G-MDSCs express Ly-6G and low levels of Ly-6C (Figure 4) (Youn et al 2008a). Furthermore, M-MDSCs can be distinguished from G-MDSCs by CD115 and CCR2 staining, which is hardly expressed by G-MDSCs (Veglia et al 2018). In contrast to M-MDSCs, suppressive macrophages express low levels of Ly-6C but are $CD11c^{+}$ MHC class II^{+}, the latter markers generally being absent on MDSCs (Movahedi et al 2008b). Human MDSCs express CD11b, CD33, and $CD66b^{+}$ but lack HLA-DR expression. M-MDSCs are defined as $CD14^{+}$ $CD15^{-}$ $HLA\text{-}DR^{low}$, and G-MDSCs are $CD14^{-}$ $CD15^{+}$ $HLA\text{-}DR^{low}$ (Bronte et al 2016). Intracellular effector markers expressed by human and mouse MDSCs include iNOS for M-MDSCs and ROS for G-MDSCs, whereas and both subsets express Arg1, S100A8, and S100A9 (Veglia et al 2021b). M-MDSCs and G-MDSCs are the major MDSC subsets, but there is also evidence for the presence of other subsets, namely the early MDSCs (Bronte et al 2016) and eosinophilic MDSCs (Goldmann et al 2017). Early MDSCs express CD11b in mice and co-express CD11b and CD33 in humans but lack any markers for monocytes and neutrophils like GR-1 in mice or CD14 and CD15 in humans (Cassetta et al 2020, Zhang et al 2018). Eosinophilic MDSCs were identified in mouse chronic staphylococcal infection and were defined as $Ly6C^{low}$ $Ly6G^{-}$ $CCR3^{low}$ $Siglec\text{-}F^{low}$ $IL\text{-}5R^{low}$ (Goldmann et al 2017).

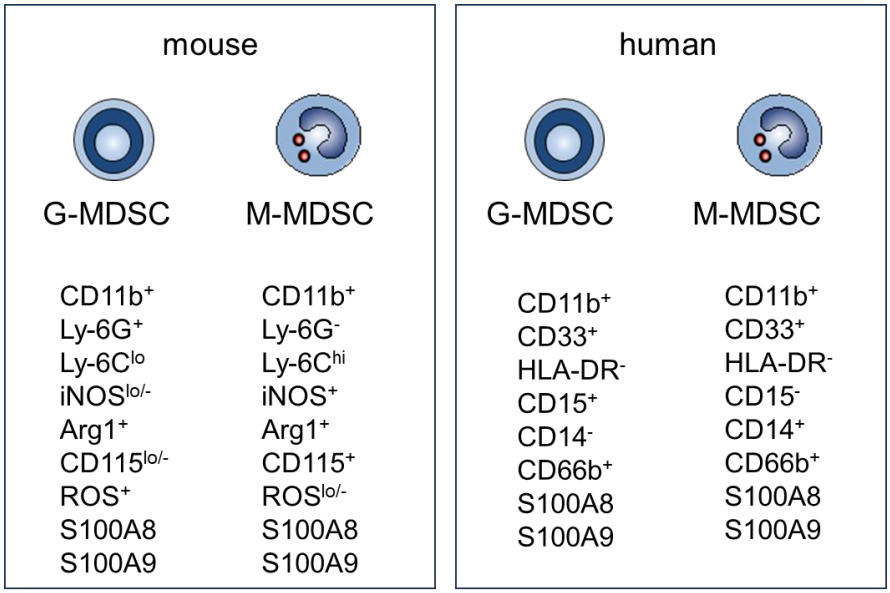

Figure 4: Marker expression by M-MDSCs and G-MDSCs. Indicated markers are expressed by murine and human MDSC subsets. Figure credit: Prof. Manfred Lutz (modified).

1.2 T cell subsets and their function

T cells are important mediators of the adaptive immune system. T cell precursors origin in the bone marrow and migrate to the thymus, where a repertoire of T cell receptors with a unique specificity for each T cell is generated (Germain 2002, Pennock et al 2013). The diversity of T cell receptors provides the ability of T cells to respond to a huge variety of pathogens. Naïve T cells recirculate between blood and the secondary lymphoid organs (spleen and lymph nodes) in order to increase their chance to find the specific antigen. CD62L expression enables the entry of naïve T cells into lymph nodes (Gallatin et al 1983). The T cells migrate to the T cell zones driven by a gradient in the chemokine CCL19, which is produced in the T cell area and binds to CCR7 on T cells (Kaiser et al 2005). The activation of specific T cells requires three signals: antigen recognition (signal 1), co-stimulation (signal 2), and cytokines released by DCs (signal 3) (Gutcher & Becher 2007). The peptide antigen is presented by DCs on an MHC molecule, and the T cell receptor recognizes the combination of MHC molecule and peptide. During signal 2, costimulatory receptors (e.g. CD28) on T cells bind to their ligands on DCs (e.g. B7-1 and B7-2) (Sharpe 2009). Besides the costimulatory molecules also coinhibitory molecules exist, including CTLA-4 competing with B7 molecules for CD28 ligation, and PD-L1 binding to PD-1 on T cells. T cell activation results in massive proliferation the antigen-specific T cell clones, followed by the egress from the lymph node and entry into the site of infection. CD69 expressed upon T cell activation prevents the exit of T cells from secondary lymphoid organs and is downregulated upon T_{eff} cell differentiation (Shiow et al 2006). CD62L expression is downregulated by T_{eff} cells as well, which reduces their potential to enter the lymph nodes (Yang et al 2011). CD44 expression is upregulated on effector and memory T cells and is implicated in cell adhesion and migration (Baaten et al 2012).

T cells are classified by their major function: $CD8^+$ cytotoxic T cells kill infected or cancer cells which present antigens on MHC class I, whereas $CD4^+$ helper T cells recognize peptides bound to MHC class II on professional antigen presenting cells like DCs, macrophages, and B cells, leading to the production of cytokines enhancing cytotoxic T cell and innate immune cell functions (Laidlaw et al 2016). $CD4^+$ T_{eff} cells are further divided into Th1, Th2 and Th17 cells. Th1 cells are generated in the presence of IFN-γ and IL-12 and secrete IFN-γ and TNF-α, which activates macrophages to kill intracellular pathogens and $CD8^+$ T cells to kill infected cells (Tau et al 2000). Th2 cells are produced in response to IL-4 and secrete IL-4, IL-5, and IL-13, which increases the defense against extracellular pathogens by inducing class switching of antibodies produced by B cells (Ouyang et al 2000, Shimoda et al 1996). Th17 cells need the presence of

IL-6 or IL-21 and TGF-β for their differentiation and produce IL-17, IL-21, IL-22, and GM-CSF, providing protection against bacterial and fungal infections (Korn et al 2009).

Besides the generation of T_{eff} cells, a small number of memory T cells is generated after T cell activation, which can be re-activated rapidly by antigen presenting cells after encounter of the specific antigen. Central memory T cells express CD62L and CCR7, which are associated with recirculation through the T cell areas of secondary lymphoid tissues similar to naïve T cells. On the other hand, effector memory T cells are $CCR7^-$ but express chemokine receptors required for the homing to inflamed tissues (Sallusto et al 2004, Sallusto et al 1999). Tissue resident memory cells do not survey tissues through blood and lymph but are retained in the tissue by CD69 and CD103 (Szabo et al 2019).

Tregs play an important role in preventing autoimmunity by limiting T cell activation (Caramalho et al 2015). Natural Tregs are generated in the thymus, whereas induced Tregs develop from $CD4^+$ T cells in peripheral tissues in the presence of IL-10 or TGF-β (Workman et al 2009). Natural and a subset of induced Tregs express the transcription factor FoxP3, which is required for Treg development and function (Sakaguchi et al 2010). Tregs suppress conventional T cells by secreting the suppressive cytokines IL-10, TGF-β, and IL-35 (Schmidt et al 2012). Furthermore, Tregs consume IL-2 by expressing high levels of CD25, a component of the high affinity IL-2 receptor, leading to an inhibition of $CD4^+$ T cell priming (Tang et al 2006) and $CD8^+$ T cell differentiation (McNally et al 2011). Moreover, Tregs can downregulate costimulatory molecules on antigen presenting cells through CTLA-4 and kill T_{eff} cells using granzyme and perforin (Schmidt et al 2012).

1.3 Function of myeloid cell subsets

Hematopoiesis in the bone marrow starts from hematopoietic stem cells which further differentiate into various progenitors. The granulocyte-monocyte progenitor can give rise to neutrophils and macrophage-dendritic cell progenitors, which further can differentiate into monocytes and DCs (Zhu et al 2016). Neutrophils defend the host against pathogens by phagocytosing microbes, cytokine production, releasing granules, and forming neutrophil extracellular traps (Rosales 2018).

Classical monocytes are present in the blood and are recruited to sites of inflammation, followed by a differentiation to macrophages or DCs in inflamed tissues (Ginhoux & Jung 2014). Non-classical monocytes survey the blood vessels and, upon infection, migrate into the tissue, where they differentiate into macrophages and initiate the immune response (Auffray et al 2007). M1 macrophages phagocytose and kill pathogens, activate Th1 cells, and produce pro-inflammatory cytokines including IL-1β and IL-6, whereas M2 macrophages are implicated in

tissue repair and wound healing, activate Th2 cells, and produce anti-inflammatory cytokines like IL-10 and TGF-β (Murray & Wynn 2011, Zhang et al 2021a).
CDC1s efficiently cross-present extracellular antigens to $CD8^+$ T cells, whereas cDC2s induce the polarization of helper and regulatory T cells (Rhodes et al 2019). Mo-DCs can develop from monocytes upon migration into inflamed tissues (Ginhoux & Jung 2014).

1.4 Organization of immune cells in the spleen

The spleen is a secondary lymphoid organ organized in the red pulp and the white pulp areas, which are parted by the marginal zone in mice and by the perifollicular zone in humans (Bronte & Pittet 2013, van Krieken & te Velde 1988). The blood flows through afferent arterioles to the marginal zone, where it enters an open blood system lacking endothelial linings. Then, the blood in the sinusoid spaces and the red pulp is led to the efferent splenic veins (Bronte & Pittet 2013). The white pulp consists of spatially separated T cell and B cell areas, through which naïve T cells and B cells circulate in order to find the cognate antigen and where the clonal expansion takes place. In the red pulp and the marginal zone mainly innate immune cells are located. Phagocytes including DCs, monocytes, and macrophages monitor the blood for pathogens and initiate and shape adaptive immune responses, but also filter opsonized, aged, and dead cells (Bronte & Pittet 2013). NK cells reside in the red pulp but can migrate into the white pulp upon infection and contribute to T cell polarization (Bekiaris et al 2008). Also, effector and memory T cells are located in the splenic red pulp (Bajénoff et al 2010, Jung et al 2010, Unsoeld et al 2004). MDSCs were shown to accumulate in human and murine spleens (Jordan et al 2017a, Youn et al 2008a). We found that MDSCs were located in the red pulp in an *M.tb* vaccine model but can be activated to migrate into the white pulp upon activation with LPS and IFN-γ to kill DCs (Ribechini et al 2019).

1.5 MDSCs in pathologies

MDSCs were initially described in cancer, and the majority of publications concerning MDSCs is still associated with this field. Apart from their crucial role in cancer, MDSCs are implicated in a variety of other pathologies, including chronic bacterial and parasitic infections (Ost et al 2016, Van Ginderachter et al 2010), traumatic stress (Cuenca et al 2011), sepsis (Delano et al 2007), and transplantation (Dugast et al 2008). Recently, M-MDSC and G-MDSC subsets were found in the peripheral blood of severe cases with COVID-19 infections and were associated with a poor prognosis (Agrati et al 2020, Schulte-Schrepping et al 2020, Xu et al 2020), however it is not clear yet if MDSCs are recruited in severe cases to protect the host from immunopathology or if they contribute to disease severity. MDSCs are also recruited during

autoimmune diseases including MS (Ioannou et al 2012), type 1 diabetes (Yin et al 2010b), rheumatoid arthritis (Evans et al 2009), inflammatory bowel disease, (Kim et al 2015) and autoimmune hepatitis (Hammerich & Tacke 2015). MDSC injection led to an improvement of the disease in mouse models like type I diabetes (Yin et al 2010a), rheumatoid arthritis (Fujii et al 2013), and colitis (Däbritz et al 2016).

1.5.1 MDSCs in cancer

Cancer belongs to the leading causes of death among people under the age of 70 in the majority of countries worldwide, with breast and lung cancer being the most common cancer types (Sung et al 2021). Early during tumorigenesis, the malignant cells are eliminated by $CD8^+$ T cells and NK cells, leading to a selection of cancer cells with little immunogenicity (Teng et al 2015). In order to prevent tumor destruction by the immune system, the cancer cells manipulate the immune system towards favoring immunosuppression. DCs express low levels of costimulatory molecules but express PD-L1 and CTLA-4, inducing T cell anergy (Labani-Motlagh et al 2020). Tregs produce immunosuppressive cytokines and their infiltration is associated with reduced patient survival (Kobayashi et al 2007, Yang & Lattime 2003). Tumor-associated macrophages promote tumor growth by secreting VEGF, MMP-7, MMP-9, IL-10, and TGF-β and suppress T cells by arginase production (Colegio et al 2014, Labani-Motlagh et al 2020). Reactivating T cell functions by blocking PD-L1 and CTLA-4 with antibodies resulted in an increased survival rate of cancer patients (Waldman et al 2020).

MDSC numbers correlated with the cancer stage and metastasis (Najjar & Finke 2013). MDSCs accumulated in response to M-CSF, G-CSF, and GM-CSF (Groth et al 2019). Cytokines produced by the tumor like IL-6 and IFN-γ were shown to activate MDSCs *in vitro*, however their role in MDSC function is not clear in *vivo* yet (Marvel & Gabrilovich 2015). MDSCs in tumor-bearing mice and cancer patients suppressed T cells by producing iNOS, IDO, arginase, TGF-β, and IL-10 (Hu et al 2011, Huang et al 2006a, Youn et al 2008a), and the suppression took place in the spleen as well as in the tumor (Kumar et al 2016). Treg accumulation was induced by MDSCs and depended on CD40 expression on MDSCs (Pan et al 2010). Furthermore, MDSCs were found to remodel the tumor micro-environment by secreting factors promoting angiogenesis and invasion, including VEGF and MMP9 (Tartour et al 2011). MDSCs furthermore promoted metastasis by inducing epithelial-to-mesenchymal transition (Toh et al 2011) and by infiltrating premetastatic organs and establishing the niche by tissue remodeling with MMP9 and immunosuppression (Yan et al 2010).

1.5.2 Role of MDSCs in multiple sclerosis and EAE

MS is a chronic autoimmune disease of the central nervous system where myelinated axons are destroyed leading to disability. The cause of MS is uncertain, but associated risk factors include ultraviolet B light, vitamin D, Epstein-Barr virus infection, obesity, smoking, and specific genes like HLA-DRB1*15:01 (Ascherio 2013, Sawcer et al 2011). Most patients show the relapsing-remitting form of disease, where relapses are followed by improvement or absence of symptoms, however this may develop into secondary progressive disease where the symptoms continuously get worse (Goldenberg 2012). Some patients develop primary progressive disease, where the MS progresses without remission from the beginning on. Symptoms include problems with vision, movement, and breathing as well as cognitive impairment (Ghasemi et al 2017).

Innate and adaptive immune cells infiltrate the brain and spinal cord and promote the demyelination and damage oligodendrocytes and axons (Dendrou et al 2015). The accumulation of immune cells causes the development of large demyelinated lesions, which are a hallmark of MS. $CD8^+$ T cell and B cell numbers are associated with lesion activity and axonal damage (Frischer et al 2009). $CD4^+$ T cells are less frequent than $CD8^+$ T cells and recognize antigens like MOG and myelin basic protein (Bielekova et al 2004, Frischer et al 2009). Th1 and Th17 cells are implicated in disease progression. Th1 cells are thought to activate microglia, whereas Th17 cells contribute to disrupting the blood brain barrier and upregulate the production of pro-inflammatory cytokines by astrocytes (Elain et al 2014, Kunkl et al 2020, Tahmasebinia & Pourgholaminejad 2017).

The EAE mouse model is mostly used for experimental MS research (Farooqi et al 2010). The mice are immunized with myelin antigen and adjuvants inducing the generation of Th1 and Th17 cells, and pertussis toxin injection further increases the EAE by opening the blood brain barrier and inducing clonal expansion of Th1 cells (Libbey & Fujinami 2011, Shive et al 2000). Despite the high similarity of MS and EAE, some differences between the mouse model and the human disease can be observed. Besides the artificial induction of the autoimmunity, the disease course during EAE is monophasic with the outbreak of disease followed by remission (Bettelli et al 2003). In human MS $CD8^+$ T cells are the prominent pathological cell type, while $CD4^+$ T cells drive the development of murine EAE (Dendrou et al 2015). GM-CSF is mainly produced by Th1 cells in humans, whereas in mouse EAE Th17 cells are the major source of GM-CSF (Codarri et al 2011, Noster et al 2014).

M-MDSC and G-MDSC subsets were found to be increased during relapsing-remitting MS but not during secondary progressive disease (Iacobaeus et al 2018). In mice with EAE, $Arg1^+$

MDSCs were found to induce apoptosis in T cells in the spinal cord (Moliné-Velázquez et al 2011). Furthermore, M-MDSCs with the potential of iNOS upregulation were detected in the spleen, bone marrow, blood, and spinal cord of mice with EAE (Zhu et al 2007). G-MDSCs on the other hand were shown to increase their suppressive potential upon IFN-β treatment and escalating dose immunotherapy using myelin basic protein of EAE (Melero-Jerez et al 2019, Wegner et al 2017). Moreover, G-MDSCs reduced the frequency of GM-CSF-producing B cells leading to disease recovery (Knier et al 2018). MDSCs generated *in vitro* with GM-CSF reduced the clinical score of mice when injected prior to EAE induction, and similar results were obtained when GM-CSF was injected before and during EAE induction (Ribechini et al 2017).

1.5.3 MDSCs during tuberculosis infection

M.tb infection is a leading cause of mortality worldwide (Raviglione & Sulis 2016). *M.tb* infection is mostly a pulmonary disease leading to symptoms including fever, weight loss, persistent cough, and haemoptysis. The disease is classified into latent and active infection. *M.tb* mainly infect alveolar macrophages, which internalize the bacteria by phagocytosis, however fusion of the phagosome with the lysosome is blocked by *M.tb*. When the bacteria gain access to the lung parenchyma, monocytes and DCs transport the bacteria to the draining lymph nodes, leading to the recruitment of immune cells and the formation of a granuloma enclosing the bacteria (Pai et al 2016). The granuloma contains monocytes, macrophages, DCs, as well as B and T cells. On the one hand, the granuloma limits the spreading of *M.tb*, but also creates a survival niche containing phagocytes which the bacteria infect and replicate in (Ehlers & Schaible 2013). If the bacterial load inside the granuloma gets too high, the bacteria egress from the granuloma and the disease transitions into the active stage, becoming symptomatic and contagious (Pai et al 2016). The progression into active tuberculosis can occur within months or several years after infection, and 85% of infected individuals remain latently infected (Andrews et al 2012, Vynnycky & Fine 1997).

BCG, a live attenuated strain of *Mycobacterium bovis*, is used as a vaccine against tuberculosis since 1921 mainly in newborn children (Dye 2013). The efficacy ranges from 0% to 80%, however it is not understood what leads to such a high variability. The efficacy tends to be reduced in individuals which were exposed to *M.tb* prior to the vaccination (Mangtani et al 2014). Despite the BCG vaccine of newborns shows good protection of children, the efficacy of adults varies (Dockrell & Smith 2017).

M.tb as well as BCG have been shown to induce MDSCs (Knaul et al 2014, Martino et al 2010).

Factors implicated in MDSC licensing and activation found upon mycobacteria infection include GM-CSF, IL-6, S100A8/A9, and IFN-γ (Magcwebeba et al 2019). Both M-MDSCs and G-MDSCs were found in the blood of tuberculosis patients, whereas mainly G-MDSCs were present in the bronchoalveolar lavage and M-MDSCs were found in pleural effusions (du Plessis et al 2013, El Daker et al 2015, Yang et al 2014). Early after *M.tb* infection (acute phase) in mice, low numbers of MDSCs were already present in the lungs, which highly expanded during the chronic phase (Tsiganov et al 2014). MDSCs were located at the edges of necrotic granulomas in *M.tb* susceptible mice (Obregón-Henao et al 2013). We found MDSCs recruited to the spleen in an *M.tb* prime-boost vaccination scenario using Freund's adjuvant in mice (Ribechini et al 2019). Upon activation with LPS and IFN-γ the MDSCs migrated from the red pulp to the white pulp where they induced apoptosis in DCs.

For the research on *M.tb* and BCG, mouse models of intranasal or intratracheal infection are most commonly used, since the pathogen reaches the lungs (Orme & Roberts 2001). However, most mouse strains lack the development of granulomas with central necrosis, which is thought to be an important feature triggering therapy resistance (Driver et al 2012). Therefore, mouse models are not suitable for tuberculosis drug development. An exception is the C3HeB/FeJ mouse model, which forms granulomas with high similarities to the human disease (Kramnik et al 1998). Some mouse strains are more susceptible to *M.tb* infection and develop progressive disease with premature death, while resistant strains are capable of controlling the growth and spread of bacteria (Chackerian & Behar 2003). CBA, C3HeB/FeJ, DBA/2, and 129SvJ belong to the susceptible mouse strains, whereas C57BL/6J and BALB/c are resistant (Medina & North 1998). In both resistant and susceptible strains MDSCs are recruited to the lungs, however in susceptible mice MDSCs are more abundant (Knaul et al 2014).

1.5.4 Manipulation of MDSCs for therapy

MDSC function can be inhibited in different ways. Low doses with distinct chemotherapeutic agents like cisplatin and gemcitabine induced the depletion of MDSCs and increased the immune response to tumors (Huang et al 2016, Yang et al 2013). STAT3 is an important transcription factor for MDSC activation, and STAT3 inhibition decreased G-MDSC frequencies in the blood of lymphoma patients and an increased frequencies of T cells and macrophages (Reilley et al 2018). Inhibiting prostaglandin E2 catabolism resulted in repression of arginase and ROS production by MDSCs (Eruslanov et al 2010), whereas Phosphodiesterase-5 was shown to reduce the expression of arginase and iNOS (Serafini et al 2006). Another strategy to inhibit MDSCs is to induce their differentiation. All-trans-retinoic acid reduced MDSC numbers and restored T cell function in mice and human (Iclozan et al

2013, Mirza et al 2006). Inhibiting the homing of MDSCs to the tumor by blocking chemokine receptors like CCR5 (Blattner et al 2018) and CXCR2 (Steele et al 2016) improved the immune response to the tumor.

Besides inhibiting MDSCs for cancer therapy, injecting or inducing MDSCs for the treatment of autoimmune diseases showed beneficial effects in preclinical models. GM-CSF injection increased the amount of suppressive $CD11b^+$ $Gr\text{-}1^+$ cells in the peripheral blood and spleen of mice with graft-versus-host-disease and improved the lethality (Joo et al 2009). Adoptive transfer of MDSCs prolonged the survival of murine allografts of heart, kidney, skin, and islets (Zhang et al 2021b). Various murine autoimmune diseases exhibited amelioration upon MDSC injection, including EAE, autoimmune arthritis, inflammatory bowel disease, psoriasis, type 1 diabetes, autoimmune hepatitis, and systemic lupus erythematosus (Zhang et al 2021b).

1.6 VLA-1 integrin

The main focus of our study lies on the characterization of the integrin VLA-1as a potential marker for M-MDSCs. Integrins are important receptors for cell adhesion to the extracellular matrix or to other cells, but are also linked to the cytoskeleton, which activates intracellular signaling pathways upon adhesion (Hynes 2002). Integrins are non-covalently linked heterodimers composed of one α and one β subunit. 18 types of α subunits and 8 types of β subunits have been identified, which combine to 24 different integrins with various functions (Figure 5) (Hynes 2004). Several integrins are specific for leukocytes, mediating cell-cell contacts, including integrins αX (CD11c) β2 and αM (CD11b) β2, which are mainly expressed by innate immune cells (Barczyk et al 2009, Podolnikova et al 2016, Vorup-Jensen et al 2007). Other groups of integrins bind with a high affinity to collagen, laminin, or the amino acid sequence RGD (Barczyk et al 2009, Swirski et al 2009b). VLA-1 consists of the α1β1 (CD49a/CD29) subunits and binds with a unique affinity to collagen IV, but also to collagen I and with a low affinity to laminin (Briesewitz et al 1993, Riikonen et al 1995). Besides binding to extracellular matrix components, VLA-1 was shown to bind the cell surface molecules Sema7A (Suzuki et al 2007) and collagen XIII (Nykvist et al 2000). VLA-1 is expressed on mesenchymal cells as well as on immune cells including T cells, NK cells, and macrophages (Ben-Horin & Bank 2004). While naïve T cells lack VLA-1 expression, VLA-1 is upregulated earliest at 5-6 days after T cell activation and is maintained on memory T cells, which favor Th1 over Th2 development (Goldstein et al 2003a). In a study on human peripheral blood lymphocytes, VLA-1 was co-expressed with CD62L and VLA-4, but not with lymph node homing receptor CCR7 (Goldstein et al 2003a). Furthermore, VLA-1 was expressed by a subset of $CD69^+$ $CD8^+$ tissue resident memory T cells in the skin, lung, liver, as well as tumor and is

associated with high cytotoxic activity (Cheuk et al 2017, Ghilas et al 2020, Haddadi et al 2017, Murray et al 2016). In macrophages, VLA-1 was shown to inhibit the egress from inflammatory tissues (Becker et al 2013). A subset of human liver-resident macrophages expressed VLA-1, which exhibited higher baseline production of TNF-α, IL-12, and IL-10 but were less responsive to TLR stimulation compared to VLA-1$^-$ macrophages (Martrus et al 2019).

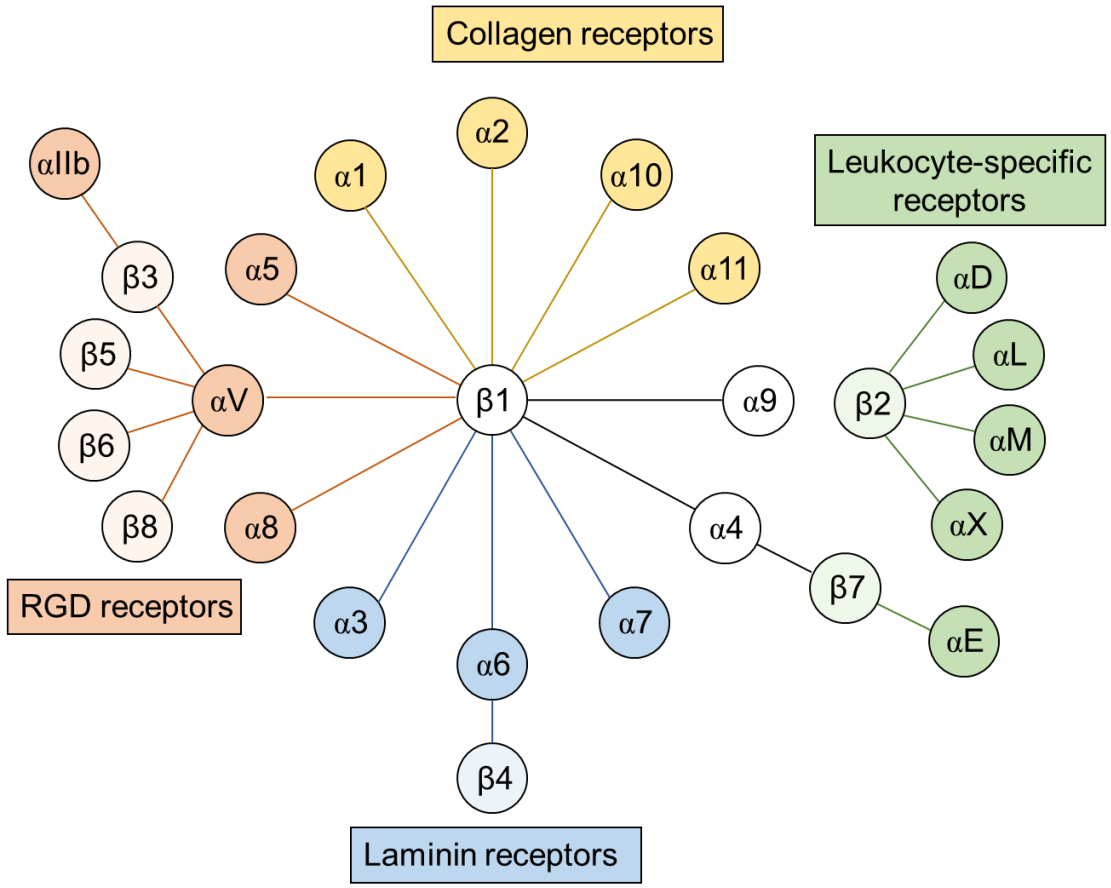

Figure 5: Combinations of α and β integrin subunits. Integrins are divided into 4 groups, the laminin, RGD, collagen and leukocyte-specific receptors. 24 different integrins are known which are composed of a combination of the 18 different α subunits and the 8 types of β subunits (Barczyk et al 2009, Hynes 2002).

1.7 CD16.2

Another MDSC marker candidate is CD16.2 (FcγRIV). The human homologue protein to the mouse CD16.2 is CD16A (FcγRIIIA) (Mao et al 2021). CD16.2 and CD16A are receptors for the Fc region of antibodies and bind IgG with a low affinity compared to FcγRI (Dekkers et al 2017). The sialylation of antibodies was found to be critical for IVIG, which induces anti-inflammatory responses when administered at high doses during autoimmune diseases like MS and systemic lupus erythematosus (Alter et al 2018b). CD16.2 was shown to bind sialylated IgG2b (Kaneko et al 2006) and MDSCs were found to be increased when human spleen cells were treated with IVIG (Aslam et al 2018). Therefore, CD16.2 expressed by MDSCs may be

implicated in the suppressive effect of IVIG and may serve as a new functional marker for MDSCs.

1.8 Objective

Although MDSCs were discovered decades ago, there are still no specific surface markers available to distinguish MDSCs from non-suppressive neutrophils or monocytes. This leads to the requirement of intracellular effector or licensing marker staining or proving the MDSC function with suppression assays. Therefore, specifically sorting live MDSCs without monocyte or neutrophil contamination is not yet possible. These reasons make the characterization of specific surface markers urgently required. Hence, we sought to identify novel surface markers for MDSCs in this study.

1.8.1 VLA-1-dependent T_{eff} cell suppression by MDSCs

We found that VLA-1 expression is upregulated on *in vitro* generated M-MDSCs (BM-MDSCs). Since T_{eff} cells but not naïve T cells express VLA-1 as well (Goldstein et al 2003a), we hypothesized that VLA-1^+ M-MDSCs and T_{eff} cells home to the same area, where T cell suppression can take place. The spleen is a major organ for MDSC-mediated suppression

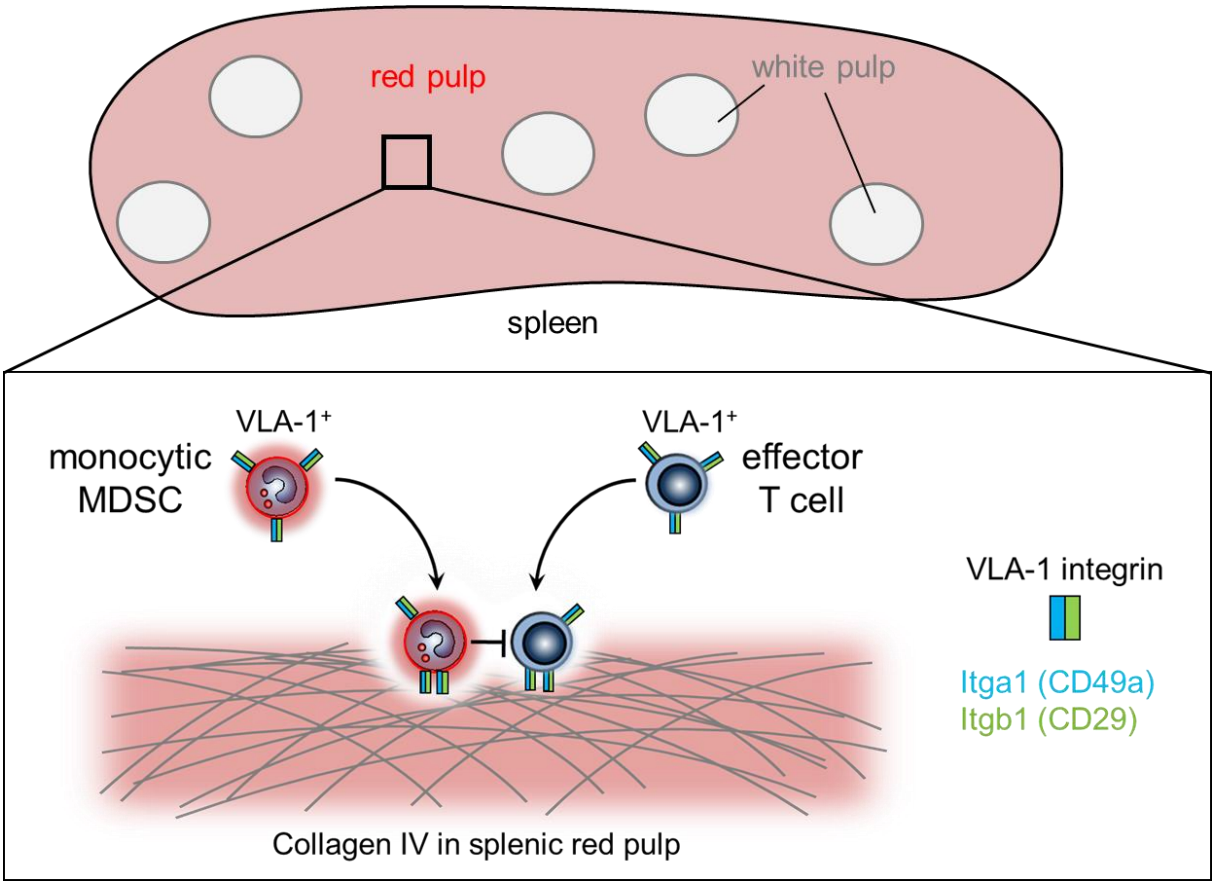

Figure 6: Hypothesis: VLA-1-expressing M-MDSCs home to the collagen-rich splenic red pulp and suppress VLA-1^+ T_{eff} cells there.

(Bronte & Pittet 2013, Greifenberg et al 2009), however it is not clear how MDSCs home to and migrate within the spleen. Collagen IV is only freely accessible in the red pulp of the spleen (Liakka et al 1995, Lokmic et al 2008), where monocytes and T_{eff} cells can be found (Jung et al 2010, Ugel et al 2012a), indicating that MDSC-mediated T_{eff} cell suppression takes place in the red pulp (Figure 6). In this study, aimed to investigate the relevance of VLA-1 for the homing and the suppressive function of MDSCs.

1.8.2 Marker expression by MDSCs in BCG-infected mice

Since BCG infection is known to induce MDSC accumulation in mice (Knaul et al 2014), we used this model to investigate the marker expression of endogenous MDSCs. For analyzing acute BCG infections, the timepoint 2 weeks after infection is established (Heldwein et al 2003, Nicolle et al 2004), whereas chronic BCG infection can be studied after 6 weeks (Clements et al 2001). We believe that generation of MDSCs upon intranasal BCG infection in our mouse model occurs as shown in figure 7. The bacteria in the lung activate resident DCs, which then prime T cells in the lymph node. The activated T cells migrate to the lung, where they kill

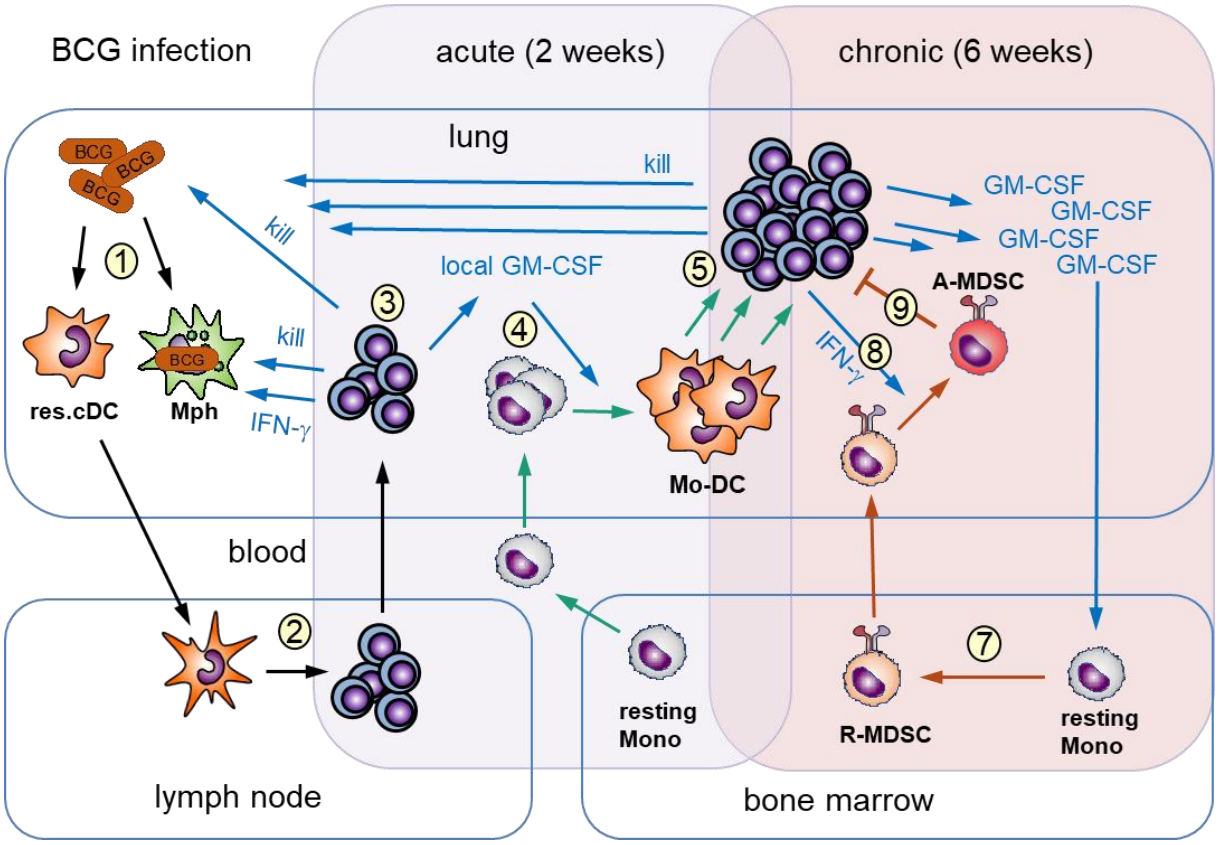

Figure 7: MDSC generation by BCG in mice. 1: BCG activate DCs and macrophages in the lung. 2: DCs prime T cells. 3: Infiltrating T_{eff} cells kill bacteria and infected macrophages. 4: Local GM-CSF secreted by activated T cells induces the differentiation of monocytes into Mo-DCs. 5: T cell response is enhanced by Mo-DCs. 6: GM-CSF produced by the activated T cells reaches systemic levels. 7: GM-CSF in the bone marrow induces R-MDSC generation. 8: Infiltrating R-MDSCs are activated by IFN-γ. 9: A-MDSCs suppress the T cells in the lung. Figure credit: Prof. Manfred Lutz (modified).

infected macrophages and bacteria. GM-CSF locally produced by the T cells induces the differentiation of infiltrating monocytes into mo-DCs, resulting in an augmentation of the T cell response. In the chronic phase, the large number of T cells produce high amounts of GM-CSF, which reach systemic levels and induces the generation of R-MDSCs in the bone marrow. Upon migrating to the lung, R-MDSCs are activated by IFN-γ produced by the T cells, followed by effector T cell suppression. Using this mouse model, we analyzed the expression of the potential MDSC marker candidates VLA-1 and CD16.2 by endogenous MDSCs in the spleen, lung and bone marrow.

2 Material and methods

2.1 Reagents

Table 1. Reagents

Product	Supplier
Agarose	Roth (Karlsruhe, Germany)
Ammonium Chloride (10% solution)	Applichem (Darmstadt, Germany)
Antisedan	Orion Pharma (Hamburg, Germany)
Avidin/Biotin Blocking Kit	Vector Laboratories (Newark, United States)
β-mercaptoethanol	Sigma-Aldrich (Deisenhofen, Germany)
Brefeldin A (from *Penicillium brefeldianu*)	Sigma-Aldrich (Deisenhofen, Germany)
BSA	Roth (Karlsruhe, Germany)
CellTrace™ Violet Cell Proliferation Dye	Invitrogen (Darmstadt, Germany)
CFSE	Invitrogen (Darmstadt, Germany)
Collagenase IV	Worthington (Lakewood, Canada)
Collagen IV	Sigma-Aldrich (Deisenhofen, Germany)
Complete Freund's Adjuvant	Sigma-Aldrich (Deisenhofen, Germany)
CpG ODN	Sigma-Aldrich (Deisenhofen, Germany)
DMSO	Sigma-Aldrich (Deisenhofen, Germany)
DNase	Roche (Basel, Switzerland)
EDTA	Applichem (Darmstadt, Germany)
eFluor™ 670 Cell Proliferation Dye	Invitrogen (Darmstadt, Germany)
Ethanol	Applichem (Darmstadt, Germany)
Ethidium Bromide	Roth (Karlsruhe, Germany)
FCS (Fetal Calf Serum)	Sigma-Aldrich (Deisenhofen, Germany)
Fibronectin	Sigma-Aldrich (Deisenhofen, Germany)
Fluoromount-G	Serva Electrophoresis (Germany)
Formaldehyde (37%)	Roth (Karlsruhe, Germany)
HEPES	Gibco (Waltham, United States)
Hydrogen Peroxide (30%)	Applichem (Darmstadt, Germany)
IFNγ	ImmunoTools (Friesoythe, Germany)
Isopropanol	Applichem (Darmstadt, Germany)
Ketamine	Serumwerk (Bernburg, Germany)
L-Glutamine	PAA Laboratories (Pasching, Austria)
LPS (E. coli 0127:B8)	Sigma-Aldrich (Deisenhofen, Germany)
M. tuberculosis (heat-killed)	BD Difco (Schwerte, Germany)
Medetomidine	Orion Pharma (Hamburg, Germany)
Methanol	Applichem (Darmstadt, Germany)
MOG Peptide (35-55)	China Peptides (Shanghai, China)
OVA-peptide$_{327-339}$	CharitéCentrum (Berlin, Germany)
Paraformaldehyde	Sigma-Aldrich (Deisenhofen, Germany)
Penicillin/Streptomycin	PAA Laboratories (Pasching, Austria)
Pertussis Toxin	List Biological Laboratories (Campbell, USA)
Sodium azide (NaN3)	Roth (Karlsruhe, Germany)
Sodium (meta)periodate	Sigma-Aldrich (Deisenhofen, Germany)
Sodium phosphate dibasic	Sigma-Aldrich (Deisenhofen, Germany)
Sodium phosphate monobasic	Sigma-Aldrich (Deisenhofen, Germany)
Sucrose ≥99.5%	Sigma-Aldrich (Deisenhofen, Germany)
Tris	Applichem (Darmstadt, Germany)
Tissue-tek	Sakura (Umkirch, Germany)
Triton X-100	Sigma-Aldrich (Deisenhofen, Germany)
Trypan blue	Sigma-Aldrich (Deisenhofen, Germany)

2.2 Antibodies

Table 2. Antibodies for surface antigens

Antigen	Conjugate	Dilution	Clone	Isotype	Company
B220	Pacific blue	1:100	RA3-6B2	Rat IgG2a, κ	BioLegend
CCR2	PE Brilliant Violet 605	1:25 1:200			BioLegend
CD3ε	FITC	1:100	145-2C11	Armenian Hamster IgG	BioLegend
CD4	PerCP/Cy5.5 PE Alexa Fluor 488	1:200 1:400	GK1.5	Rat IgG2b, κ	BioLegend
CD8a	APC Pacific blue FITC	1:200 1:200 1:200	53.6-7	Rat IgG2a, κ	BioLegend
CD11b	APC PerCP/Cy5.5 Alexa Fluor 700	1:300 1:600 1:200	M1/70	Rat IgG2b, κ	BioLegend
CD11c	PE/Cy7	1:600	N418	Armenian Hamster IgG	BioLegend
CD16.2	Alexa Fluor 647	1:100	9E9	Armenian Hamster IgG	BioLegend
CD25	Biotin PE	1:100 1:300	PC61	Rat IgG1, λ	BioLegend
CD44	Alexa Fluor 647	1:100	IM7	Rat IgG2b, κ	BioLegend
CD45	Brilliant Violet 785 Alexa Fluor 488	1:300 1:200	30-F11	Rat IgG2b, κ	BioLegend
CD49a	PE PerCP/Cy5.5	1:100 1:300	HMα1	Armenian Hamster IgG	BioLegend
CD64	PE	1:200	X54-5/7.1	Mouse IgG1, κ	BioLegend
CD62L	Alexa Fluor 700	1:100	MEL-14	Rat IgG2a, κ	BioLegend
CD69	APC Alexa Fluor 488	1:100 1:100	H1.2F3	Armenian Hamster IgG	BioLegend
CD90.1	PerCP/Cy5.5	1:200	OX-7	Mouse IgG1, κ	BioLegend
CD103	Biotin	1:100	2E7	Armenian Hamster IgG	BioLegend
CD274	APC	1:100	10F.9G2	Rat IgG2b, κ	BioLegend
F4/80	Brilliant Violet 711	1:300	BM8	Mouse IgG1, κ	BioLegend
I-A/I-E	Alexa Fluor 700	1:600	M5/114.15.2	Rat IgG2b, κ	BioLegend
Ly6C	Brilliant Violet 510 PE Alexa Fluor 647	1:200 1:600 1:200	HK1.4	Rat IgG2c, κ	BioLegend
Ly6G	APC/Fire Brilliant Violet 650	1:200 1:300	1A8	Rat IgG2a, κ	BioLegend
NK1.1	Brilliant Violet 421	1:200	PK136	Mouse IgG2a, κ	BioLegend
Vα2	APC/Cy7	1:400	B20.1	Rat IgG2a, λ	BioLegend

Antigen	Conjugate	Dilution	Clone	Isotype	Company
Vβ 5.1, 5.2	Biotin	1:200	MR9-4	Mouse IgG1, κ	BD Pharmingen

Table 3. Antibodies for intracellular antigens

Antigen	Conjugate	Dilution	Clone	Isotype	Company
Arginase 1	APC	1:100	A1exF5	Rat IgG2a, κ	Invitrogen
NOS2	PE FITC	1:300 1:300	CXNFT	Rat IgG2a, κ	eBioscience

Table 4. Antibodies for intranuclear antigens

Antigen	Conjugate	Dilution	Clone	Isotype	Company
Ki-67	Alexa Fluor 647 FITC	1:200 1:200	16A8	Rat IgG2a, κ	BioLegend
FoxP3	Alexa Fluor 488	1:200	MF-14	Rat IgG2b, κ	BioLegend

Table 5. Antibodies used for microscopy

Antigen	Conjugate	Dilution	Clone	Isotype	Company
CD11b	Alexa Fluor 488	1:100	M1/70	Rat IgG2b, κ	BioLegend
CD49a	Alexa Fluor 488	1:100	HMα1	Armenian Hamster IgG	BioLegend
CD90.1	Biotin	1:100	HIS51	Rat IgG2a, κ	eBioscience
CD169	Alexa Fluor 647	1:150	3D6.112	Rat IgG2a, κ	BioLegend

Table 6. Secondary antibodies

Antigen	Conjugate	Dilution	Company
Streptavidin	Cy3	1:300	BioLegend
Streptavidin	FITC	1:300	BioLegend
Streptavidin	Brilliant Violet 510	1:300	BioLegend
Streptavidin	PE-Cy7	1:300	BioLegend

2.3 Buffers, media, and solutions

Table 7. Buffers, media, and solutions

Buffer	Composition
PBS, pH7.4	0.2 mg/ml Potassium chloride (Sigma-Adrich) 8.0 mg/ml Sodium chloride (Sigma-Adrich) 1.15 mg/ml Monopotassium phosphate (Sigma-Adrich) 1.15 mg/ml Disodium phosphate (Sigma-Adrich) In Millipore water

Buffer	Composition
RPMI 1640 complete medium	500ml RPMI 1640 (Sigma-Adrich) 10% heat-inactivated sterile filtered FCS (Sigma-Adrich) 100U/ml Penicillin (Sigma-Adrich) 100µg/ml Streptomycin (Sigma-Adrich) 2mM L-glutamine (Sigma-Adrich) 50mM β-mercaptoethanol (Sigma-Adrich)
10x Erythrocyte lysis buffer	150 mM Ammonium chloride (Roth) 10 mM Sodium bicarbonate (Roth) 0.1 mM EDTA (Sigma-Aldrich) In Millipore water
Lung digestion buffer	10mM HEPES (Gibco) 0.25 mg/ml Liberase (Roche) In DMEM (Gibco)
Stop solution (for lung digest)	50 µM b-Mercaptoethanol In PBS
Spleen digestion mix II	1 mg/ml Collagenase IV (Worthington) 20 µg/ml DNase I (Roche) 2% FCS In RPMI-1640 medium
Spleen digestion mix I	1 mg/ml Collagenase IV (Worthington) 20 µg/ml DNase I (Roche) 2% FCS In RPMI-1640 medium
MACS Buffer	0.5% BSA (Roth) 2 mM EDTA (Sigma-Aldrich) In PBS
FACS Buffer	0.1% BSA (Roth) 0.1% Sodium azide (Roth) In PBS
ELISA wash buffer	0.05% Tween 20 (Applichem) In PBS
TBST wash buffer	20 mM Tris-hydrochloride pH 7.6 (Sigma-Aldrich) 150 mM Sodium chloride (Sigma-Aldrich) 0.05% Tween 20 (Applichem) In PBS

2.4 Primary cell techniques

2.4.1 Handling of cells

All procedures were performed under sterile conditions using a class II biological safety cabinet (Thermo Scientific) and sterile materials. The cells were cultured in an incubator (Thermo Scientific) at 37 °C and 7% CO_2. Before splitting or using cultured cells for assays, the medium was pre-warmed to 37°C. Centrifugation was performed for 10 min at 1200 rpm and room temperature. For counting, the cells were diluted 1:10 in trypan blue (Sigma-Aldrich) for discriminating dead cells and counted using a Neubauer counting chamber (Hartenstein) and an

Axiostar plus microscope (Carl Zeiss). The cell number per ml was calculated by the following formular:

$$\frac{\text{number live cells large quadrant 1} + \text{number live cells large quadrant 2}}{2} \; x \text{ dilution } x \; 10^4$$

2.4.2 Generation of GM-CSF supernatant

The supernatant for BM-MDSC generation was obtained from a murine GM-CSF transfected X63-Ag8.653 myeloma cell line kindly provided by B. Stockinger (London, UK). The cells were thawed according to the standard procedure and cultured in a T75 culture flask (Greiner Bio-One) in RPMI 1640 complete medium. After 2 days, 10^7 cells were harvested and transferred to a T182 culture flask (Greiner Bio-One). When reaching a confluency of around 90% after 3-4 days, the supernatant was harvested and centrifuged at 1000 rpm for 10 min. Subsequently, the culture supernatant was sterile-filtered with Minisart syringe filters (Sartorius) and stored at -20 °C before using for BM-MDSC generation.

2.4.3 BM-MDSC generation

Murine BM-MDSCs were generated as described before (Lutz et al 1999) based on a modified protocol for BM-DC generation (Rössner et al 2005). Briefly, femur and tibia of 6–12-week-old mice were removed and soaked for 1-2 min in ethanol for disinfection. Then, the bones were transferred into a 6 cm petri dish (Greiner Bio-One) filled with PBS. For isolating the cells, the ends of the bones were removed with scissors and flushed with PBS using a 10 ml syringe (Pentaferte) and a 27-gauge needle (Neoject). Next, the cells were centrifuged, resuspended in RPMI 1640 complete medium, and counted. $3x10^6$ BM cells were cultured in 10 cm petri dishes (Greiner Bio-One) in 10 ml RPMI 1640 complete medium with 10% GM-CSF supernatant for 3 days. The R-MDSCs can be activated by incubation for 16 h with 100 ng/ml LPS (Sigma-Aldrich) and 100 U/ml IFN-γ (Peprotech) or for 4 h with 1 µg/ml LPS and 0,5 µg/ml IFN-γ.

2.4.4 Generation of single cell suspensions of spleen and lymph nodes

Spleens and lymph nodes from 6-12-week-old OT-II CD09.1 mice were removed, and single cell suspensions were prepared by mashing the organs with a syringe plunger through 70 µm cell strainers (Greiner Bio-One) placed in a 6 cm petri dish (Greiner Bio-One) filled with PBS. Erythrocytes in the spleen cell suspension were lysed by incubation with 4 ml 1x erythrocyte lysis buffer for 1-2 min at room temperature. The lysis was stopped by adding 10 ml RPMI 1640 complete medium. Next, spleen and lymph node cells were centrifuged, resuspended in RPMI 1640 complete medium and counted.

2.4.5 Generating singe cell suspension of lungs

Lungs of mice were removed, placed in a 2 ml tube (Eppendorf), and chopped in small pieces on ice. Then, the tissue was transferred to a 50 ml falcon (Greiner Bio-One) and incubated with 2 ml digestion mix for 45 min at 37 °C and 120 rpm on a shaker. Subsequently, 20 ml of stop solution were added and the tissue suspension was mashed through a 70 µm cell strainer (Greiner Bio-One). After 10 min centrifugation, the single cells were incubated with 1 ml erythrocyte lysis buffer for 1 min. The reaction was stopped by adding 10 ml RPMI 1640 complete medium, followed by centrifugation and cell counting.

2.4.6 Effector OT-II T cell generation

Spleen and lymph nodes were removed, and single cell suspensions were prepared. $2x10^6$ pooled spleen and lymph node cells were cultured in a 24 well plate (Greiner Bio-One) for 6-7 days in 2 ml RPMI 1640 complete medium with 1 µM OVA-peptide$_{327-339}$ (CharitéCentrum Berlin). After 3-4 days, new medium was added depending on the intensity of yellow coloring of the medium.

2.4.7 T cell suppressor assay

WT or Itga1$^{-/-}$ BM-MDSCs were harvested and seeded into a round bottom 96 well plate (Greiner Bio-One) and co-cultured with syngeneic pooled spleen and lymph node cells or *in vitro* generated effector OT-II T cells in 200 µl RPMI 1640 complete medium. Depending on the assay, either 20,000 or 200,000 T cells were added per well. MDSCs were seeded in triplicates of different MDSC to T cell-ratios. The T cells were stimulated with 2.5 µg/ml αCD3 and 2.5 µg/ml αCD28 antibodies. If additional MDSC stimulation was required, 100 ng/ml LPS and 100 U/ml IFN-γ were added to the culture. After 3 days, the cells were harvested, the triplicates were pooled, and the T cell proliferation was analyzed by flow cytometry using the Ki-67 marker.

2.4.8 *In vitro* migration assay of MDSCs and T_{eff} cells

WT or *Itga1*$^{-/-}$ A-MDSCs were labeled with CFSE and mixed with OT-II dsRed T_{eff} cells at a 1:2 ratio (MDSC:T). Next, the cells were transferred into a µ-slide 8 well chamber (IBIDI) which was coated with 20 µg/ml fibronectin (Sigma-Aldrich) or 100 µg/ml collagen IV (Sigma-Aldrich). Images were recorded using an inverted LSM 780 confocal microscope (Zeiss) with an XL incubator suitable for live cell imaging. Images were acquired every 15 s for 60 min and analyzed with the Imaris software (Bitplane).

2.4.9 MACS of CD11b$^+$ cells

CD11b$^+$ cells were isolated from murine spleen or lung cells using the CD11b MicroBeads (Miltenyi Biotec) according to the manufacturer's instructions. Briefly, the cells were centrifuged and resuspended in 90 µl MACS buffer per 10^7 cells. Next, 10 µl MicroBeads were added and incubated for 15 min at 4 °C, followed by washing with 2 ml MACS buffer. For the magnetic separation, LS MACS columns (Miltenyi Biotec) were placed in MACS separator (Miltenyi Biotec) and rinsed with 5 ml MACS buffer. Then, the labeled cells were loaded in 500 µl MACS buffer per 10^8 cells onto the MACS column and washed 3 times with 3 ml MACS buffer. Finally, the column was removed and placed on a collection tube and flushed out with 5 ml MACS buffer using a plunger. The purity was assessed by CD11b staining and analyzing the cells by flow cytometry.

2.4.10 FACS

BM-MDSCs were kept at room temperature during the staining and sorting processes. First, the cells were harvested, washed, and resuspended in RPMI 1640 complete medium and adjusted to 50x10^6 cells per ml. Next, the antibodies were added with a dilution of 1:100, followed by 20 min incubation and washing. Subsequently, the cells were resuspended in RPMI 1640 medium supplemented with 5% FCS at 10x10^6 cells per ml. Immediately before sorting, the cells were filtered using a round bottom polystyrene test tube with a 70 µm cell strainer snap cap (Falcon). Sorting was performed with a FACS Aria III (BD) using a 100 µm nozzle and a flow rate not exceeding 9000 cells/s.

2.5 In vivo mouse experiments

2.5.1 Mice

All mice were housed in the animal facilities of the Institute of Virology and Immunobiology at the University of Würzburg. C57BL/6 wildtype and C57BL/6 CD45.1 mice were purchased from Charles River and bred in house. C57BL/6 OT-II dsRed mice were kindly provided by Andreas Beilhack, Würzburg, Germany. C57BL/6 OT-II (kindly provided by Francis Carbone, Melbourne, Australia), C57BL/6 *Itga1*$^{-/-}$ (kindly provided by Humphrey Gardener, Cambridge, England, and Jyrki Heino, Turku, Finland) (Gardner et al 1996) and C57BL/6 Sema7A$^{-/-}$ mouse lines (kindly provided by Jeroen Pasterkamp, Utrecht, Netherlands) were each crossed with C57BL/6 CD90.1 congenic mice. All animal experiments were approved by the local authorities (Regierung von Unterfranken) and were performed according to the German animal protection law.

2.5.2 Adoptive transfer of labeled MDSCs and T cells

T_{eff} cells were generated from C57BL/6 OT-II CD90.1 congenic mice, allowing their discrimination from the CD90.2$^+$ host by antibody staining. R-MDSCs and A-MDSCs were generated from C57BL/6 WT and *Itga1*$^{-/-}$ mice and were labeled with CFSE (Invitrogen), CellTrace Violet (Invitrogen) or eFluor 670 (Invitrogen) following the manufacturer's instructions. Briefly, the cells were harvested, washed, and resuspended either with 2.5 µM CFSE or 1.75 µM eFluor 670 in 1 ml PBS per 2x10^7 cells, followed by incubation for 10 min at room temperature in the dark and washing with 1 ml FCS and 40 ml PBS. The staining with CellTrace Violet was performed by incubating 1x10^7 cells per ml PBS with 5 µM CellTrace Violet for 6 min in the dark at room temperature. Next, the cells were washed with 500 µl FCS and 5 ml RPMI for 5 min at 37 °C.

7-10x10^6 MDSCs were injected alone or co-injected with T_{eff} cells at a 1:1 ratio in 100 µl PBS into the lateral tail vein of 8–12-week-old C57BL/6 WT mice. The spleens were harvested at different time points to perform microscopy or flow cytometry. For isolating VLA-1$^+$ cells from the spleen for flow cytometry, the organ was placed in a 6 well plate (Greiner Bio-One) on ice and flushed with spleen digestion mix I using a 1 ml syringe (Chirana) and A 25 gauge needle (Neoject). Next, the spleen was chopped into small pieces with a scalpel and subsequently incubated in spleen digestion mix I for 45 min at 37 °C. Singe cell suspensions were prepared by mashing the organ suspension through 70 µm cell strainers (Greiner Bio-One) with a syringe plunger, followed by washing, erythrocyte lysis and counting.

2.5.3 Intravital microscopy of injected T cells and MDSCs

For live tracking the migration of T_{eff} cells and WT or *Itga1*$^{-/-}$ A-MDSCs in the spleen, the MDSCs were labeled with CFSE, and the T_{eff} cells were used from OT-II dsRed transgenic mice. 1x10^7 cells each were injected intravenously at a 1:1 ratio. After 1 h, the mice were anaesthetized with isoflurane, positioned on a heated pad and the spleen was exposed by performing a small incision. The spleen was placed under a glass cover slip with two custom-made holders and the moisture of the tissue was maintained using sterile 0.9 NaCl. The data was acquired using a multiphoton microscope TrimScope II equipped with a Chameleon Ultra II titanium sapphire laser (Coherent), beam splitters at 500, 570, and 655 nm, bandpass filters 420/50, 535/50, 605/70, and photomultipliers (LaVision BioTec). The light intensity was increased between 5% and 30% depending on the penetration depth along the Z-axis. Images of the splenic subcapsular sinus were recorded every 30 s for 30-90 min with 70-90 µm in the Z-plane. Analysis was performed using the Imaris software (Bitplane). The cell tracking was

corrected manually, no filters were applied to process the data, and tracks with durations exceeding 60 s were excluded.

2.5.4 Induction of EAE

When inducing EAE, we aimed for 100% disease penetrance and a maximum score of 3-4. We found best results using 200 µg MOG_{35-55} peptide (ChinaPeptides) and 200 ng pertussis toxin (List Biological Laboratories) per mouse, however the dose of new MOG_{35-55} peptide batches needs to be re-evaluated.

First the water-in-oil emulsion with MOG_{35-55} peptide was prepared. Therefore, complete Freund's adjuvant (Sigma-Aldrich) supplemented with 10 mg/ml heat-killed *M. tuberculosis* (Difco) was mixed with MOG_{35-55} peptide in PBS at a 1:1 ratio and attached to a vortex (Scientific Industries) for 1,5 h, until a thick emulsion was formed. Before injection (day 0), 8-week-old female C57BL/6 WT mice were anesthetized with 2 mg Ketamine (Serumwerk) and 20 µg Medetomidine (Orion Pharma) in 100 µl PBS per mouse intraperitoneally. Then, 100 µl of the MOG/CFA emulsion were injected subcutaneously at the lower back of the mice. 100 µl pertussis toxin in PBS were injected intraperitoneally at day 0 and day 2. The anesthesia was antagonized with Antisedan (Orion Pharma). The score of the mice was monitored according to table 8 from day 8 until the end of the experiment. In case a mouse exhibited breathing problems or lost more than 20% of bodyweight, the mouse was sacrificed.

Table 8. EAE score

Score	Symptoms
1	Full tail paralysis
2	Complete paralysis of one hind leg or partial paralysis of both hind legs
3	Complete or near-complete paralysis of both hind legs, no impairment of front legs
4	Beginning weakness of front legs, breathing normal
5	Front leg paralysis, mouse needs to be sacrificed

For analysis of the spleens via flow cytometry or ELISA, the spleens were removed on day 15 after EAE induction. The restimulation for ELISA was performed by culturing $4x10^5$ spleen cells per well in a flat bottom 96 well plate (Greiner Bio-One) in serum-free HL-1 medium (Lonza BioWhittaker) with concentrations of 30 µg/ml, 10 µg/ml, and 3 µg/ml MOG_{35-55} peptide. After 3 days, cells were stained for flow cytometry and the supernatants were removed and stored at -20°C until performing the ELISA assay.

2.5.5 Mouse infection with BCG

The bacteria for the infection were harvested during the exponential growth phase. 8–12-week-old male C57BL/6 WT mice were anaesthetized with an intraperitoneal injection of 2 mg Ketamine and 20 µg Medetomidine in 100 µl PBS per mouse. Then, $1x10^7$ colony forming units BCG in 20 µl PBS were slowly administered intranasally using a pipet. After approximately 15 min, the anesthetics were antagonized with 250 µg Antisedan in 100 µl PBS. After 2 and 6 weeks, the spleens, lungs, and bone marrow were harvested for analysis. Since high cell numbers were required for the analysis, the spleens were cut into small pieces with scissors in a 1.5 ml tube (Eppendorf) and incubated with 1 ml spleen digestion mix II for 20 min, followed by mashing through a 70 µm cell strainer (Greiner Bio-One). The bacterial load of the lungs was measured by adding 100 µl of the lung single cell suspension to agar plates and dispensed using glass beads (3 mm diameter, Hartenstein). The plates were sealed with parafilm, cultured for 4 weeks at 35 °C and then the formed bacteria colonies were counted manually.

2.5.6 Tumor induction of mice

67NR breast cancer cells were cultured in Dulbecco's Modified Eagle Medium (Gibco) supplemented with 10% FBS (Sigma-Aldrich), 100 U/ml Penincillin (Sigma-Adrich) and 100 µg/ml Streptomycin (Sigma-Adrich). Before injection, the cells were treated with 2 µg/ml Puromycin (Gibco) for 24 h. For tumor induction, 8-12-week-old female BALB/c mice were anaesthetized with isoflurane and in each side $1x10^5$ 67NR cells in 50 µl of 50% matrigel:PBS were injected orthotopically into the fourth mammary fat pad. As soon as the tumor became palpable, the tumor size was measured 3 times per week using sliding calipers and the mice were sacrificed when the tumor reached a size of 1x1 cm. Tumor infiltrating cells were isolated by cutting the tumor into small pieces using a scalpel, followed by a digestion with 1 mg/ml collagenase A (Sigma-Aldrich), 1 mg/ml collagenase D (Sigma-Aldrich) and 0.4 mg/ml DNase I (Sigma-Aldrich) for 2 h at 37 °C on a shaker.

2.6 Analysis

2.6.1 Flow Cytometry

The single cell suspension was washed with FACS buffer and Fc receptors were blocked by incubation with 10% supernatant derived from the 2.4G2 hybridoma cell line (anti-Fc-gamma-RII/III, ATCC) in FACS buffer for 15 min at 4 °C. Next, the cells were stained with Fixable Viability Dye eFluor™ 780 (eBioscience) diluted 1:1000 in PBS for 15 min at 4 °C. After washing with FACS buffer, the surface markers were stained by incubating the cells with the

antibodies from table 2 for 15-30 min. For staining intracellular antigens (table 3), the cells were fixed with 2% formaldehyde (Roth) for 20-60 min at room temperature, whereas for nuclear antigen staining (table 4) the cells were treated with Cytofix/Cytoperm solution (eBioscience) for 20-60 min at room temperature. After washing, the antibodies were incubated for 45-60 min at room temperature. For apoptosis detection using annexin V, the cells were stained with 0.5 µl annexin V in 50 µl annexin V binding buffer (BD Pharmingen) for 15 min at room temperature. Then, 100 µl annexin V binding buffer were added, and the samples were measured within 1 h. The samples were acquired using the Attune Nxt V6 (ThermoFisher Scientific) or the LSR II (BD) Flow Cytometers and the data was analyzed via FlowJo 10 (Tree Star) and Prism 9.1.1 (GraphPad). The spectral overlap was compensated using OneComp beads or cells stained with a single fluorochrome-conjugated antibody using the FlowJo software, and eventual compensation mistakes were corrected manually according to Figure 8. The MFI was calculated with the FlowJo software using the geometric mean.

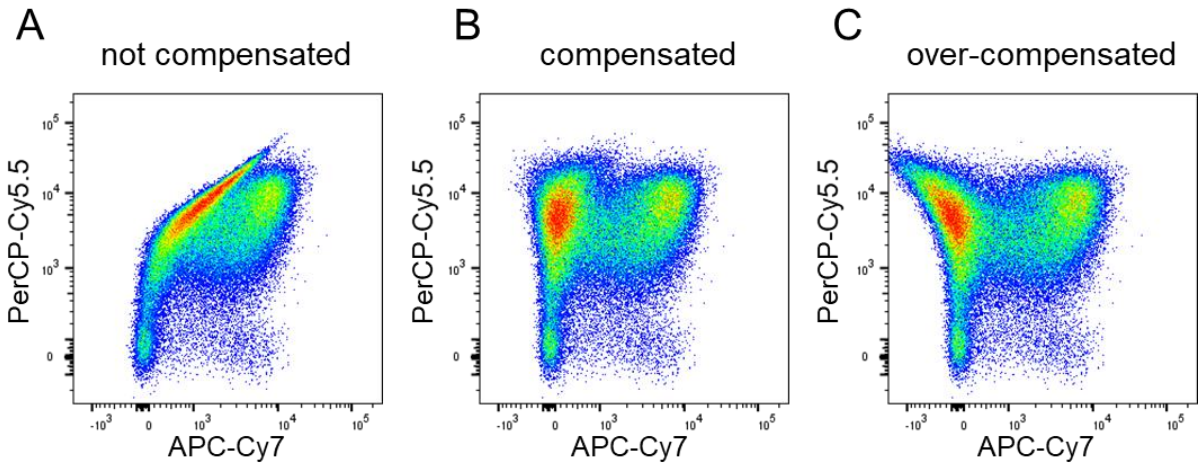

Figure 8: Compensation of spectral overlap. (A) Fluorescence spillover results in false positive signals. **(B)** The MFI of the positive and negative population should be similar in the channel where the false signal is detected. **(C)** Over-compensation results in a lower MFI of the positive population compared to the negative.

2.6.2 Confocal microscopy

Spleens were harvested, embedded in Tissue-Tek (Sakura), immediately frozen, and stored at -80 °C. 10 µm thick cryosections were prepared using a cryotome (Leica) and stored at -20 °C. Directly before staining, the sections were thawed for 10 min at room temperature. Next, the slides were fixed with 4% paraformaldehyde (Sigma-Aldrich) in PBS for 10 min and washed twice with PBS. The tissue was then permeabilized using 0.1% Triton X-100 (Sigma-Aldrich) in cold PBS for 5 min and washed. In case of staining with biotinylated antibodies, the slides were treated with the Avidin/Biotin Blocking Kit (Vector Laboratories) according to the manufacturer's instructions. Briefly, the slides were incubated with Avidin D solution for 15

min, followed by incubation with Biotin solution for another 15 min. Next, unspecific binding of antibodies was blocked by incubating the tissue with 5% BSA (Roth) in PBS for 20 min. The primary antibodies (table 5) diluted in 1% BSA in PBS were stained for 16 h at 4 °C in a wet chamber, followed by washing and secondary antibody (table 6) staining for 1 h at room temperature in a wet chamber. After washing three times, the slides were dried, embedded in Fluoromount G (SouthernBiotech) and covered with a coverslip. The tissue sections were visualized and analyzed using a confocal fluorescence microscope (Zeiss LSM780) and the ZEN Black 8.1 software (Zeiss) and processed via the ImageJ 1.51h software.

When using the αCD90.1 antibody, the previously described method did not result in any staining, therefore we used the following protocol. The cryosections were fixed with acetone for 7 min at room temperature, followed by treatment with the Biotin/Avidin Blocking Kit. Primary antibodies were diluted in PBS with 2% FCS and incubated for 1 h at room temperature in a wet chamber. After washing, the secondary antibodies were stained for 30 min at room temperature in a wet chamber. The covering, acquiring, and processing was continued as described above.

2.6.3 Cytokine detection via ELISA

Culture supernatants of MOG_{35-55} peptide re-stimulated spleen cells were analyzed for their cytokine levels using commercially available IL-10 and IL-17 ELISA kits (BioLegend) according to the manufacturer's instructions. All washing steps were performed with an automated 96-plate washer (Tecan Group) using ELISA wash buffer or TBST wash buffer. First, 96 well Costar plates (Corning Life Sciences) were coated with capture antibodies overnight using the respective coating buffer based on the manufacturer's instructions. 50 µl of the samples and standard dilutions were added to the wells in duplicates and incubated for 2 h at room temperature. The captured cytokines were detected by incubation with 100 µl biotinylated detection antibody for 1 h at room temperature, followed by incubation with avidin-horseradish peroxidase solution. After washing, 100 µl TMB substrate was added and incubated for 10 min at room temperature in the dark. Finally, 100 µl of stop solution were added and the absorbance was measured at 450 nm with a Vmax kinetic microplate reader (Molecular Devices) and analyzed using the SOFTmax PRO 3.0 Software (Molecular Devices)

2.6.4 Statistical analyses

Data are presented as means plus standard deviation. Differences between groups were compared using unpaired Student's t test or 2-way ANOVA. P values <0.05 were considered statistically significant.

3 Results

3.1 Expression and function of VLA-1 on MDSCs

3.1.1 Identification of mouse BM-MDSC subsets via flow cytometry

In this study, we used *in vitro* generated MDSCs for the identification of new surface markers. MDSCs with T cell suppressive capacities were generated by culturing bone marrow cells in the presence of GM-CSF for 3-4 days (Rössner et al 2005). Using flow cytometry, $CD11b^{+}$ $Ly\text{-}6C^{hi}$ $Ly\text{-}6G^{-}$ monocytes or M-MDSCs and $CD11b^{+}$ $Ly\text{-}6C^{low}$ $Ly\text{-}6G^{+}$ granulocytes or G-MDSCs can be defined (Figure 9A). This marker combination was not specific for MDSCs since monocytes and granulocytes expressed the same markers. Culture with GM-CSF resulted

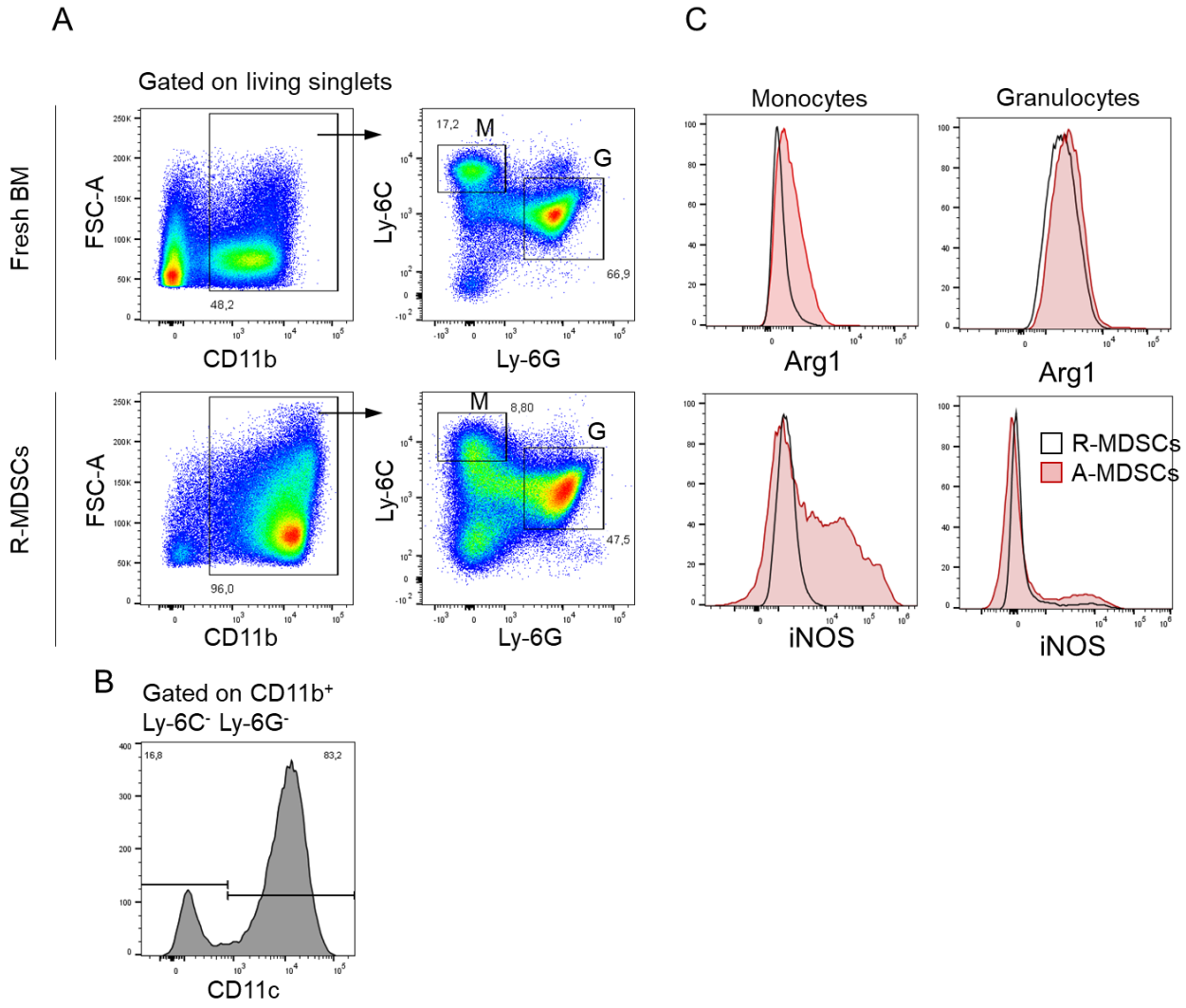

Figure 9: Identification of murine MDSC subsets by flow cytometry. BM-MDSCs were generated by culturing mouse bone marrow cells in the presence of GM-CSF for 3 days and analyzed by flow cytometry using the following gating strategy. **(A)** $CD11b^{+}$ $Ly\text{-}6C^{hi}$ $Ly\text{-}6G^{-}$ M-MDSCs and $CD11b^{+}$ $Ly\text{-}6C^{low}$ $Ly\text{-}6G^{+}$ G-MDSCs in the cultures expressed the same surface markers as monocytes and granulocytes, respectively, in fresh bone marrow. **(B)** $CD11c^{+}$ dendritic cells and macrophages accumulated in the culture as well. **(C)** Effector markers iNOS and Arg1 were upregulated by M-MDSCs after activation with LPS + IFN-γ for 16 h, but not by G-MDSCs.

in a nearly pure population of $CD11b^+$ cells. Apart from the generated M-MDSCs and G-MDSCs, the culture contained $CD11b^+$ $CD11c^+$ Ly-$6C^-$ Ly-$6G^-$ mo-DCs and macrophages (Figure 9B), as well as dendritic cell precursors (Lutz et al 1999) and $CXCR4^+$ neutrophil precursors (Capucetti et al 2020), which are not suppressive (unpublished data). Upon activating the R-MDSCs with LPS and IFN-γ, M-MDSCs expressed Arg1 and iNOS (Figure 1C), whereas G-MDSCs did not exhibit an increased iNOS and Arg1 expression when comparing A-MDSCs with R-MDSCs (Figure 9C). Using the described markers is the standard method of MDSC identification (Lutz & Eckert 2021).

3.1.2 VLA-1 expression on MDSCs and T cells

Due to the lack of surface markers for MDSC identification, we sought for new markers which could be used in addition to CD11b, Ly-6C and Ly-6G and would allow a better discrimination of MDSCs from non-suppressive cells. We found VLA-1 to be expressed by $CD11b^+$ Ly-$6C^{hi}$ Ly-$6G^-$ M-MDSCs but not by $CD11b^+$ Ly-$6C^{low}$ Ly-$6G^+$ G-MDSCs (Figure 10A). VLA-1 was already expressed by monocytes in the bone marrow, however GM-CSF culture led to an

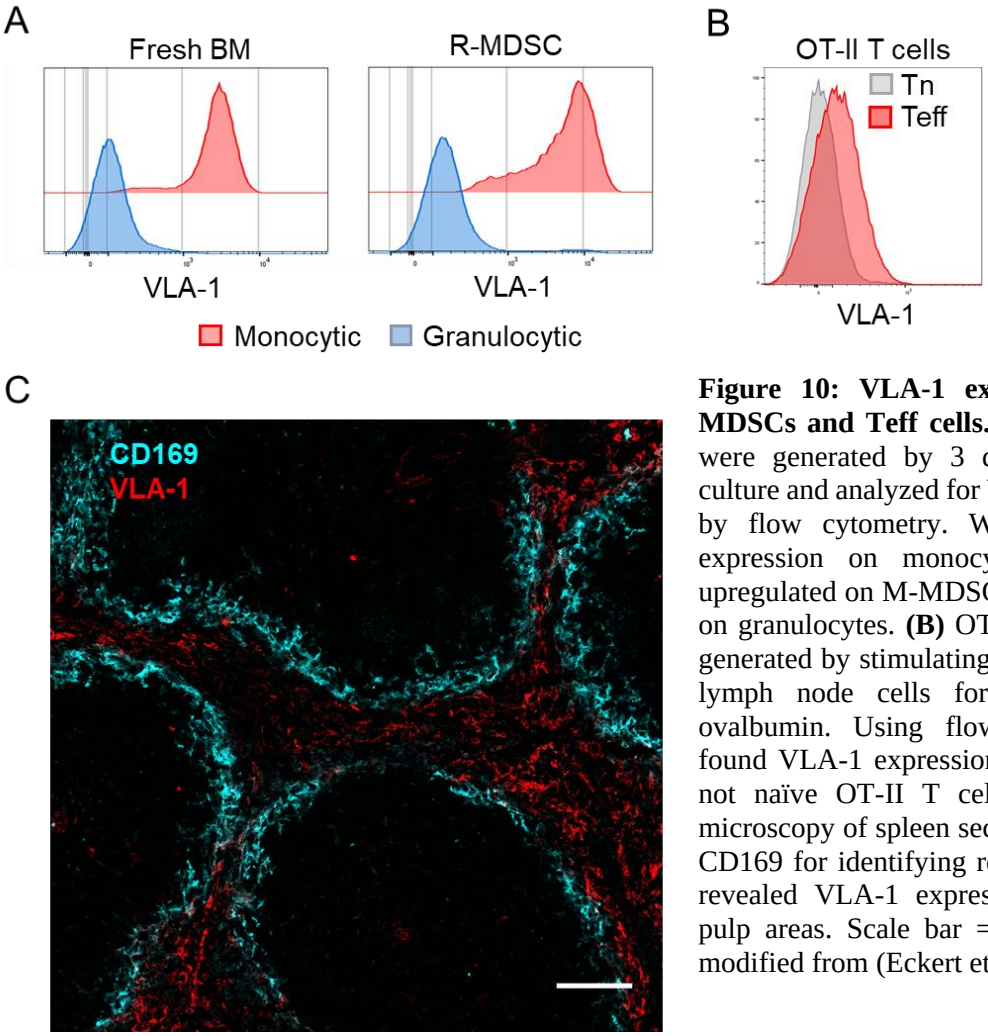

Figure 10: VLA-1 expression by M-MDSCs and Teff cells. (A) BM-MDSCs were generated by 3 days of GM-CSF culture and analyzed for VLA-1 expression by flow cytometry. We found VLA-1 expression on monocytes, which was upregulated on M-MDSCs, but not present on granulocytes. **(B)** OT-II T_{eff} cells were generated by stimulating OT-II spleen and lymph node cells for 6-7 days with ovalbumin. Using flow cytometry, we found VLA-1 expression on T_{eff} cells but not naïve OT-II T cells. **(C)** Confocal microscopy of spleen sections stained with CD169 for identifying red and white pulp revealed VLA-1 expression only in red pulp areas. Scale bar = 100 µm. Figure modified from (Eckert et al 2021b)

upregulation of VLA-1 expression (Figure 10A). Besides the expression on M-MDSCs, VLA-1 was expressed by T_{eff} cells but not naïve T cells (Ray et al 2004), which we validated by generating OT-II T_{eff} cells and analyzing the VLA-1 expression by flow cytometry (Figure 10B). Confocal microscopy of spleen sections revealed that VLA-1$^+$ cells were almost exclusively present in the red pulp areas (Figure 10C), where monocytes and effector or memory T cells are located, but not in the white pulp, where naïve T cells search for antigens (Bajénoff et al 2010, Bronte & Pittet 2013, Jung et al 2010, Unsoeld et al 2004). The borders between red and white pulp were visualized using the αCD169 antibody, which stains the marginal zone macrophages. Expression of the same homing receptor by both cell types indicates that MDSCs and T_{eff} cells might home to the same organ.

3.1.3 VLA-1 expression has no impact on MDSC subset distribution and iNOS expression

After identifying the expression of VLA-1 on M-MDSCs, we analyzed cell populations derived from *Itga1*$^{-/-}$ mice, which lack the alpha chain of the VLA-1 (CD49a) integrin. When examining the distribution of monocytic and granulocytic subsets of WT and *Itga1*$^{-/-}$ BM-MDSCs by flow cytometry, we observed no difference when MDSCs lacked VLA-1 (Figure 11A). Likewise, we found no difference in iNOS expression of WT and *Itga1*$^{-/-}$ MDSCs upon LPS + IFN-γ activation (Figure 11B). However, we observed that the iNOS expressing cells were positive for VLA-1 (Figure 11C), indicating that VLA-1 may be a marker to identify the iNOS$^+$ M-MDSCs. Activation of the M-MDSCs with LPS and IFN-γ did not result in a further upregulation of VLA-1 expression (Figure 11D).

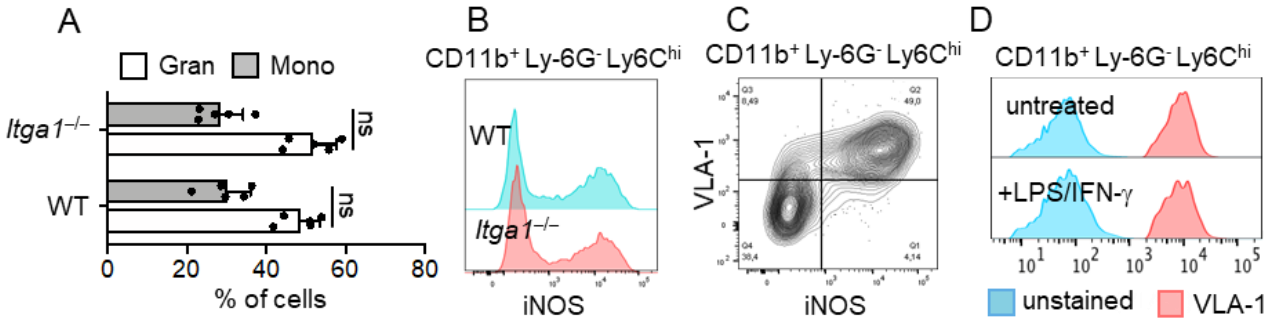

Figure 11: Examining VLA-1-expressing cells by flow cytometry. (A) BM-MDSCs generated from WT and Itga1$^{-/-}$ mice exhibited similar frequencies of monocytic and granulocytic subsets. Pooled data of n=5 independent experiments. **(B)** BM-MDSCs were stimulated with LPS and IFN-γ for 16 h and analyzed by flow cytometry. CD11b$^+$ Ly-6C^{hi} M-MDSCs expressed similar levels of iNOS independent of VLA-1 deficiency. Representative of n=3 independent experiments. **(C)** Setup as in (B). iNOS expressing M-MDSCs were positive for VLA-1 staining. **(D)** Setup es in (B). VLA-1 is not upregulated upon stimulation with LPS and IFN-γ. Statistics by student's unpaired t-test. ns=non-significant. Figure modified from (Eckert et al 2021b)

3.1.4 T cell suppression of VLA-1 deficient MDSCs is not reduced *in vitro*

We hypothesized, that T_{eff} cells are more prone to MDSC-mediated suppression. In order to test this, we performed a T cell suppressor assay comparing naïve and T_{eff} cells. We titrated different numbers of MDSCs to 200,000 T cells, stimulated with αCD8 and αCD28 antibodies, and analyzed the proliferation by flow cytometry using Ki-67. As expected, we found that less MDSCs were required to suppress T_{eff} cells compared to naïve T cells (Figure 12A). Next, we compared the suppressive capacity of WT and *Itga1*$^{-/-}$ R-MDSCs and A-MDSCs towards naïve or effector T cells. We did not observe a difference in naïve and effector T cell suppression between WT and *Itga1*$^{-/-}$ MDSCs, whereas activation of the MDSCs resulted in a significantly enhanced suppression (Figure 12B). These data indicate VLA-1 has no impact on T cell suppression in the artificial *in vitro* setting.

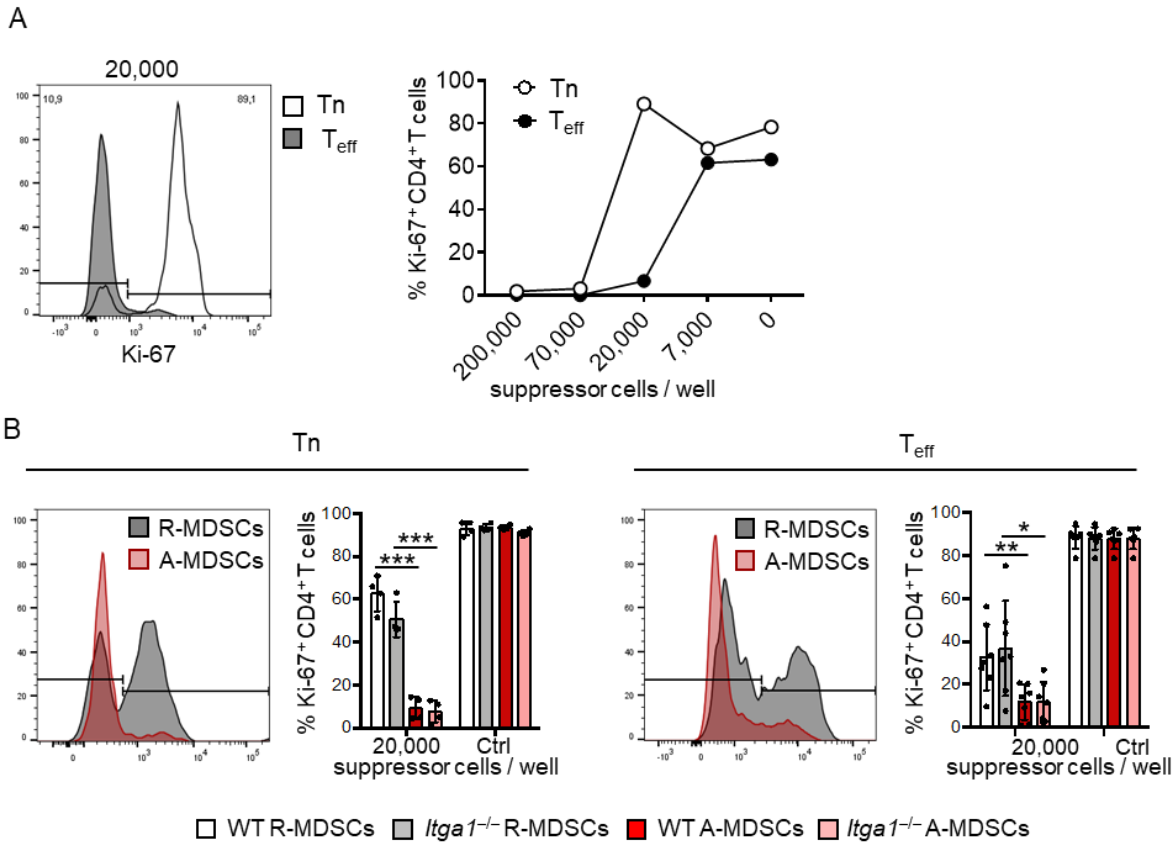

Figure 12: T cell suppression by WT and Itga1$^{-/-}$ R-MDSCs and A-MDSCs. (A) 200,000 naïve and effector T cells were cultured with different numbers of BM-MDSCs in the presence of αCD8 and αCD28 antibodies. Proliferation was measured by Ki-67 antibody staining of CD4^{+} living cells after 3 days of co-culture. T_{eff} cell suppression required less MDSC numbers compared to naïve T cells. Representative of n=3 experiments. **(B)** 20,000 naïve or effector T cells were cultured with 20,000 MDSCs, stimulated, and analyzed by flow cytometry after 3 days. For activating MDSCs, LPS and IFN-γ were added to the cultures. VLA-1 deficiency had no impact in T cell suppression, whereas MDSC activation increased the suppression. Pooled data of n=4 (Tn) or n=7 (T_{eff}) experiments. Statistics by student's unpaired t-test. *p<0.05, **p<0.01, ***p<0.005. Figure modified from (Eckert et al 2021b)

3.1.5 VLA-1 has no impact on homing of MDSCs to the spleen

For examining the effect of VLA-1 on the homing efficiency of MDSCs, we injected *in vitro* generated WT and *Itga1*$^{-/-}$ R-MDSCs and A-MDSCs intravenously into syngeneic mice. The MDSCs were labeled with CFSE, eFluor 670 or CellTrace violet to allow their detection via flow cytometry. The CD11b^{+} live cell labeling dye^{+} injected MDSCs were further discriminated into monocytic and granulocytic subsets based on their Ly-6C and Ly-6G expression (Figure 13A). We found that R-MDSCs appeared mainly in spleens and lungs upon injection, but hardly in the bone marrow and lymph nodes (Figure 13B). Monocytic and granulocytic subsets occurred at similar frequencies in the spleen (Figure 13C). However, we did not observe a significant difference in cell recovery between WT and *Itga1*$^{-/-}$ R-MDSC (Figure 13B+C). MDSCs lacking VLA-1 exhibited a slightly reduced recovery to the lung compared to WT MDSCs. VLA-1 expression of injected WT MDSCs is significantly increased in M-MDSCs compared to the background staining observed in *Itga1*$^{-/-}$ MDSCs in the spleens and lungs but not in G-MDSCs and bone marrow (Figure 13D), indicating that VLA-1^{+} M-MDSCs are present in the spleens and lungs but not in the bone marrow. Next, we injected A-MDSCs and harvested the spleens after 6 h and 24 h. Consistently, A-MDSCs exhibited no altered recovery in the absence of VLA-1. The majority of MDSCs disappeared already 4 h after injection, particularly the monocytic subset (Figure 13E+F). These data indicate that VLA-1 is not implicated in homing of MDSCs to the spleen.

3.1.6 MDSC-mediated T cell suppression in part depends on VLA-1

Next, we sought to assess the functional relevance of VLA-1 on T cell suppression. The spleen is a major organ where T cell suppression by MDSCs takes place (Bronte & Pittet 2013, Ugel et al 2012b), therefore we focused on this organ. Monocytes were shown to reside in the collagen-rich subcapsular red pulp of the spleen (Swirski et al 2009a). Also effector T cells but not naïve T cells localize in the splenic red pulp (Unsoeld et al 2004). In order to investigate the location of the *in vitro* generated cells in the spleen, we injected BM-MDSCs and T_{eff} cells intravenously and analyzed the spleens using confocal microscopy. The red pulp area was discriminated by CD169 staining. As expected, we found CD11b^{+} WT and *Itga1*$^{-/-}$ MDSCs exclusively in the red pulp of spleens 6 h and 24 h after MDSC injection, independent of their activation status (Figure 14A+B). Also the *in vitro* generated OT-II T_{eff} cells occurred in the splenic red pulp (Figure 14B), indicating that interaction of MDSCs and T_{eff} cells may take place at this site.

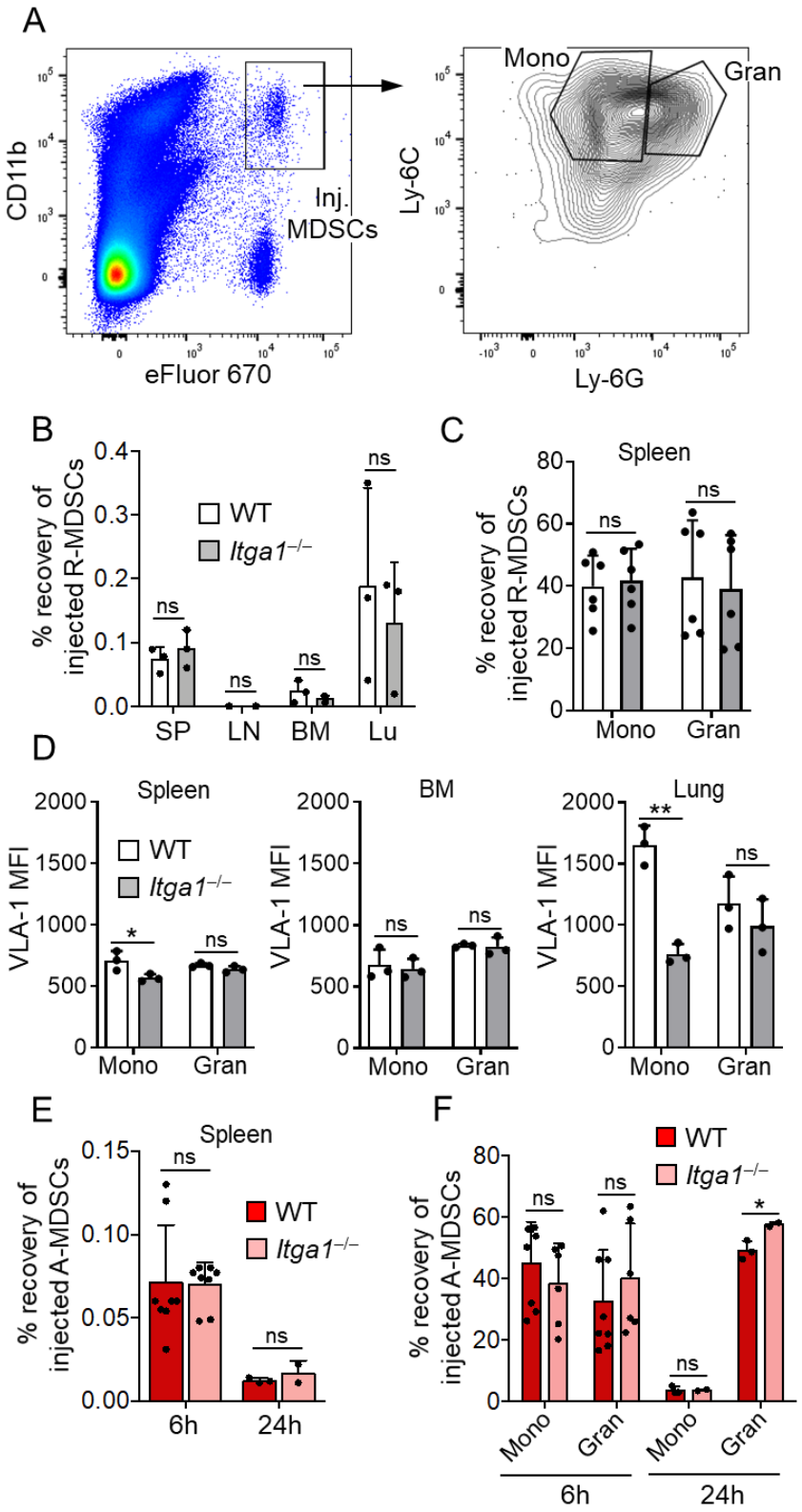

Figure 13: Homing of MDSCs to the spleen is independent of VLA-1. (A) R-MDSCs were generated from WT and *Itga1*$^{-/-}$ mice, labeled, and injected intravenously into syngeneic mice. The injected cells were identified by CD11b and live dye, and further divided into monocytic and granulocytic MDSCs by Ly-6C and Ly-6G staining. **(B)** Injected R-MDSCs in spleen, lymph nodes, bone marrow, and lungs were analyzed by flow cytometry and quantified (n=3). **(C)** Recovery of R-MDSC subsets to the spleen was quantified (n=6). **(D)** VLA-1 expression of monocytic and granulocytic subsets of injected WT and *Itga1*$^{-/-}$ R-MDSCs was examined in spleen, bone marrow and lung by flow cytometry. **(E)** MDSCs were activated with LPS + IFN-γ for 4h and injected intravenously. Recovery to the spleen was checked after 6 h and 24 h (n=2-6). **(F)** A-MDSC subsets were quantified in the spleens 6 h and 24 h after injection. Statistics by student's unpaired t-test. ns=non-significant, *p<0.05, **p<0.01. Figure modified from (Eckert et al 2021b)

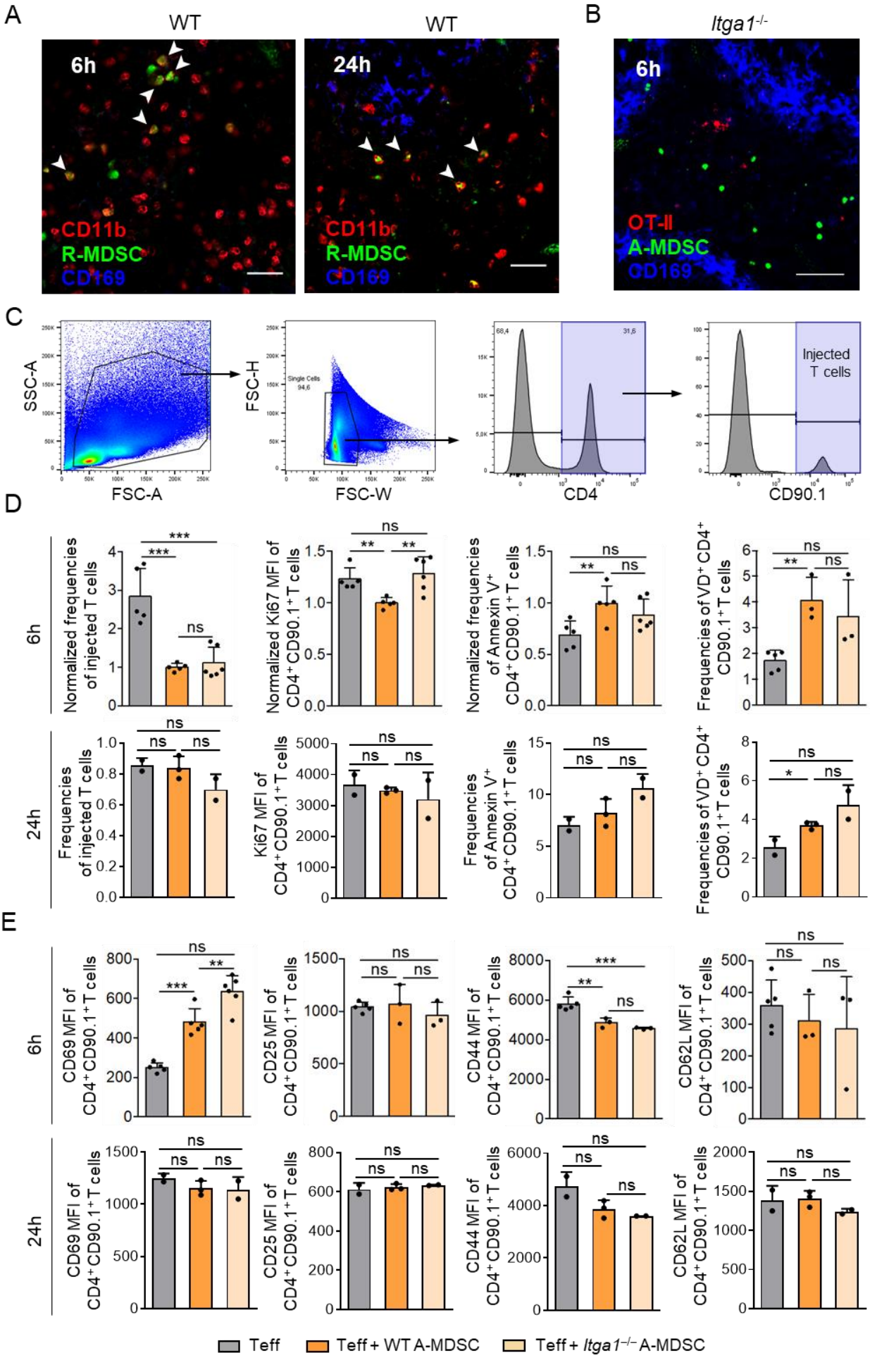
A
WT
WT
6h
24h
CD11b
R-MDSC
CD169
B
Itga1-/-
6h
OT-II
A-MDSC
CD169
C
SSC-A
FSC-A
FSC-H
FSC-W
Single Cells
94,6
68,4
31,6
CD4
CD90.1
Injected
T cells
D
6h
24h
Normalized frequencies of injected T cells
Normalized Ki67 MFI of CD4+CD90.1+T cells
Normalized frequencies of Annexin V+ CD4+CD90.1+T cells
Frequencies of VD+CD4+ CD90.1+T cells
Frequencies of injected T cells
Ki67 MFI of CD4+CD90.1+T cells
Frequencies of Annexin V+ CD4+CD90.1+T cells
Frequencies of VD+CD4+ CD90.1+T cells
E
CD69 MFI of CD4+CD90.1+T cells
CD25 MFI of CD4+CD90.1+T cells
CD44 MFI of CD4+CD90.1+T cells
CD62L MFI of CD4+CD90.1+T cells
Teff
Teff + WT A-MDSC
Teff + Itga1−/− A-MDSC

Figure 14: T cell suppression by MDSCs is partially dependent on VLA-1. (A) R-MDSCs were labeled with CFSE and injected intravenously into syngeneic recipients. Spleens were collected after 6 h and 24 h and stained for confocal microscopy with αCD11b and αCD169 antibodies, the latter marking the borders of the red pulp. $CD11b^+$ $CFSE^+$ injected MDSCs were detected exclusively in the red pulp. Scale bar = 30 µm. Representative of sections from n=3 mice. **(B)** *Itga1*$^{-/-}$ BM-MDSCs were activated with LPS+IFN-γ for 4 h, labeled with CFSE, co-injected with *in vitro* generated OT-II $CD90.1^+$ T_{eff} cells at a 1:1 ratio intravenously into syngeneic mice, and spleens were analyzed by confocal microscopy. Injected T_{eff} cells were identified with αCD90.1 antibody staining, and the red pulp was discriminated by CD169 staining. A-MDSCs and T_{eff} cells appeared in the red pulp. Scale bar = 50 µm. Representative of sections from n=3 mice. **(C)** Experimental setup as in (B). WT or *Itga1*$^{-/-}$ A-MDSCs were co-injected with T_{eff} cells and the spleens ware analyzed using flow cytometry after 6 h and 24 h. $CD4^+$ $CD90.1^+$ single cells were studied further. n=2-6 mice. **(D)** Experimental setup as in (C). Frequency as well as Ki-67, Annexin V and viability dye staining was performed to assess T_{eff} cell suppression. **(E)** Experimental setup as in (C). Injected T_{eff} cells were stained for CD69, CD25, CD44, and CD62L as markers for activated or effector T cells. Statistics by student's unpaired t-test. ns=non-significant, *p<0.05, **p<0.01, ***p<0.005. Figure from (Eckert et al 2021b)

In order to investigate the impact of VLA-1 expression on MDSC-mediated T cell suppression, we co-injected WT or *Itga1*$^{-/-}$ MDSCs and OT-II CD90.1 T_{eff} cells. OT-II T cells are $CD4^+$ and express a transgenic T cell receptor specific for ovalbumin (Derkow et al 2007), and the CD90.1 congenic marker enables the tracking of injected T cells in the $CD90.2^+$ B6 mice (Hickey et al 2002). 6 h and 24 h after the injection, we analyzed the spleens via flow cytometry. After excluding the doublets, we analyzed the CD90.1 congenic injected OT-II Teff within the $CD4^+$ T cell population (Figure 14C). We found a significantly reduced T_{eff} cell recovery to the spleen when WT A-MDSCs were co-injected compared to the control, as well as reduced proliferation measured by Ki-67, increased apoptosis indicated by Annexin V staining, and increased cell death shown by viability dye staining 6 h after injection (Figure 14D). When co-injecting *Itga1*$^{-/-}$ A-MDSCs, the T_{eff} cell proliferation was restored to similar levels of control T_{eff} cells. T cell apoptosis and viability dye staining were visibly but non-significantly reduced when *Itga1*$^{-/-}$ A-MDSCs were co-injected compared to WT A-MDSCs. 24 h after injection, the T cell recovery and proliferation remained unaltered upon WT and *Itga1*$^{-/-}$ A-MDSC injection. The frequency of apoptotic and dead cells was slightly increased when WT A-MDSCs were co-injected, and this effect was stronger when the MDSCs lacked VLA-1. The T cell activation marker CD69 was up-regulated 6 h after WT-MDSC co-injection, which was even enhanced when *Itga1*$^{-/-}$ A-MDSCs were co-injected (Figure 14E). This effect was lost 24 h after injection. CD25 and CD62L expression was not altered by MDSC co-injection. The effector marker CD44 was downregulated when MDSCs were co-injected, however we did not observe a difference between WT and *Itga1*$^{-/-}$ MDSC injection. Altogether, we found that co-injection of A-MDSCs with T_{eff} cells resulted in a strong T cell suppression indicated by reduced T cell frequency and proliferation, as well as increased apoptosis and cell death. This effect was

partially dependent on VLA-1 expression by MDSCs, indicating that VLA-1 is implicated in T cell suppression *in vivo*.

3.1.7 MDSC-mediated suppression of WT and Sema7A deficient T_{eff} cells is not significantly different

Since we found VLA-1 deficient BM-MDSCs to be less suppressive compared to WT MDSCs, we sought to investigate the suppressive mechanism. Sema7A is expressed by activated T cells and was found to negatively regulate T cell activation and function (Czopik et al 2006). Sema7A was shown to interact with VLA-1 (Suzuki et al 2007), therefore we performed a suppressor assay with Sema7A$^{-/-}$ OT-II transgenic T_{eff} cells. We titrated different amounts of BM-MDSCs to 200,000 WT or Sema7A deficient T_{eff} cells and analyzed the proliferation via flow cytometry using Ki-67 staining. We found that the proliferation of Sema7A$^{-/-}$ T_{eff} was slightly but non-significantly increased compared to WT T_{eff} cells at 70,000 suppressor cells per well (Figure 15). These data indicate that Sema7A expression on T_{eff} cells might have a small impact on M-MDSC-mediated suppression, however the difference between WT and Sema7A$^{-/-}$ was rather small and the standard deviation was high.

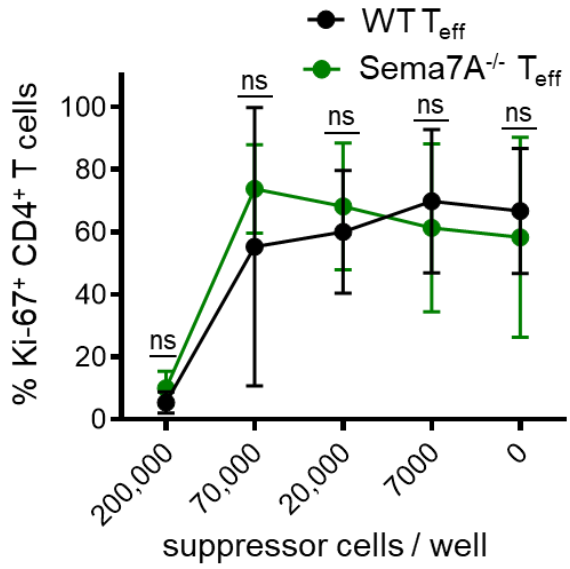

Figure 15: Sema7A$^{-/-}$ T_{eff} cell suppression is non-significantly less effective compared to WT T_{eff} cell suppression. WT OT-II and Sema7A$^{-/-}$ OT-II T_{eff} cells were generated by culturing spleen and lymph node cells for 6 days in the presence of OVA. Different numbers of R-MDSCs were titrated to 200,000 WT or Sema7A$^{-/-}$ T_{eff} cells and activated with αCD3 and αCD28 antibodies. T cell suppression was assessed by Ki-67 using flow cytometry. Statistics by student's unpaired t-test. ns=non-significant

3.1.8 VLA-1 is implicated in MDSC-T cell interaction on collagen IV *in vitro*

The following experiments were performed by Dr. Eliana Ribechini and are part of our common publication (Eckert et al 2021b). They are displayed here to complete the understanding of the VLA-1 functions on MDSCs as outlined in the publication. iNOS expression was not reduced in VLA-1 deficient BM-MDSCs and the suppressive capacity of *Itga1*$^{-/-}$ MDSCs was not impaired compared to WT MDSCs *in vitro*, whereas T_{eff} cell suppression by *Itga1*$^{-/-}$ MDSCs was reduced *in vivo*. To investigate the basis of this discrepancy, we analyzed MDSC motility

and T cell interaction on collagen IV, since VLA-1 is a high affinity receptor for this substrate. Therefore, we coated a µ-slide 8 well chamber with collagen IV or fibronectin as a control, added WT or *Itga1*$^{-/-}$ A-MDSCs and T_{eff} cells at a 1:2 ratio and analyzed the MDSC behavior by live cell imaging using a confocal microscope (Figure 16A). We did not find a difference between WT or *Itga1*$^{-/-}$ MDSC in track speed mean, track length, and track displacement length as indicators of MDSC migration on fibronectin and on collagen IV (Figure 16B). However, we observed that MDSC-T cell interaction time was reduced when MDSCs lacked VLA-1 on collagen IV, but not on fibronectin (Figure 16C). These data indicate that binding of VLA-1 to collagen IV is implicated in MDSC-T_{eff} cell interaction but not in MDSC migration.

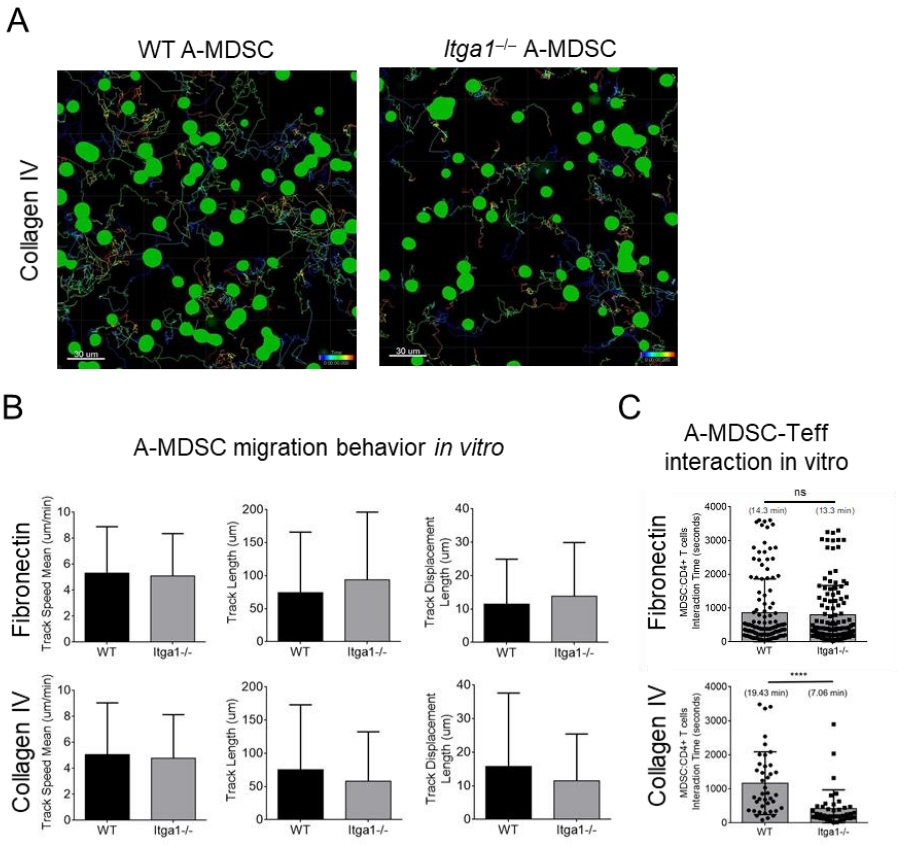

Figure 16: VLA-1 binding to collagen IV is required for MDSC-T cell interaction but not for MDSC migration. WT or *Itga1*$^{-/-}$ MDSCs were activated with LPS+IFN-γ, labeled with CFSE, and mixed with dsRed OT-II T_{eff} cells at a 1:2 ratio (MDSC:T_{eff}). The mixed cells were transferred into a µ-slide 8 well chamber coated with fibronectin or collagen IV and acquired using an inverted Confocal Laser Scanning Microscope recording consecutive pictures in 4 different quadrants per 15 s. **A.** Example of A-MDSC tracking. **B.** Quantification of MDSC migration parameters indicated by track speed mean, track length, and tack displacement length. **C.** Quantification of MDSC-T_{eff} cell interactions. Numbers between brackets indicate MDSC-T_{eff} cell interaction time. Statistics by unpaired student's t-test, ns=non-significant, **** $p<0.001$. Figure from (Eckert et al 2021b), data by Dr. Eliana Ribechini

3.1.9 VLA-1$^{-/-}$ MDSCs exhibit a deficit in interaction with T_{eff} cells in the splenic red pulp

The following experiments were performed by Dr. Eliana Ribechini and are part of our common publication (Eckert et al 2021b). They are displayed here to complete the understanding of the VLA-1 functions on MDSC as outlined in the publication. In order to confirm our data obtained from the previous *in vitro* experiment, we performed intravital 2-photon microscopy of spleens of mice co-injected with dsRed T_{eff} cells and CFSE-labeled A-MDSCs. Due to the high light absorbance of erythrocytes, which are present in the spleen at high numbers, we focused on the subcapsular sinus area of the red pulp with a range of 70–90 μm in the z-plane. We found co-localization of T_{eff} cells and A-MDSCs in the subcapsular red pulp (Figure 17A+B) and analyzed the migration behavior and interaction time. As expected, we found no difference between WT and *Itga1*$^{-/-}$ MDSC migration indicated by track speed mean, track length, track displacement length, track area mean, speed, and distance from the origin (Figure 17C). Similar to the data from the previous *in vitro* experiment, we observed a reduced interaction time when MDSCs were deficient of VLA-1 (Figure 17D). In conclusion, these data validate the findings showing that VLA-1 is dispensable for MDSC migration but playing a role in T cell suppression by facilitating MDSC-T cell interaction.

3.1.10 VLA-1 deficient MDSCs are less efficient in reducing EAE score compared to WT MDSCs

After discovering a role of VLA-1 in T cell suppression, we wanted to validate this finding using the disease model EAE. Injection of R-MDSCs is known to reduce the clinical score of EAE (Ribechini et al 2017), therefore we used this model for our studies. We injected WT, *Itga1*$^{-/-}$ MDSCs, or PBS into syngeneic mice 4 days before EAE induction (Figure 18A). We observed a significant reduction of the clinical score of mice receiving a WT MDSC injection compared to PBS or *Itga1*$^{-/-}$ MDSC-injected mice (Figure 18B). *Itga1*$^{-/-}$ MDSC injection reduced the clinical score slightly but non-significantly. MDSCs were shown to induce Treg development (Huang et al 2006b), therefore we analyzed Treg frequencies of the spleens via flow cytometry. We found that significantly lower Treg frequencies were present in *Itga1*$^{-/-}$ MDSC-injected mice compared to WT mice (Figure 18C). However, the Treg frequencies of PBS-injected mice were at similar levels compared to WT MDSC-injected mice. Next, we wanted to determine the cytokine levels of IL-10, which exerts immunosuppression and is produced by Tregs and MDSCs (Saraiva & O'Garra 2010), and IL-17, which is a critical effector cytokine during EAE (Minton 2020). ELISA of spleen cells restimulated with MOG peptide revealed significantly higher IL-10 production in WT MDSC-injected mice compared to PBS-

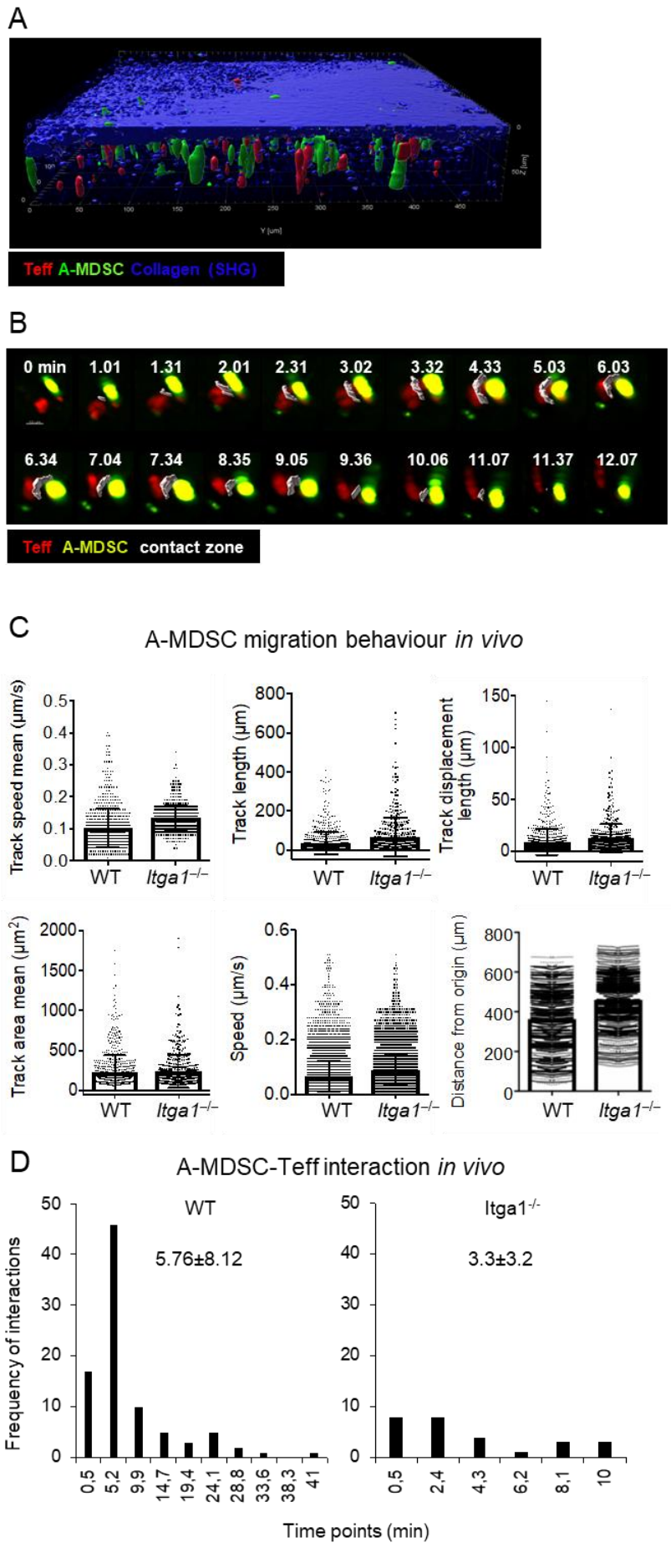

Figure 17: MDSC-T_{eff} cell interaction but not MDSC migration is dependent on VLA-1 expression. BM-MDSCs were activated for 4 h, labeled with CFSE and co-injected with OVA-stimulated T_{eff} cells at a 1:1 ratio (7×10^6 cells of each). After 1-4h, intravital 2-photon microscopy of the subcapsular area of the spleens was performed and analyzed using Imaris software. **(A)** T_{eff} and A-MDSCs co-localize in the collagen-rich (blue, SHG, second harmonic generation) subcapsular area. Representative of n=2 experiments. **(B)** Example of MDSC-T_{eff} cell interaction. Consecutive time points from emergence until termination of the interaction are shown. Contact zone is displayed as white surface. **(C)**. 749 tracks for WT MDSCs and 489 tracks for *Itga1*$^{-/-}$ MDSCs were analyzed for the indicated parameters for cell migration, revealing no deficit in MDSC migration in the absence of VLA-1. **(D)** MDSC-T_{eff} cell interaction was quantified. From the total amount of tracks, 12.14% of WT MDSC tracks resulted in T cell interaction with a medium duration of 5.76 min, whereas 5.52% of *Itga1*$^{-/-}$ MDSC tracks resulted in interaction with a mean value of 3.2 min. Figure from (Eckert et al 2021b), data by Dr. Eliana Ribechini

injected mice at 30 µg MOG. This effect was visibly but non-significantly reduced in *Itga1*$^{-/-}$ MDSC-injected mice. A similar pattern with reduced IL-10 concentrations was present at lower MOG concentrations and without MOG, indicating that this effect is only partially antigen

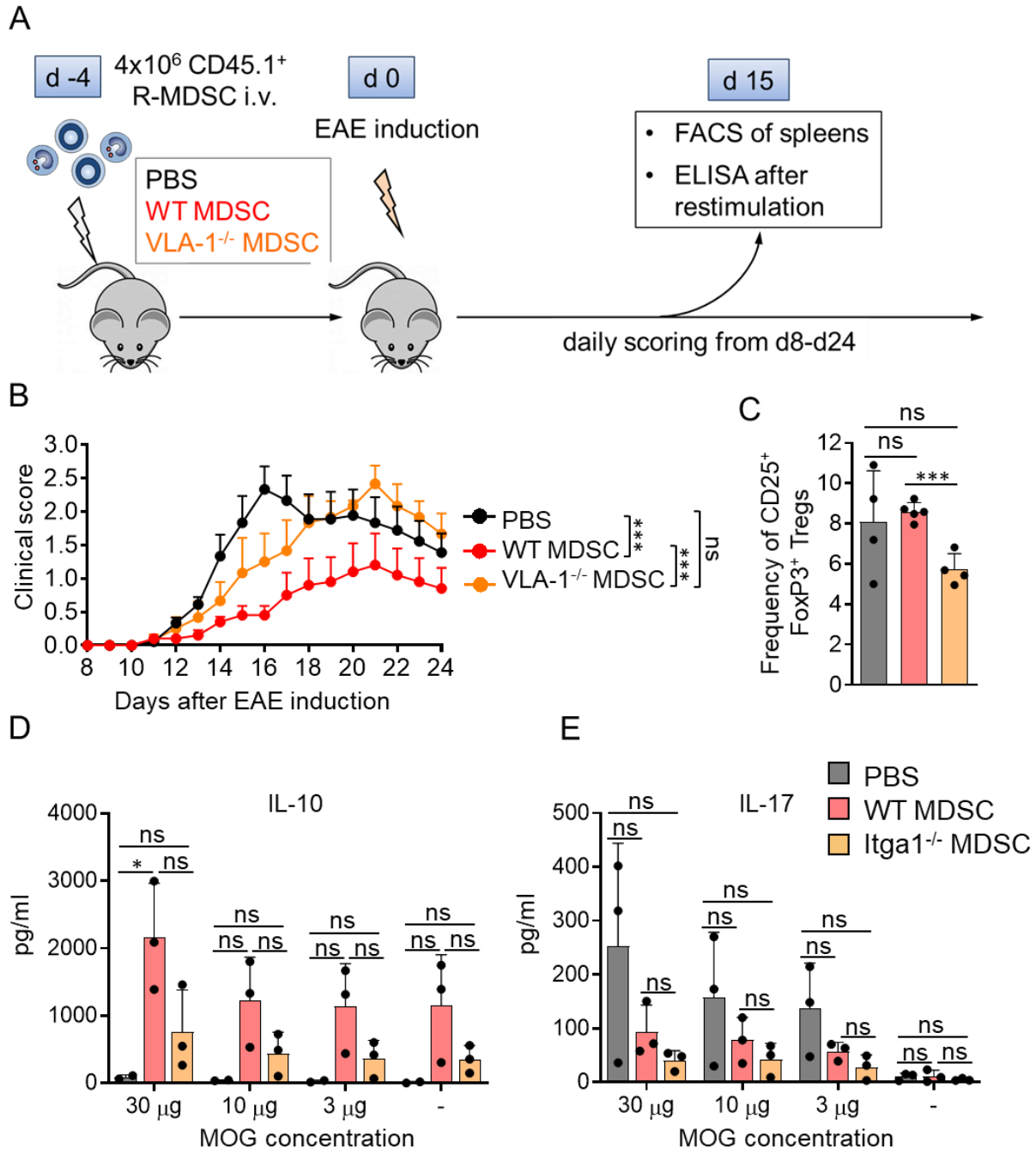

Figure 18: VLA-1 is implicated in immunosuppression of EAE. 4x10^6 R-MDSCs of WT or *Itga1*$^{-/-}$ mice or PBS were injected into syngeneic mice 4 days before EAE induction. Mice were scored from day 8-24. On day 15, spleens were analyzed for Treg frequencies and cytokines were measured by ELISA after restimulation. **(A)** Scheme of the experimental setup. **(B)** Clinical score of the mice showing amelioration of disease of WT MDSC-injected mice. Data from 2 independent experiments with WT (n=10), *Itga1*$^{-/-}$ (n=6), PBS (n=9) mice. Statics by two-way ANOVA with Geisser-Greenhouse correction, ***p<0.005. **(C)** Flow cytometry of FoxP3$^+$ CD25$^+$ Treg frequencies in the spleen. n=4, statistics by unpaired T test, ***p<0.001. **(D)** IL-10 ELISA of spleen cells restimulated with MOG peptide for 3 days. n=2-3, statistics by unpaired T test, ns=non-significant, *p<0.05. **(E)** IL-17 ELISA of restimulated splenocytes with MOG peptide for 3 days. n=3, statistics by unpaired T test

specific (Figure 18D). As expected, IL-17 production was highest in the PBS-injected mice and reduced upon MDSC injection. VLA-1 deficiency slightly further reduced the IL-17 production (Figure 18E). Altogether, we showed that VLA-1 is implicated in MDSC-mediated immunosuppression during EAE and might involve the presence of Tregs and IL-10 production.

3.1.11 G-MDSCs are partially responsible for the suppressive effect of MDSCs during EAE

Since we injected bulk BM-MDSCs in the previous EAE experiment, we wanted to assess which cells from the mixture in the culture are responsible for the reduction of the clinical score. Innate immune memory is called trained immunity and is in contrast to adaptive immunity not antigen specific (Netea et al 2019). Trained immunity is achieved by epigenetic remodeling upon infection of immune cells as well as encountering pathogen-associated molecular patterns and cytokines (Divangahi et al 2021). LPS tolerance was shown to be induced by epigenetic changes in macrophages, which was not propagated to daughter cells and therefore differs from

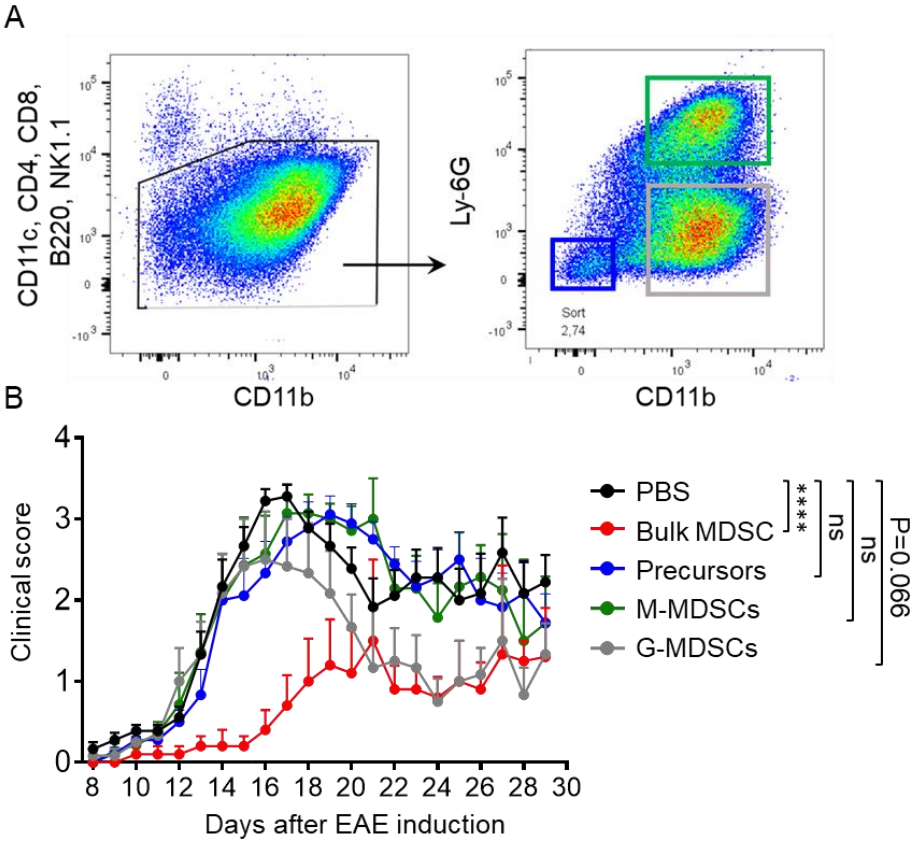

Figure 19: The reduction of clinical EAE score upon MDSC injection partially depends on G-MDSCs. $CD11b^+$ $Ly\text{-}6G^-$ M-MDSC, $CD11b^+$ $Ly\text{-}6G^+$ G-MDSCs, and $CD11b^-$ $Ly\text{-}6G^-$ precursors were sorted from BM-MDSCs by FACS and injected intravenously into mice 4 days before EAE induction. Bulk MDSC and PBS injections served as control. **(A)** Sorting strategy of G-MDSC, M-MDSC and precursor populations. **(B)** Clinical score was measured from day 8 until day 29. Data from 2 independent experiments with precursors (n=9), M-MDSCs (n=7), G-MDSCs (n=6), bulk MDSCs (n=5), and PBS (n=9) mice. Statics by two-way ANOVA with Geisser-Greenhouse correction, ns=non-significant, ****p<0.001.

trained immunity (Foster et al 2007). Because MDSCs were injected already 4 days before EAE induction and previous experiments showed injected MDSCs disappearing already after 24h (Figure 13), we wanted to investigate if the culture with GM-CSF leads to epigenetic changes of precursors which are prone to develop into MDSCs. Therefore, we FACS sorted CD11b$^-$ Ly-6G$^-$ cells which include macrophage dendritic cell precursors (Liu et al 2019) (Figure 19A). Furthermore, we sorted CD11b$^+$ Ly-6G$^-$ M-MDSC and CD11b$^+$ Ly-6G$^+$ G-MDSCs from BM-MDSC cultures of WT mice. We injected the sorted M-MDSCs, G-MDSCs and precursors as well as bulk MDSCs and PBS as controls 4 days prior to EAE induction and observed the disease score (Figure 19B). We found that bulk MDSC injection was significantly more efficient in EAE suppression than the injection of the sorted populations. M-MDSC and precursor injection did not exhibit any immunosuppressive effect on the EAE score and were in a similar range to the score of PBS-injected mice. G-MDSC injection had no effect on the EAE curve during the early phase of disease, however around day 16, the score decreased and reached similar levels to the bulk MDSC-injected mice. Taken together, we found that G-MDSCs are partially responsible for the reduction of the EAE score, but not M-MDSCs or CD11b$^-$ Ly-6G$^-$ precursors.

3.1.12 MDSC identification using a new marker strategy by flow cytometry

We recently published a strategy of MDSC identification using more markers than the common combination of CD11b, Ly-6C and Ly-6G (Eckert et al 2021a). After excluding cell debris and doublets, we first detected CD11b$^+$ Ly-6G$^+$ granulocytes and further analyzed CD11b$^+$ Ly-6G$^-$ cells which include the monocytic populations (Figure 20A). We examined the Ly-6C expression in combination with the expression of CD11c, MHC-II, and CD69 markers of untreated, LPS-activated, and LPS + IFN-γ-activated MDSCs (Figure 20B). M-MDSCs were Ly-6C^{hi}, CD69$^+$, CD11c$^{low/-}$ and MHC II$^{low/-}$. CD11c, MHC II and CD69 were highly expressed by dendritic cells and macrophages, which lack Ly-6C expression, resulting in a waterfall-shaped distribution of CD69$^+$ Ly-6C$^+$ CD11c$^-$ monocytes differentiating into CD69$^+$ Ly-6C$^-$ CD11c$^+$ mo-DCs and macrophages. While CD11c and MHC II were already expressed by untreated GM-CSF-cultured cells, CD69 expression was only induced after activation with LPS or LPS + IFN-γ. For distinguishing MDSCs from non-suppressive cells, the staining of effector molecules like iNOS and Arg1 is required. iNOS was expressed only after MDSC activation with LPS + IFN-γ by the monocytic but hardly by the granulocytic subset (Figure 20C). Arg1 was exclusively expressed by a portion of iNOS$^+$ cells, and correspondingly, Arg1 was only expressed by monocytic but not granulocytic A-MDSCs as well (Figure 20D). When analyzing the iNOS expression in all CD11b$^+$ Ly-6G$^-$ populations unstimulated and stimulated with LPS

or LPS + IFN-γ, we found as expected no iNOS expressed by the unstimulated subsets (Figure 20E). The highest iNOS expression was present in Ly-6C^{+} CD11c^{+} cells, but low frequencies of iNOS producing cells were also present in Ly-6C^{+} CD11c^{-} and Ly-6C^{-} CD11c^{+} populations.

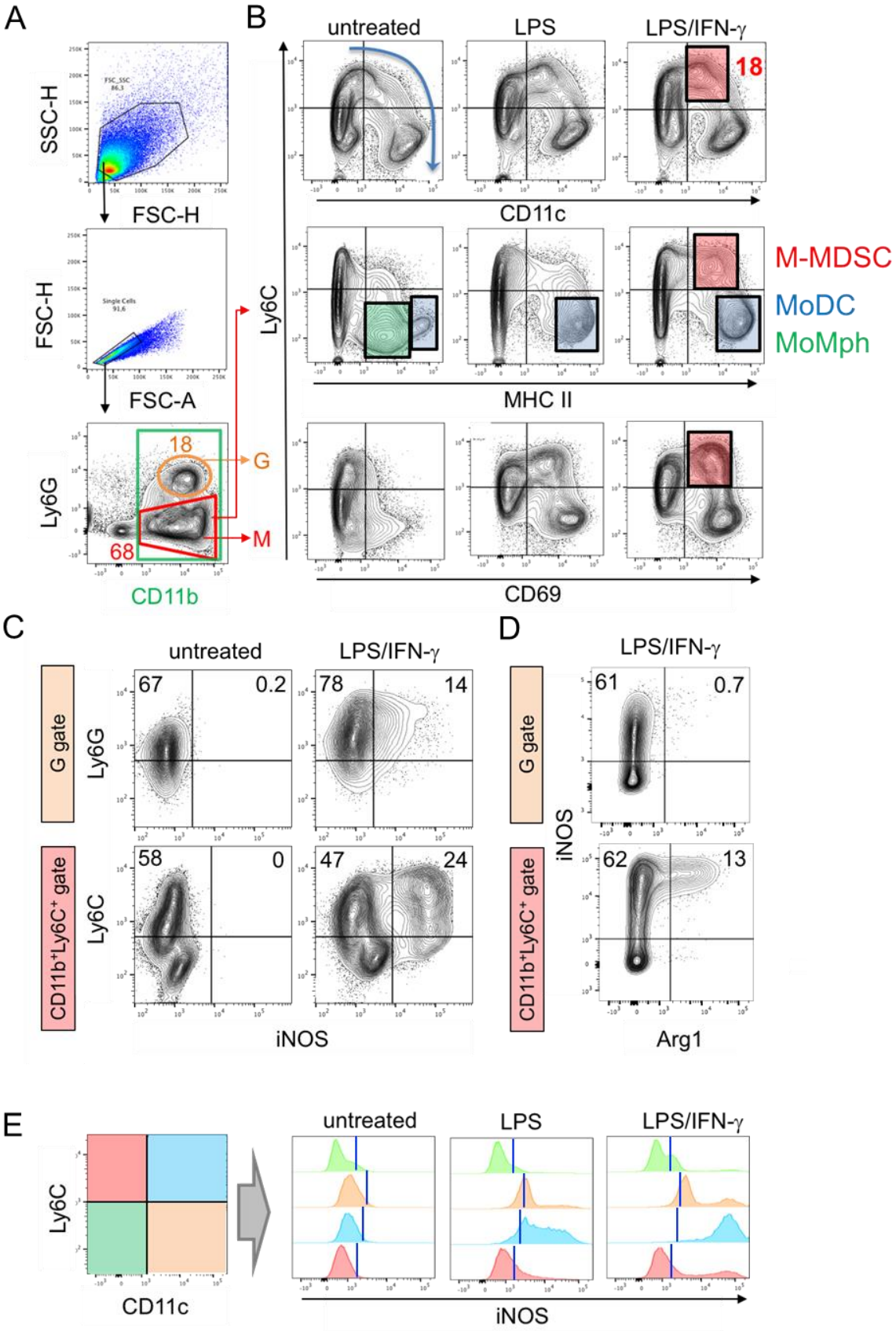

Figure 20: Analysis of BM-MDSCs using a new combination of markers by flow cytometry. BM-MDSCs were generated by 3 days of GM-CSF culture and activated with LPS or LPS + IFN-γ for 16 h. Antibody staining for flow cytometry was performed using the indicated markers. **(A)** After excluding debris and doublets, the $CD11b^+$ cells (green) were divided into granulocytes (orange) and monocytic cells (red). **(B)** Monocytic cells were further analyzed using Ly-6C, CD11c, MHC II, and CD69 staining. M-MDSCs expressed Ly-6C and low levels of CD11c, MHC II and CD69, the latter only after activation. Mo-DCs and macrophages lacked Ly-6C expression but expressed high levels of CD11c, MHC II and CD69. Ly-$6C^{hi}$ monocytes differentiating into dendritic cells or macrophages lose their Ly-6C expression and become MHC II^+ and $CD11c^+$, which results in a pattern resembling a waterfall (blue arrow). **(C)** iNOS was expressed by *in vitro*-generated M-MDSCs activated with LPS + IFN-γ, but not by G-MDSCs or R-MDSCs. **(D)** Arg1 was expressed by activated M-MDSCS but not G-MDSCs. All Arg1-expressing cells were $iNOS^+$. **(E)** iNOS-expressing cell populations of *in vitro*-generated resting, LPS-activated or LPS + IFN-γ-activated MDSCs were identified. MDSCs were pre-gated on $CD11b^+$ Ly-$6G^-$ cells and four quadrants of differentially Ly-6C and CD11c-expressing cells (color-coded) were analyzed. Highest iNOS expression was present in Ly-$C6^+$ $CD11c^+$ cells upon activation with LPS + IFN-γ. Figure from (Eckert et al 2021a)

Ly-$6C^-$ $CD11c^-$ cells did not exhibit any iNOS expression. LPS + IFN-γ stimulation resulted in a higher production of iNOS compared to stimulation with LPS alone. Using additional markers to the standard CD11b, Ly-6C and Ly-6G staining protocol like CD11c, MHC II or CD69 resulted in a better resolution myeloid of cell populations within the mixture of BM-MDSC culture.

3.1.13 Integration of VLA-1 into the identification strategy of M-MDSCs results in a better definition of myeloid populations

Since we identified VLA-1 as a novel marker, we sought to incorporate VLA-1 for staining M-MDSCs. Therefore, we performed flow cytometry staining of BM-MDSCs and either used $CD11b^+$ Ly-$6G^-$ cells (Figure 21A) or $CD11b^+$ VLA-1^+ cells (Figure 21B) for further analysis. Using the VLA-1 staining, the subsets identified with Ly-6C and CD11c staining displayed as cleaner populations and the contaminating Ly-$6C^{-/low}$ $CD11c^-$ population, which likely consists of neutrophil precursors (Capucetti et al 2020), was lacking. Using the VLA-1 strategy, iNOS and Arg1 expression were not only detected in Ly-$6C^+$ $CD11c^+$ cells, but also in the Ly-$6C^+$ $CD11c^-$ population (Figure 21C). We henceforth referred to these two distinct populations as transitory cells and monocytes, respectively, instead of terming them M-MDSCs, which was used for Ly-$6C^+$ $CD11c^+$ cells in the previous section. We used the term "transitory cells" since this population may be at a transitional stage of monocytes developing into macrophages or mo-DCs. Macrophage and DC populations did not express iNOS or Arg1. Taken together, these data show that including VLA-1 as an M-MDSC marker led to a cleaner separation of MDSC populations. MDSC effector molecules were expressed by monocytes as well as transitory cells.

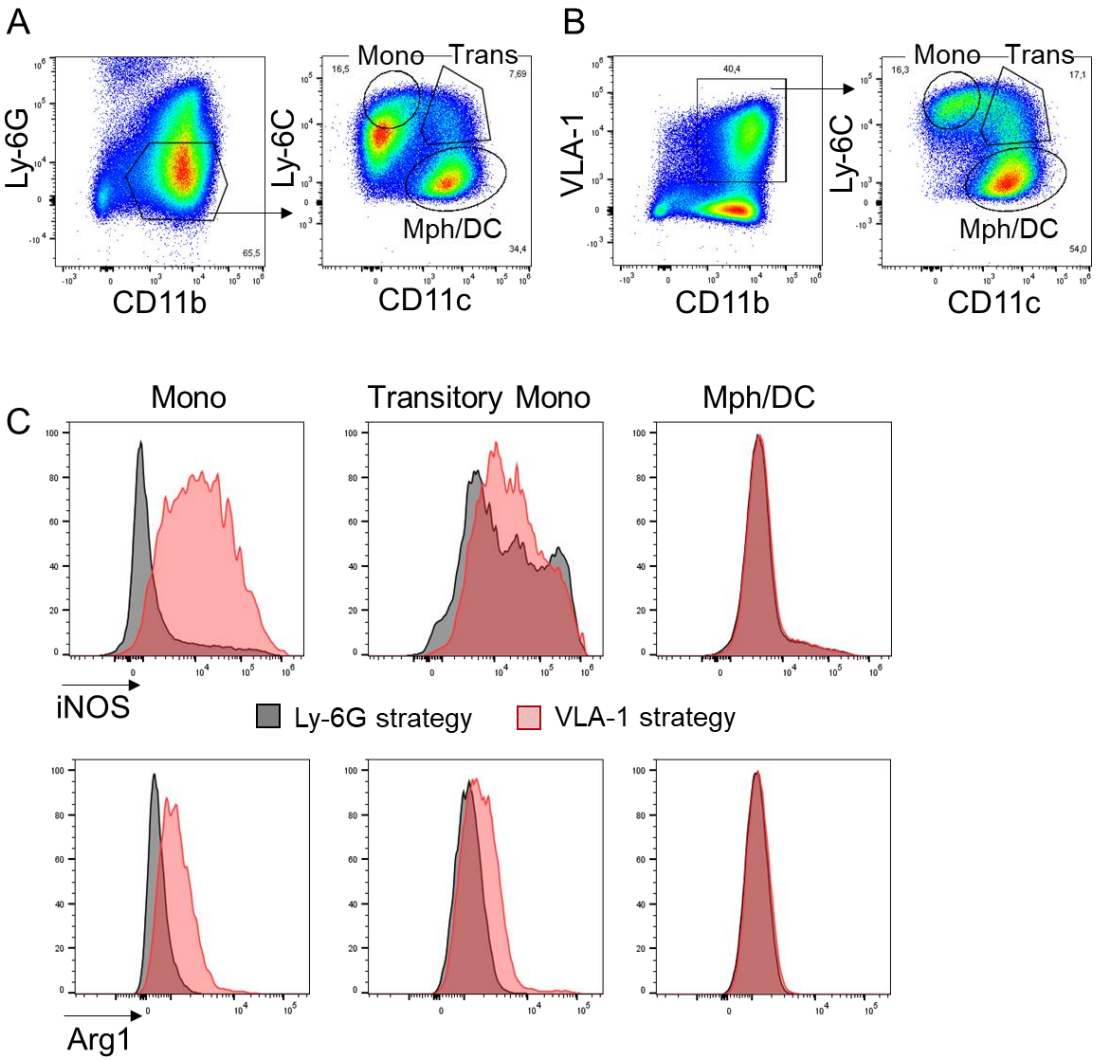

Figure 21: Using VLA-1 as an M-MDSC marker results in a clearer separation of monocytic populations. BM-MDSCs were generated by culturing bone marrow cells for 3 days with GM-CSF. Cells were analyzed by flow cytometry for the indicated markers. **(A)** Monocytic, transitory and macrophage / dendritic cell subsets after gating on $CD11b^+$ $Ly\text{-}6G^-$ cells. **(B)** Cell populations as in (A) after gating on $VLA\text{-}1^+$ $CD11b^+$ cells. **(C)** Using the strategy of staining $CD11b^+$ $VLA\text{-}1^+$ cells instead of $CD11b^+$ $Ly\text{-}6G^-$ cells prior to identifying monocyte, transitory and macrophage / dendritic cell populations resulted in higher frequencies of iNOS producing monocytes.

3.1.14 VLA-1 is not expressed by tumor-infiltrating MDSCs in murine breast cancer

Finally, we wanted to investigate if VLA-1 is not only a good marker for M-MDSCs *in vitro* but also for endogenous MDSCs of tumor-bearing mice. Therefore, we orthotopically injected 67NR breast cancer cells into female mice (Heppner et al 2000) and analyzed the monocytic infiltrates in the tumors via flow cytometry. In contrast to our *in vitro* data, VLA-1 was not expressed by any cells in the tumor (Figure 22A). Thus, we used the initial strategy excluding $Ly\text{-}6G^+$ cells instead of further analyzing $VLA\text{-}1^+$ cells (Figure 22B), which led to a contamination of $Ly\text{-}6C^-$ $CD11c^-$ cells probably consisting of eosinophils and neutrophil

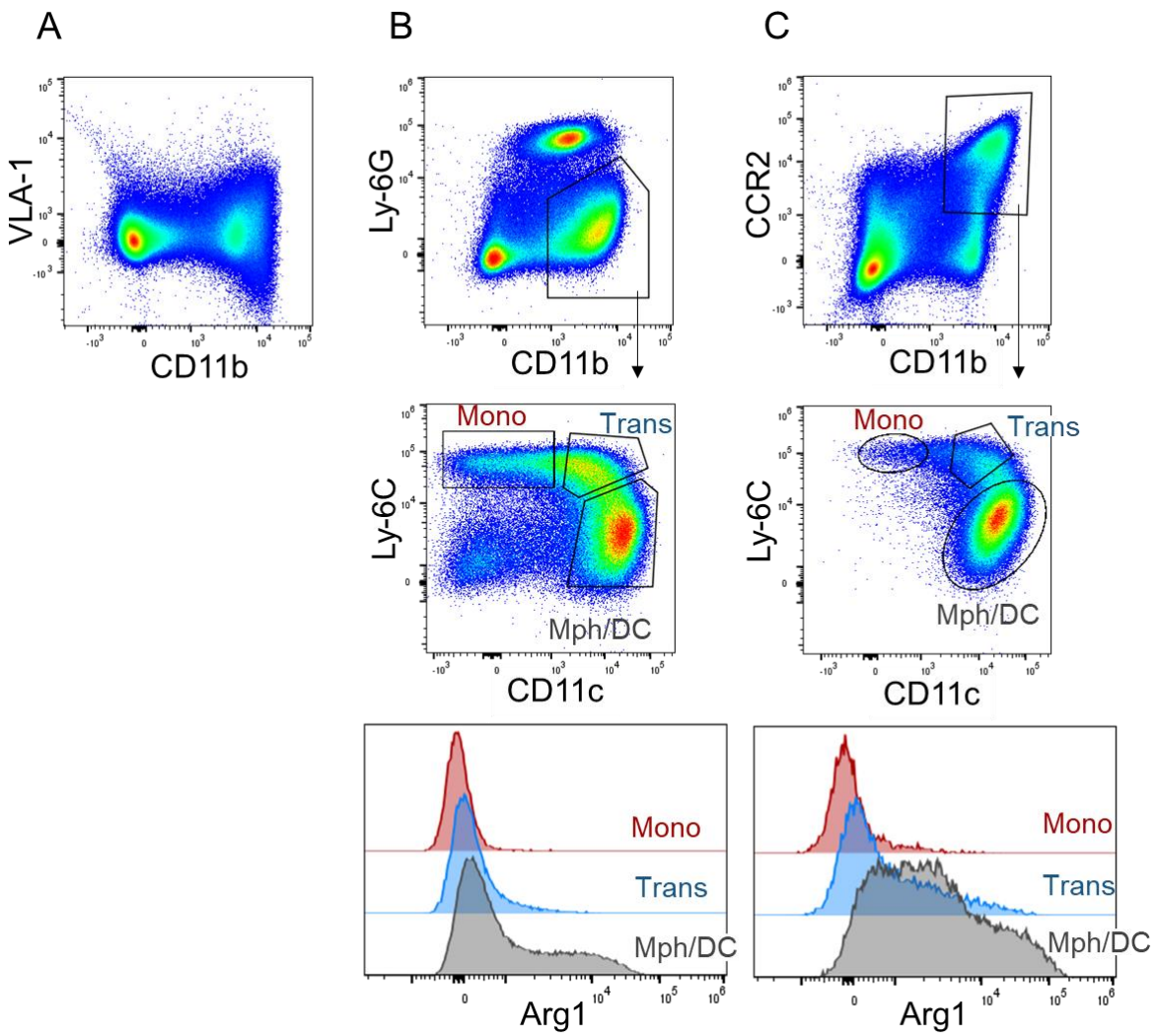

Figure 22: VLA-1 is not expressed by monocytic infiltrates in murine breast cancer but can be replaced with the marker CCR2. BALB/c WT mice were orthotopically injected with 67NR breast cancer cells into two mammary fat pats and tumors were examined by flow cytometry after 4 weeks. Living $CD45^+$ cells were analyzed (n=3). Example stainings are shown. **(A)** VLA-1 is not expressed by tumor-infiltrating cells. **(B)** Monocytes, transitory cells and Mph/DCs of Ly-$6G^-$ $CD11b^+$ cells were analyzed and Arg1 expression was examined. **(C)** Arg1 expression and subset distribution of monocyte, transitory cell, and Mph/DC subsets of $CCR2^+$ $CD11b^+$ cells were analyzed. Data was generated in collaboration with Dr. Angela Riedel and Greta Mattavelli.

precursors (Capucetti et al 2020, Hey et al 2016). Therefore, we replaced the VLA-1 marker with CCR2, which is expressed by monocytes and macrophages and is implicated in homing to inflamed tissues (Desalegn & Pabst 2019). Examining $CCR2^+$ $CD11b^+$ cells lead to an exclusion of the Ly-$6C^-$ $CD11c^-$ population (Figure 22C) and resulted in a higher frequency of Arg1 producing macrophages / DCs as well as transitory cells (Figure 22B+C). Summed up, we found that VLA-1 is not expressed by 67NR breast tumor-infiltrating cells but may be replaced with CCR2 in this setting.

3.2 Analysis of MDSCs in BCG-infected mice

3.2.1 Lung bacterial load corresponds with lung T cell proliferation and splenic monocyte numbers

M.tb as well as BCG infection was shown to induce the accumulation of MDSCs (Magcwebeba et al 2019). Therefore, we used a mouse model of intranasal BCG infection for studying MDSC marker expression and finding new surface markers. For analyzing the acute phase of BCG

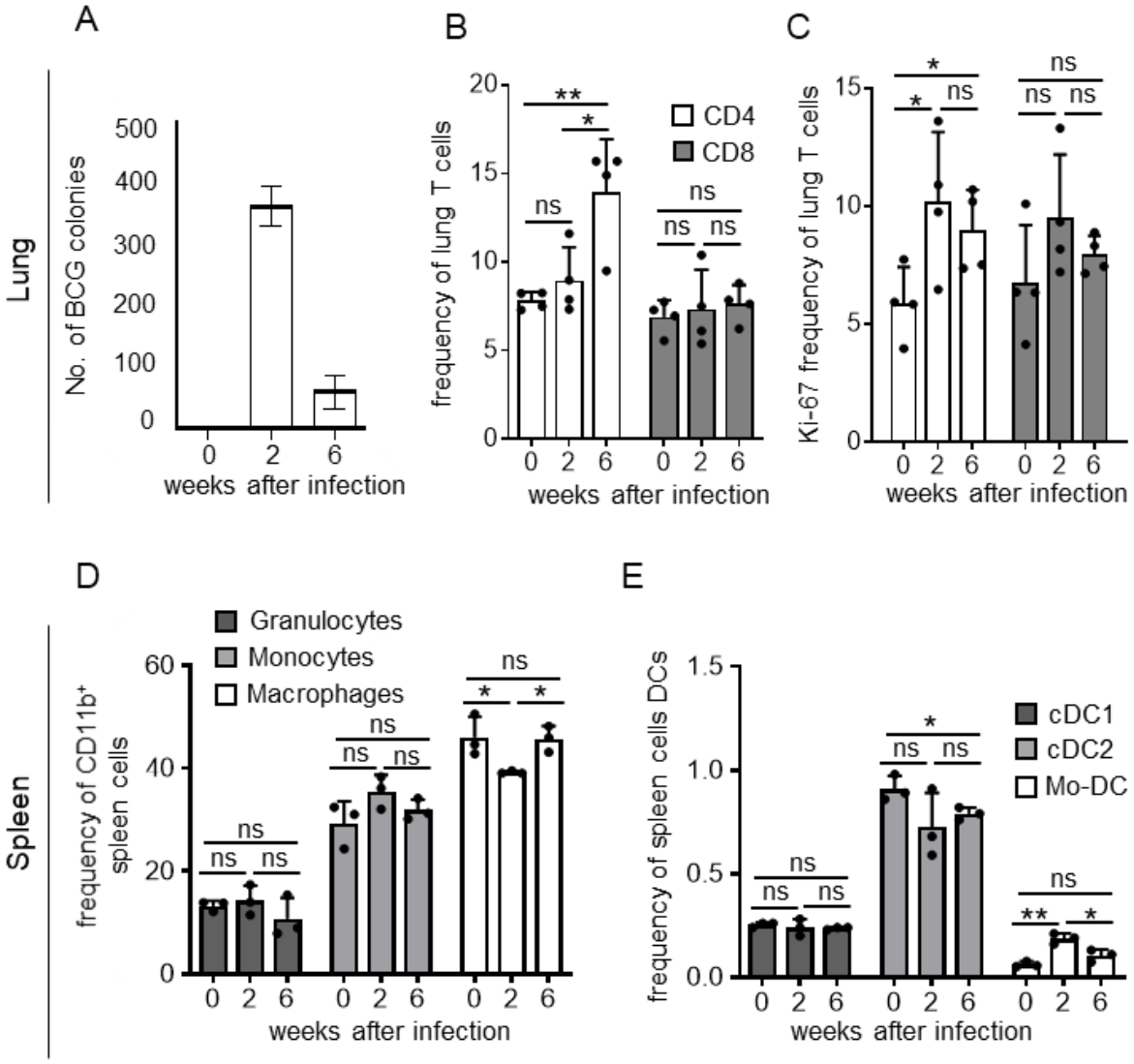

Figure 23: Lung bacterial load corelates with T cell proliferation and monocyte and mo-DC frequencies. B6 WT mice were infected intranasally with BCG for 2 or 6 weeks or left untreated as control. Representative of 3 independent experiments with n=3 mice. Statistics by student's unpaired t-test, ns=non-significant, *p<0.05, **p<0.01. **(A)** Bacterial load of lung single cell suspensions was measured by counting colonies 4 weeks after plating the suspension on agar. **(B)** Frequency of living $CD4^+$ and $CD8^+$ T cells of the lung was assessed by flow cytometry. **(C)** Proliferation of lung $CD4^+$ and $CD8^+$ T cells was measured by Ki-67 staining. **(D)** Frequencies of splenic $CD11b^+$ $Ly\text{-}6G^+$ $Ly\text{-}6C^{low}$ granulocytes, $CD11b^+$ $Ly\text{-}6C^{hi}$ $Ly\text{-}6G^-$ monocytes and $CD11b^+$ $Ly\text{-}6G^-$ $Ly\text{-}6C^-$ macrophages were analyzed using flow cytometry. **(E)** Frequencies of $CD11c^+$ $B220^-$ $Ly\text{-}6C^-$ $CD64^+$ mo-DCs, $CD11c^+$ $B220^-$ $Ly\text{-}6C^-$ $CD64^-$ $CD8^+$ $CD11b^-$ cDC1s and $CD11c^+$ $B220^-$ $Ly\text{-}6C^-$ $CD64^-$ $CD8^-$ $CD11b^+$ cDC2s were measured by flow cytometry. Data was generated in collaboration with Dr. Vini John.

infection, we harvested the organs 2 weeks after infection, whereas for chronic infection we sacrificed the mice after 6 weeks. Healthy mice were used as controls. We found that the bacterial growth of lung single cell suspensions was almost 4-fold higher at 2 weeks compared to 6 weeks after infection (Figure 23A). Next, we examined T cell and myeloid cell populations from the lung and the spleen, respectively, of BCG-infected mice via flow cytometry. In the lung, $CD4^+$ T cell frequencies were not altered after 2 weeks but significantly increased 6 weeks after infection, whereas $CD8^+$ T cell frequencies did not change (Figure 23B). $CD4^+$ T cell proliferation indicated by Ki-67 staining was already increased after 2 weeks and slightly but non-significantly decreased after 6 weeks compared to 2 weeks after infection (Figure 23C). A similar pattern could be observed for $CD8^+$ T cells without statistical significance. When analyzing myeloid populations, we found a significant increase of mo-DCs, a slight expansion of monocytes, and a decrease of macrophages after 2 weeks of infection, which was abolished after 6 weeks (Figure 23D+E). cDC2s were reduced 2 and 6 weeks after infection. Granulocyte and cDC1 frequencies displayed hardly any changes. These data showed that the bacterial load in the lungs of BGC-infected mice correlated with T cell proliferation as well as the frequencies of monocytes and mo-DCs.

3.2.2 Upregulation of CD16.2, PD-L1 and iNOS in myeloid cells is most prominent in the lungs 6 weeks after BCG infection

PD-L1, iNOS and Arg1 are important suppressive molecules upregulated by MDSCs compared to monocytes and granulocytes (Gabrilovich & Nagaraj 2009a), therefore we analyzed the expression of these markers on monocytes, granulocytes and macrophages isolated from lungs, spleens and bone marrow of BCG-infected mice and healthy controls. Since bone marrow contains no macrophages, we analyzed only monocytes and granulocytes of this organ. PD-L1 expression was not altered in the myeloid cells from spleens and bone marrow of BCG-infected mice but was upregulated in monocytes, granulocytes, and macrophages from lungs after 2 weeks and further increased after 6 weeks compared to healthy controls (Figure 24A). iNOS expression was slightly upregulated in monocytes and granulocytes from bone marrow 2 and 6 weeks after infection, whereas in the lung the iNOS upregulation occurred only 6 weeks after infection in monocytes, granulocytes, and macrophages (Figure 24B). iNOS expression in the spleen remained unaltered upon infection. Arg1 expression was increased in granulocytes from the lungs 2 weeks but not 6 weeks after BCG infection (Figure 24C). All analyzed populations from spleens and bone marrow as well as monocytes and macrophages from the lungs exhibited no changes in Arg1 expression upon infection. Previous *in vitro* experiments by our group indicated that CD16.2 might be a potential marker for MDSCs. Frequencies of CD16.2

expressing cells were increased in granulocytes, monocytes and macrophages from bone marrow, spleens, and lungs 6 weeks after BCG infection (Figure 24D). In the lungs but not in spleens and bone marrow, CD16.2^{+} cells were expanded already 2 weeks after BCG infection, however less pronounced compared to the increase after 6 weeks. Altogether, we found that the major alteration of myeloid suppressor marker expression occurred 6 weeks after BCG infection, whereas the highest bacterial load was present at 2 weeks (Figure 23A). These data indicate, that MDSCs were mostly present 6 weeks after infection at the chronic stage of disease.

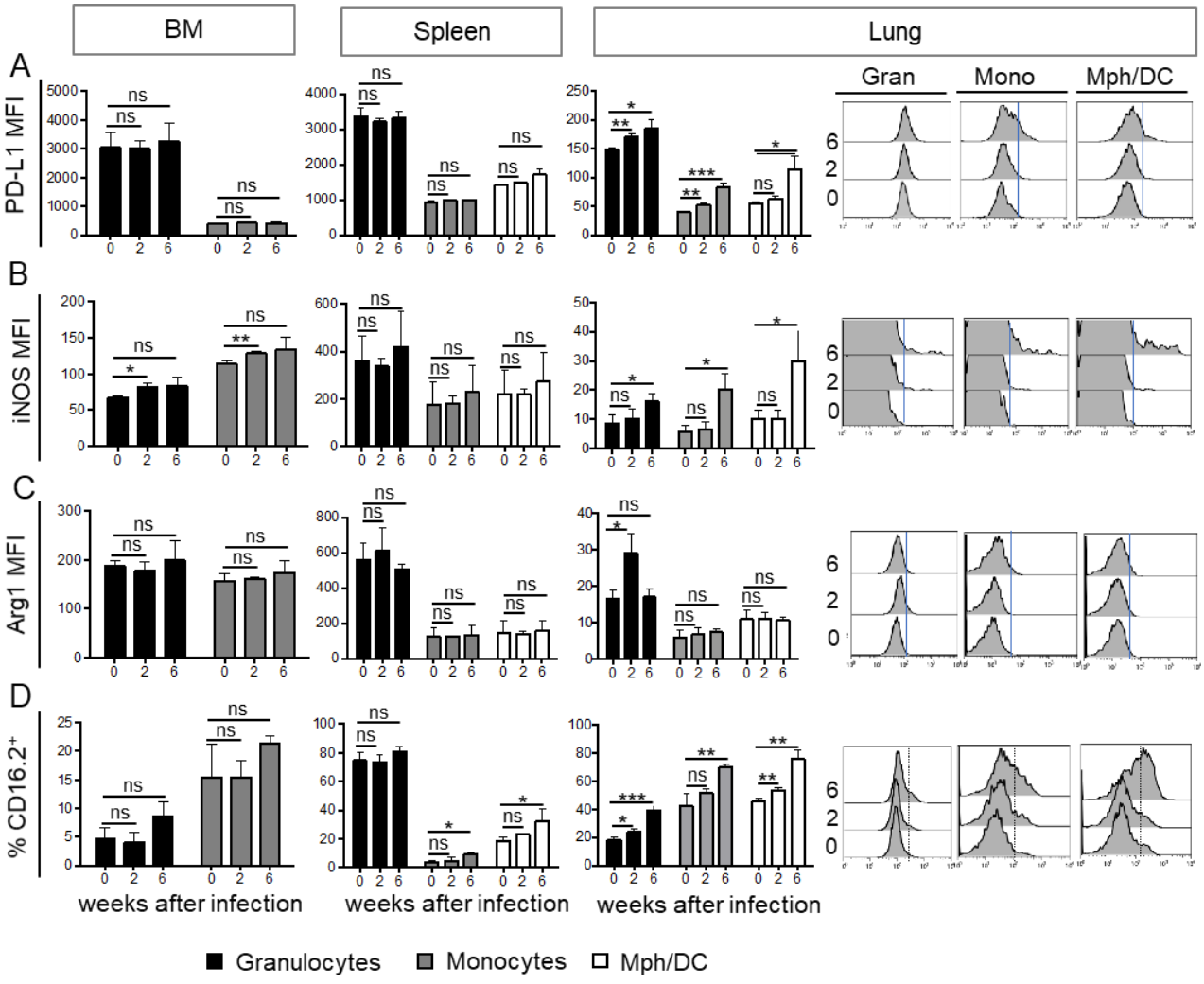

Figure 24: PD-L1, iNOS and CD16.2 are most profoundly upregulated 6 weeks after BCG infection. B6 WT mice received an intranasal BCG administration followed by bone marrow, spleen, and lung analysis 2 and 6 weeks after infection using flow cytometry. Representative of 3 independent experiments with n=3 mice. Statistics by student's unpaired t-test, ns=non-significant *p<0.05, **p<0.01, ***p<0.001. **(A)** PD-L1 MFI of CD11b^{+} Ly-6G^{+} Ly-6C^{low} granulocytes, CD11b^{+} Ly-6C^{+} Ly-6G^{-} monocytes and CD11b^{+} Ly-6G^{-} Ly-6C^{-} macrophages and DCs were analyzed via flow cytometry. Quantification as bar graphs of bone marrow, spleen, and lungs and histograms of lung cytometry data are displayed. **(B)** Setup as in (A) but iNOS MFI was measured. **(C)** Setup as in (A) but arg1 MFI was examined. **(D)** Setup as in (A) but frequency of CD16.2^{+} cells was analyzed. Data was generated in collaboration with Dr. Vini John.

3.2.3 VLA-1 expression is slightly upregulated by myeloid cells only in the bone marrow of BCG-infected mice

Since we previously defined VLA-1 as a marker of *in vitro* generated M-MDSCs, we analyzed VLA-1 expression of granulocytes, monocytes, and macrophages from bone marrow, spleens, and lungs of mice infected with BCG for 2 or 6 weeks (Figure 25). We found that monocytes expressed high levels of VLA-1 already in spleens and bone marrow of healthy mice, and the expression was significantly upregulated only at 6 weeks of BCG infection in the bone marrow. VLA-1 expression in the lungs was low in granulocytes, monocytes, and macrophages and remained at similar levels upon infection.

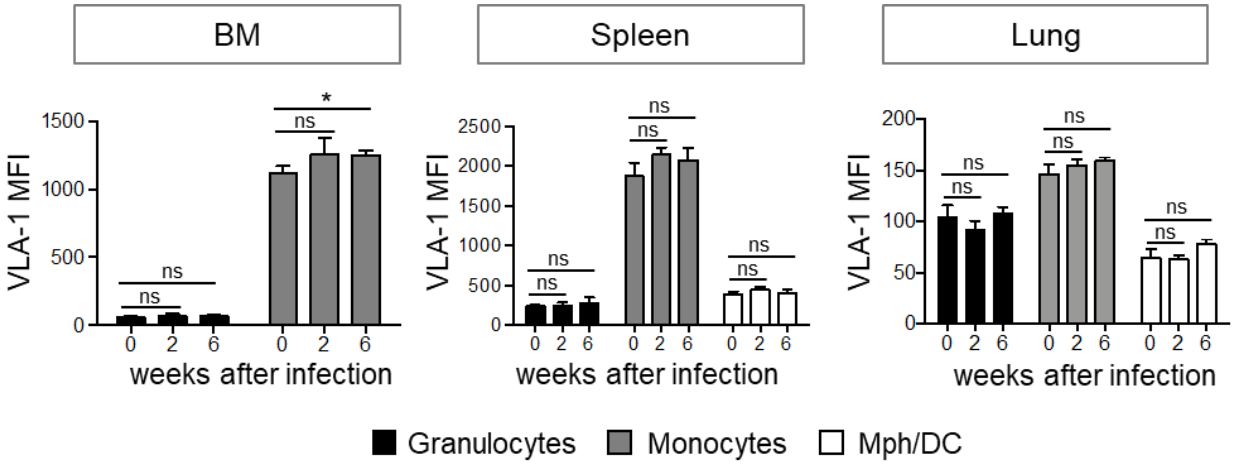

Figure 25: BCG infection induced a minor increase of VLA-1 expression on monocytes from bone marrow and spleen. B6 WT mice infected intranasally with BCG and VLA-1 expression of CD11b^{+} Ly-6G^{+} Ly-6C^{low} granulocytes, CD11b^{+} Ly-6C^{hi} Ly-6G^{-} monocytes and CD11b^{+} Ly-6G^{-} Ly-6C^{-} macrophages and DCs from bone marrow, spleens, and lungs was analyzed by flow cytometry 2 and 6 weeks after infection. Representative of 3 independent experiments with n=3 mice. Statistics by student's unpaired t-test, ns=non-significant, *p<0.05. Data was generated in collaboration with Dr. Vini John.

3.3 Meta-analysis of omics data on MDSCs from the literature

In order to find new marker candidates for future studies, we performed a meta-analysis of published MDSC-related genes identified by single cell or bulk RNA sequencing or CyTOF proteomic analyses. We only used data from studies which distinguished between M-MDSC and G-MDSC subsets. The studies examined MDSCs from different types of cancer, COVID-19, EAE, and sepsis. For our analysis we included markers appearing at least in two studies of human or murine MDSCs and as a result found 95 candidates for G-MDSCs and 31 candidates for M-MDSCs (Figure 26). Some of the identified markers are already established to be expressed by MDSCs, including PD-L1 (CD274) (Youn et al 2008a) and NOX2, required for ROS production, (NADPH oxidase, CYBB) (Corzo et al 2009) on both MDSC subsets,

arginase (ARG1 on M-MDSCs and G-MDSCs, and ARG2 on G-MDSCs) (Youn et al 2008a), and DC-HIL on M-MDSCs (Gpnmb) (Chung et al 2014). Furthermore, we found the MDSC markers S100A8, S100A9 and S100A12 upregulated in studies of M-MDSCs and G-MDSCs

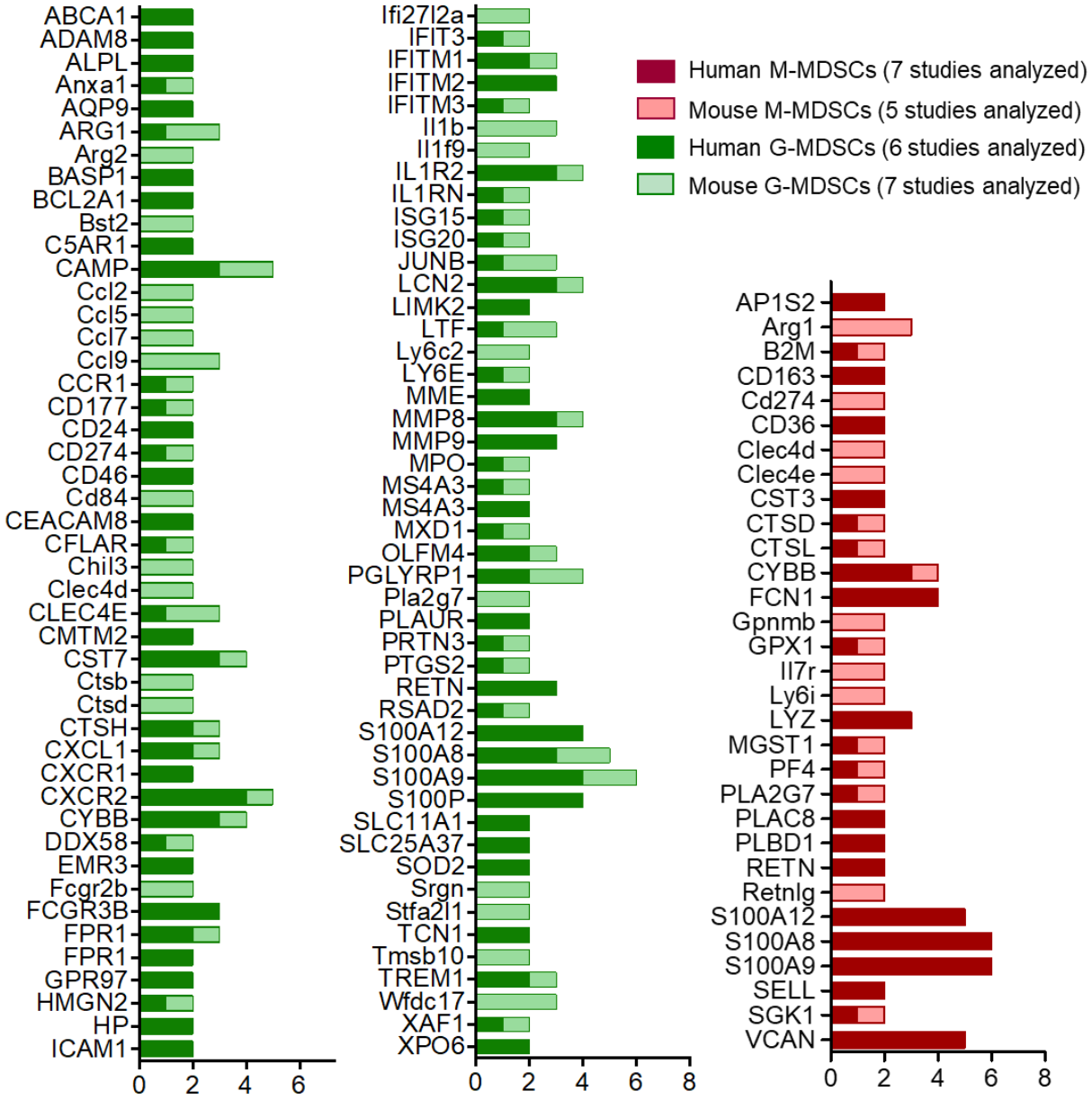

Figure 26: Meta-analysis of omics data of human and mouse M-MDSCs and G-MDSCs. We analyzed published transcriptomic and proteomic data of M-MDSCs and G-MDSCs to identify new marker candidates. We included upregulated genes or proteins which appeared at least in two studies per MDSC subset (n=5-7, as indicated). Data presented are derived from: human M-MDSC from (Alshetaiwi et al 2020, Darden et al 2020, Fultang et al 2019, Kim et al 2020, Schulte-Schrepping et al 2020, Xu et al 2020, Zhang et al 2020), human G-MDSC from (Alshetaiwi et al 2020, Condamine et al 2016, Darden et al 2020, Fultang et al 2019, Schulte-Schrepping et al 2020, Veglia et al 2021a), murine M-MDSC from (Alshetaiwi et al 2020, Halaby et al 2019, Katzenelenbogen et al 2020, Metzger et al 2019, Molgora et al 2020), and murine G-MDSC from (Alshetaiwi et al 2020, Halaby et al 2019, Knier et al 2018, Loeuillard et al 2020, Metzger et al 2019, Veglia et al 2021a, Youn et al 2012). Genes found in both mouse and human studies are shown as accumulated values in stacks. Figure from (Lutz & Eckert 2021)

(Zhao et al 2012). Ctsb and Ctsd were found to be involved in metastasis of pancreatic cancer (Dumartin et al 2011), therefore Ctsb expressed by G-MDSCs and Ctsd expressed by G-MDSCs and M-MDSCs may contribute to tumor progression by this mechanism. A variety of chemokines and chemokine receptors were altered in G-MDSCs but not in M-MDSCs, which have been associated with MDSCs but are also expressed by non-suppressive neutrophils including CXCR2 (Katoh et al 2013) and CCR1 (Li et al 2019). Neutrophil granule components with implication in tumor progression also emerged in our analysis such as MPO and MMP-8 and -9 (Rawat et al 2021), and CAMP (Minns et al 2021, Piktel et al 2016). VCAN secreted by MDSCs was shown to induce mesenchymal to epithelial transition of cancer cells in the metastatic niche (Gao et al 2012) and appeared in 5 of our analyzed studies in human M-MDSCs. FCN1 was upregulated in 4 studies of human M-MDSCs and plays an important role for innate immune defense by activating the lectin pathway of the complement system (Munthe-Fog et al 2012). Analyzing published transcriptomic and proteomic data of MDSCs we found some interesting candidates for novel MDSC markers to study in the future.

4 Discussion

MDSCs are important regulatory cells implicated in various diseases including cancer, chronic infections, and autoimmunity. Due to their high similarity to non-suppressive monocytes and neutrophils, the identification of surface markers specific for MDSCs is difficult. Here, we discovered VLA-1 as a marker expressed by *in vitro* generated M-MDSCs. We found that VLA-1 is not required for MDSC homing but is implicated in T cell suppression, which we showed using MDSC and T cell co-injection studies and a multiple sclerosis mouse model. VLA-1 was important for the interaction of MDSCs and T cells, but not for the migration of MDSCs within the spleen (Figure 27). Using VLA-1 as an additional marker for the identification of *in vitro* generated M-MDSCs resulted in cleaner separation of MDSCs from cells lacking suppressor marker expression. However, we found no VLA-1 expression on endogenous MDSCs in murine breast cancer and in the BCG disease models. Therefore, we performed a meta-analysis of publications with transcriptomic or proteomic data on MDSCs and identified potential marker candidates to study in the future.

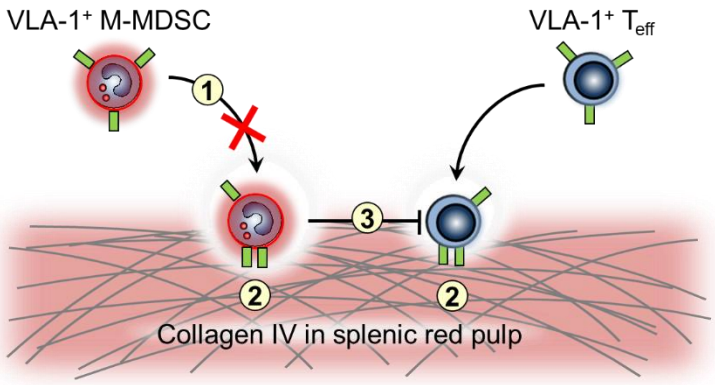

Figure 27: Function of VLA-1 on M-MDSCs. VLA-1 was not implicated in MDSC homing to the splenic red pulp (1) but in the interaction of MDSCs with T_{eff} cells on collagen IV (2). VLA-1 dependent binding on collagen IV enabled MDSC-T cell contact and T cell suppression (3).

4.1 In vitro studies of VLA-1⁺ M-MDSCs

VLA-1 is expressed by effector and memory T cells, NK cells, monocytes, and macrophages and is associated with a tissue residency (Ben-Horin & Bank 2004). In a study on human monocytes from PBMCs, VLA-1 was upregulated 12 h after stimulation with LPS and IFN-γ (Rubio et al 1995). Here, we found that VLA-1 is already expressed by monocytes isolated from bone marrow and is further upregulated on M-MDSCs after 3 days of culture with GM-CSF. The majority of VLA-1$^+$ M-MDSCs expressed iNOS, indicating that VLA-1 is expressed by MDSCs with the potential to produce effector molecules. LPS and IFN-γ treatment did not additionally upregulate the expression of VLA-1, indicating that GM-CSF and LPS + IFN-γ treatments upregulate VLA-1 expression but when combined have no additional effect. Our lab previously found that LPS and IFN-γ stimulation of GM-CSF cultured

bone marrow cells resulted in NO production, but not in fresh bone marrow cells (Greifenberg et al 2009, Ribechini et al 2017).

In vitro suppression assays showed that T_{eff} cells are more prone to MDSC-mediated suppression than naïve T cells. This was expected, since MDSCs are generated during chronic inflammation and MDSCs are rarely found in the lymph nodes (Ostrand-Rosenberg & Sinha 2009), the site of T cell priming. When comparing the suppressive activity of WT and VLA-$1^{-/-}$ MDSCs using *in vitro* suppressor assays, we did not find a difference in T cell suppression when the MDSCs lacked VLA-1. This might be the case due to the fact that the secreted NO is present in the culture supernatant (John et al 2019b) and direct interactions of MDSCs and T cells may be less important in this scenario. Furthermore, the suppressive effect of MDSCs on dendritic cells (Ribechini et al 2019) is not displayed by the suppressor assays since the T cells are activated with antibodies. Activated T cells produce cytokines which induce the iNOS expression by MDSCs, including IL-1β, TNF, IFN-γ, and IL-10 (Eckert et al 2021a), therefore the R-MDSCs are activated by the T cells during the suppression assay. Further activation of the MDSCs by adding LPS and IFN-γ to the cultures increased the suppressive activity of the MDSCs.

Sema7A is expressed already 6 h after T cell activation (Suzuki et al 2007) and was shown to negatively regulate activated T cells (Czopik et al 2006). On the other hand, Sema7A expression by activated T cells stimulates monocytes and macrophages to produce pro-inflammatory cytokines through VLA-1 ligation (Holmes et al 2002, Suzuki et al 2007). These contradicting studies also validated their data in murine disease models showing that EAE was strongly increased in the absence of Sema7A (Czopik et al 2006), whereas Sema7A deficient T cells were not capable of inducing contact hypersensitivity in mice (Suzuki et al 2007). Our data from the *in vitro* suppressor assay showed only a minor, nonsignificant decrease in T cell proliferation when T_{eff} cells expressed Sema7A in comparison to Sema7A$^{-/-}$ T cells. Further experiments have to be performed to determine whether Sema7A transduces negative signals as suggested by the results from a study showing that Sema7A ligation negatively regulates T cells, despite the other study connected the inflammatory response triggered by Sema7A to VLA-1 expression by monocytes. Since VLA-1 ligation with Sema7A on monocytes and macrophages stimulated the production of pro-inflammatory cytokines (Holmes et al 2002, Suzuki et al 2007), MDSCs may respond similarly by producing anti-inflammatory cytokines like IL-10. All in all, Sema7A expression on T_{eff} cells contributed, if at all, very little to the suppressive capacity of MDSCs, indicating that other receptors may play a role or a less

artificial mouse model requiring MDCS-T cell interaction may be necessary to determine the contribution of Sema7A ligation to T cell suppression.

4.2 VLA-1 is not required for MDSC homing

CCR2 expression by M-MDSCs and the presence of CCL2 in the tumor microenvironment were shown to be implicated in the homing of MDSCs to the tumor in various types of cancer including glioma, colon and lung cancer (Chang et al 2016, Hartwig et al 2017, Liang et al 2017). CX3CR1, which is highly expressed by M-MDSCs but hardly by G-MDSCs (Zhao et al 2015), was associated in MDSC recruitment in hepatocellular carcinoma (Chiu et al 2016). CCR1 (Inamoto et al 2016), CCR5 (Blattner et al 2018), and CXCR2 (Yu et al 2013) were found to play a role in MDSC homing the tumors as well. MDSCs not only accumulate in the effector organs during infections or cancer, but also in the spleen (Jordan et al 2017b, Periasamy et al 2016). However, it is not clear how MDSCs home to the spleen, therefore we investigated if VLA-1 is implicated in this process. When injecting MDSCs intravenously, we found that MDSCs reach the lung and the spleen, but hardly the BM and lymph nodes. This supports the hypothesis that MDSCs rather suppress T_{eff} cells during chronic inflammation in target organs when recirculating through the red pulp of the spleen instead of inhibiting T cell priming in the lymph nodes (Dorhoi & Du Plessis 2018, Ugel et al 2012a). MDSCs can be recruited from the spleen to the tumor site to suppress T cell functions (Cortez-Retamozo et al 2012, Cortez-Retamozo et al 2013). Similar to our data showing MDSCs reaching the spleens after 6 h, MDSCs were found to accumulate in the spleen 6 h after traumatic stress induction (Makarenkova et al 2006). VLA-1 was not implicated in homing of M-MDSCs to the spleen and lung, indicating that MDSCs use different homing receptors to migrate to these organs. One candidate is LFA-1, an integrin which is implicated in cell retention in the splenic red pulp and expressed by MDSCs (Bronte & Pittet 2013, Suk Lee et al 2019). VLA-1 was highly expressed by injected MDSCs in the lung and the recovery of VLA-1-deficient MDSCs was a non-significantly reduced, indicating that VLA-1 may be required for retaining MDSCs in the lung. VLA-1 was shown to be expressed by $CD8^+$ lung resident memory T cells in a model of immunization against tuberculosis (Haddadi et al 2017) and was implicated in their cell retention in the lung during influenza infection (Ray et al 2004).

4.3 VLA-1 is implicated in T_{eff} cell suppression

VLA-1 marks a subset of $CD8^+$ tissue resident memory T cells which are recruited to sites of infection and inflammation including the lung, liver, and tumors (Ghilas et al 2020, Haddadi et al 2017, Murray et al 2016). High levels of VLA-1 are also expressed by IFN-γ producing $CD4^+$

T cells (Chapman & Topham 2010, Goldstein et al 2003b). T_{eff} cells were shown to express VLA-1 in mouse models of colitis (Fiorucci et al 2002) and psoriasis (Conrad et al 2007) as well as in human atherosclerotic plaques (Stemme et al 1992). Besides the VLA-1 expression of T cells in inflamed tissues, VLA-1^+ T cells were also found in the spleen (Bradley et al 1992), which is consistent with our data of injected T_{eff} cells appearing in the spleen 6 h after injection and remaining there after 24 h. T cell suppression by inhibiting their proliferation and inducing apoptosis is a hallmark of MDSCs (Veglia et al 2018). To determine the impact of VLA-1 on T cell suppression, we injected A-MDSCs and OT-II T_{eff} cells which were generated *in vitro* by antigenic stimulation inducing Ki-67 expression. Upon injection, the T_{eff} cells transiently continue to express Ki-67 due to the lack of antigen *in vivo*. 6 h after WT A-MDSC injection, the proliferation of T_{eff} cells was reduced and apoptosis and cell death were increased, which correlated with the reduced frequencies of injected T_{eff} cells in the spleen. These effects were partially dependent on the expression of VLA-1 by A-MDSCs. 24 h after MDSC and T_{eff} cell injection, the T cell suppression was largely abolished, which is consistent with the loss of injected M-MDSCs at this timepoint. The T cell effector marker CD44 was reduced upon MDSC injection as well, which might be a result of cell death induction. The expression of CD25 and CD62L remained unchanged, however CD69 expression increased when MDSCs were co-injected, indicating that CD69 expressing T_{eff} cells are less prone to MDSC-mediated killing. The resident memory T cell marker CD69 was not expressed by the VLA-1^+ T cell subset (Goldstein et al 2003a). A proportion of the injected T_{eff} cells may become tissue resident memory T cells in the spleen, and $CD69^+$ T cells may be located in different regions of the spleen than VLA-1^+ T cells, therefore resulting in a reduced susceptibility of CD69 expressing T cells towards suppression. Further investigating the suppressive capacity of MDSCs to different T cell subsets will be interesting, since we already found that T_{eff} cells are more prone to suppression than naïve T cells.

4.4 VLA-1 is involved in MDSC-T_{eff} cell interaction on collagen IV

In vitro migration assays and intravital microscopy revealed that VLA-1 is implicated in MDSC-T_{eff} cell interaction on collagen IV. Since erythrocytes absorb light and high numbers of erythrocytes are present in the spleen, the data from the two-photon microscope could only be acquired 60-90 µm deep in the tissue. Therefore, the data was mainly generated in the subcapsular red pulp areas and might not be true for red pulp areas deeper within the spleen. Since monocytes cluster in the splenic subcapsular red pulp (Bronte & Pittet 2013), our data indicates that the subcapsular area may be an important site for T_{eff} cell suppression. Despite VLA-1 was shown to facilitate migration of influenza virus specific $CD8^+$ T cells within tissues

(Reilly et al 2020), VLA-1 deficiency did not impact MDSC motility and migration capability *in vitro* and *in vivo*.

4.5 MDSC injection prior to EAE induction reduces the disease score

Injecting R-MDSCs prior to EAE induction resulted in disease amelioration, and this effect was partially dependent on VLA-1 expression by the MDSCs. Investigating if the injection of A-MDSCs after disease onset provides similar results will be interesting since the clinical relevance is higher when using MDSCs as a treatment for EAE. Treg frequencies were reduced in *Itga1*$^{-/-}$ MDSC injected mice, however control and WT MDSC injected mice exhibited similar levels of MDSCs despite the difference in the clinical score was highest between both groups. We also found an increase in the production of the Treg signature cytokine IL-10 in MOG restimulated splenocytes in MDSC-injected mice, which was slightly reduced when MDSCs lacked VLA-1. However, this effect was only slightly above the baseline IL-10 production observed in the controls without MOG peptide. Therefore, the IL-10 production in response to antigen is very minor. Treg cells might be recruited upon MDSC injection in our model and may partially be responsible for the VLA-1 dependent clinical score reduction, since Treg recruitment and conversion are established functions of MDSCs (Gabrilovich & Nagaraj 2009a). However, the effects we observed were not completely clear and rather slight, therefore further studies are required to prove Treg involvement in the beneficial effect of injected MDSCs during EAE. The cytokine IL-17 is important for EAE development, since IL-17$^{-/-}$ mice hardly showed any disease score upon EAE induction (McGinley et al 2020). IL-17 blocking antibodies were efficient in suppressing EAE when injected at day -1 and 2 of EAE induction, but lost their efficacy when injected after the onset of symptoms (McGinley et al 2020). We found a clear but non-significant reduction of IL-17 production in MDSC injected EAE diseased mice compared to controls, indicating that MDSCs suppress IL-17 producing T cells. Since IL-17 production was required early at EAE induction and MDSCs were injected prior to EAE induction and are present only for few days, the timing of these mechanisms match, favoring the hypothesis that MDSCs suppress the IL-17 producing T cells during EAE. Administering IL-17 in MDSC injected EAE diseased may abolish the beneficial effect of MDSCs and further support the hypothesis. VLA-1 however had no impact on the reduction of IL-17 production.

When injecting sorted M-MDSCs, G-MDSCs, and macrophage dendritic cell progenitor cells from the GM-CSF cultures, we found that only G-MDSCs reduced the EAE score, however to a lesser extent than bulk MDSCs. Since both subsets were found during multiple sclerosis (Iacobaeus et al 2018) and EAE (Knier et al 2018, Zhu et al 2007) and the reduction of the

clinical score was partially dependent on VLA-1, which is not expressed by G-MDSCs, the sorting may have harmed the functionality of M-MDSCs. We also sought to find out if epigenetic imprinting of precursors may explain the fact that MDSCs disappear from the spleens after 3 days but still exert long-term functions on the disease outcome. We found that the CD11b$^-$ Ly-6G$^-$ progenitor cell population injection did not impact the EAE score. Multipotent progenitors 1 (Cabezas-Wallscheid et al 2014), common monocyte progenitors (Hettinger et al 2013), and transitional pre-monocytes express CD11b (Chong et al 2016), therefore these cells may be in part responsible for the suppressive effect since they were excluded by the sorting strategy. Hematopoietic stem cells as well as macrophage dendritic cell precursors were shown to lack CD11b expression (Grinenko et al 2018, Liu et al 2019), and common myeloid progenitors and granulocyte-monocyte progenitors were also not associated with CD11b expression (Lieu & Reddy 2012), indicating that these precursors have no impact on the MDSC-mediated EAE suppression. Further sorting specific precursor populations including multipotent progenitors 1, common monocyte progenitors, and transitional pre-monocytes and injecting the cells prior EAE induction will reveal if any of these progenitors have an impact on the clinical score of EAE.

4.6 Including VLA-1 into the strategy of M-MDSC identification *in vitro*

Many studies identify MDSCs by the markers CD11b, Ly-6C and Ly-6G, and partially even with the Gr-1 marker despite the latter being outdated. CD11c staining further allows the discrimination of macrophages and DCs from Ly-6C$^-$ CD11c$^-$ cells which include eosinophils (Hey et al 2016), facilitating the identification of suppressive macrophages. Furthermore, a Ly-6C$^+$ CD11c$^+$ transitory monocyte population could be distinguished from Ly-6C$^+$ CD11c$^-$ monocytes, which both exhibited the expression of the suppressor markers iNOS and Arg1. However, we still need to investigate if these cells are either a stable MDSC population or suppressive monocytes differentiating into macrophages by sorting this population and culturing the cells. Additionally, using VLA-1 for identifying M-MDSCs from BM-MDSC cultures resulted in a clearer separation of iNOS and Arg1 expressing cells, indicating that non-suppressive monocytes are excluded better using this strategy. Therefore, VLA-1 may be a valuable marker to separate MDSCs from non-suppressive monocytes.

4.7 VLA-1 is not a suitable marker for M-MDSCs in murine breast cancer and BCG infection

Breast cancer and tuberculosis infection are well known to recruit MDSCs in and human (Cha & Koo 2020, Knaul et al 2014, Mangtani et al 2014). In our breast cancer model, tumor

infiltrating $Arg1^+$ $CD11b^+$ cells consisted mainly of macrophages and a small portion of transitory cells, whereas monocytes did not express Arg1. This finding coincides with studies showing that M-MDSCs differentiate into tumor-associated macrophages at the tumor site depending on HIF-1α (Corzo et al 2010, Kwak et al 2020). Despite observing a strong infiltration of arginase producing $CD11b^+$ cells in murine breast tumors, we did not find any VLA-1 expression on myeloid cells. The monocyte and macrophage marker CCR2 is implicated in homing to inflamed tissues in a CCL2-dependent manner, including to skin, gut, and tumors (Ren et al 2012, Willenborg et al 2012, Zigmond et al 2012). The expression of CCR2 on M-MDSCs is well established (Lesokhin et al 2012). CCR2 deficiency reduced the egress of MDSCs from the BM and improved the survival of PD-1 treated glioma-bearing mice (Flores-Toro et al 2020). We found that CCR2 staining enriched the frequency of Arg1 producing cells within the macrophage and transitory cell populations. However, this effect can probably be explained by CCR2 staining excluding non-monocytic contaminants rather than CCR2 marking M-MDSCs, since inflammatory monocytes express CCR2 as well (Lim et al 2011). Nonetheless, CCR2 staining contributed to a better discrimination of monocytic subsets from contaminants and an enrichment of Arg1 producing cells, therefore including CCR2 as a marker was beneficial for identifying monocytes and macrophages with a potential suppressive capacity in the tumor. Since CCR2 is not required for MDSCs to home to the spleen (Serbina & Pamer 2006), this marker may be less suitable to identify splenic M-MDSCs.

Contrasting our expectations, monocytes and macrophages from spleens and lungs of BCG-infected mice did not exhibit a significant increase in VLA-1 expression compared to healthy mice. Monocytes from spleen and bone marrow of healthy and infected mice exhibited already a high $VLA\text{-}1^+$ MFI. VLA-1 expression was shown to be induced on monocytes after *in vitro* stimulation of human PBMCs with LPS and IFN-γ (Rubio et al 1995), and VLA-1 expression was upregulated on human monocytes from the blood in the systemic granulomatous disease sarcoidosis (Heron et al 2008) and on monocytes from lamina propria mononuclear cells during colitis (Fiorucci et al 2002). In mice, VLA-1 blockade was associated with a reduction of monocyte infiltrations in the lamina propria during colitis (Krieglstein et al 2002) and in corneal allografts (Chen et al 2007). We found VLA-1 expression on monocytes in spleen and bone marrow already during steady state, which is not established in the literature yet.

Despite VLA-1 showed the potential to be a marker for M-MDSCs on BM-MDSCs *in vitro*, we did not find an alteration of VLA-1 expression in the MDSC generating mouse models of breast cancer and tuberculosis, indicating that there are differences between the *in vitro* generated MDSCs and the MDSCs induced in these mouse models.

4.8 Studies of MDSCs in BCG-infected mice

Consistent with our model of acute and chronic BCG infection from figure 7, we found a high bacterial load in the lung 2 weeks after infection, which was strongly reduced after 6 weeks during the chronic stage. In line with this finding, the frequencies of monocytes and mo-DCs as well as the T cell proliferation exhibited a similar pattern. $CD4^+$ T cell frequencies were highest during the chronic stage of BCG infection, however these cells may be anergic, as anergic T cells were found in TB patients (Boer et al 2015). Macrophage frequencies decreased after 2 weeks to a similar level to the increase of monocytes in the spleen, indicating that less monocytes are differentiating to macrophages during the acute stage in the spleen. If these monocytes are R-MDSCs which migrate to the lung during the chronic stage still needs to be evaluated.

PD-L1 and iNOS were expressed by monocytes, macrophages, and granulocytes in the lungs of chronically BCG-infected mice, but not Arg1. Despite the MFI of iNOS expression was significantly increased upon chronic BCG infection, the frequency of $iNOS^{hi}$ cells was very low, therefore testing the suppressive capacity of sorted $CD11b^+$ cells will be required. Although iNOS expression is mainly linked to M-MDSCs, iNOS can also be found to be expressed by G-MDSCs (Xue et al 2020), as we also discovered iNOS expression on granulocytes 6 weeks after BCG infection. In studies with patients and nonhuman primates infected with *M.tb*, MDSCs were found to express PD-L1 (Jøntvedt Jørgensen et al 2021, Singh et al 2021). Regarding BCG infection, however, there is only *in vitro* data of MDSCs expressing PD-L1 available (John et al 2019a), which we now confirmed in a mouse model. Similar to our findings, arginase was not expressed by MDSCs in *M.tb* infected nonhuman primates (Singh et al 2021), whereas in another study on *M.tb* infected mice MDSCs were $Arg\text{-}1^+$ (Obregón-Henao et al 2013). In the latter study, the *M.tb* susceptible mouse strain C3HeB/FeJ (Kramnik et al 1998) was used in contrast to the *M.tb* resistant B6 mouse strain from our studies. Using the *M.tb* susceptible mouse model 129S2, the number of MDSCs generated during *M.tb* infection was increased compared to B6 mice (Knaul et al 2014), therefore switching the mouse model to an *M.tb* susceptible strain may be beneficial for future studies.

CD16.2 may be a new functional MDSC marker due to its capability to bind sialylated IgG2b (Kaneko et al 2006), since sialylated antibodies were implicated in the tolerogenic effects when IVIG was administered at high doses (Alter et al 2018b). In contrast to iNOS and PD-L1 expression, CD16.2 was not only upregulated in the lungs but also in the spleens during chronic BCG infection. This indicates that CD16.2 may be expressed already on R-MDSCs, which are recruited to the lungs and then activated. In *M.tb* infection, IgG binding to CD16A was

enhanced in latently infected TB patents compared to active TB patients, resulting in an increase of ADCC by CD16A expressing NK cells (Lu et al 2016b). This pro-inflammatory role of CD16A contrasts our hypothesis of its immunosuppressive role when expressed by MDSCs, however the function of the molecule may depend on the context. Binding sialylated and asialylated antibodies exhibit anti-inflammatory activity, whereas fucosylated and afucosylated antibodies promote ADCC (Alter et al 2018a).

4.9 Identifying potential new MDSC markers by analyzing omics data from the literature

Increasing numbers of transcriptomics and proteomics analyses on MDSCs open the possibility to reveal new MDSC marker candidates. We analyzed upregulated genes and proteins in MDSCs compared to non-suppressive neutrophils and granulocytes. We found three times more markers (93 vs. 31) shared between at least 2 studies for G-MDSCs than for M-MDSCS, indicating that the G-MDSC population may be more homogenous. Arg1 is frequently used as MDSC marker, which we could conform with our analysis. In 2 studies of murine G-MDSCs, Arg2 was induced, indicating that Arg2 may be a useful marker as well. The L-arginine depleting catalytic region of Arg2 is highly similar to the one of Arg1, however Arg2 is located in the mitochondria but not in the cytoplasm (Grzywa et al 2020). Contrasting our expectations, iNOS expression was upregulated by M-MDSCs only in one study (Molgora et al 2020), but also by G-MDSCs in one study (Knier et al 2018). Also, NOX2 (CYBB) upregulation was equally represented in both M-MDSCs and G-MDSCs, although ROS is mainly used as a marker for G-MDSCs (Gabrilovich & Nagaraj 2009a).

The markers S100A8 and S100A9 were upregulated in studies of M-MDSCS and G-MDSCs, which were found to be implicated in MDSC generation during cancer in mice and recruitment of MDSCs to tumors (Cheng et al 2008, Sinha et al 2008b). However, S100A8 and S100A9 can form the heterodimer calprotectin, a ligand for TLR4, which enhances autoinflammatory immune responses but not inflammation during infection (Ehrchen et al 2009). Thus, S100A8 and S100A9 expression is not limited to anti-inflammatory MDSCs and may not be optimal as an MDSC marker.

VCAN, which we found expressed by M-MDSCs in most mouse but not human studies, is an extracellular matrix proteoglycan implicated in leukocyte infiltration. VCAN expressed by stromal cells acts rather pro-inflammatory, whereas VCAN produced by myeloid cells exhibits anti-inflammatory functions (Wight et al 2020). M-MDSCs were found to secrete VCAN, and VCAN knockout in myeloid cells impaired macrometastasis formation but not MDSC

recruitment (Gao et al 2012), indicating that VCAN may be a potential MDSC marker as well as therapeutic target.

Cathepsins are lysosomal peptidases implicated in TLR signaling and cytokine secretion, and therefore play an important role for the innate immune response (Jakoš et al 2019). Various cathepsins were upregulated in our analysis, including Ctsb, Ctsd, Ctsh, and Ctsl. Ctsb was implicated in MDSC generation during polyposis (Gounaris et al 2008), and Ctsb and Ctsd were responsible for ceramidase inhibitor-induced cell death of MDSCs (Liu et al 2016). The four cathepsins we found upregulated by MDSCs were expressed in tumors (Tan et al 2013). Induction of Ctsb and Ctsd was required for metastasis of pancreatic cancer in a zebrafish model (Dumartin et al 2011). Despite their importance for MDSCs and cancer, cathepsins may be not optimal as MDSC markers due to their lysosomal location.

FCN1 was upregulated in M-MDSCs in more than half of the human studies but not in mouse studies. The pattern recognition peptide FCN1 activates the complement through the lectin pathway (Munthe-Fog et al 2012). Serum FCN1 levels in the autoinflammatory Kawasaki disease was reduced when IVIG treatment was successful, whereas FCN1 serum levels in treatment resistant individuals remained unaltered (Okuzaki et al 2017), indicating a pro-inflammatory role of FCN1. On the other hand, the complement system was found to induce T cell suppression in cancer (Roumenina et al 2019), however FCN1 was not linked to these immunosuppressive effects yet.

Chemokines and chemokine receptors were upregulated by G-MDSCs, however these markers are also expressed by non-suppressive cells like neutrophils, and therefore are not suitable markers for MDSCs. CXCR2, for instance, expressed by neutrophils is an important homing receptor for inflammatory sites (Zhang et al 2019), likewise G-MDSCs depend on CXCR2 when homing to tumors (Highfill et al 2014). Neutrophil granule components including MMP8, MMP9, and CAMP, which we found upregulated by G-MDSCs in several studies, are also not suitable as MDSC markers due to their expression by neutrophils (Minns et al 2021, Rawat et al 2021). MMP9 produced by MDSCs plays an important role for metastasis (Fleming et al 2018). CAMP expression however is reduced in MDSCs compared to polymorphonuclear leukocytes (Heim et al 2018). Despite these markers are not specific for MDSCs, they still may be valuable targets for therapeutically manipulating MDSCs.

5 Summary

MDSCs are suppressive immune cells with a high relevance in various pathologies including cancer, autoimmunity, and chronic infections. Surface marker expression of MDSCs resembles monocytes and neutrophils which have immunostimulatory functions instead of suppressing T cells. Therefore, finding specific surface markers for MDSCs is important for MDSC research and therapeutic MDSC manipulation. In this study, we analyzed if the integrin VLA-1 has the potential as a novel MDSC marker.

VLA-1 was expressed by M-MDSCs but not by G-MDSCs as well as by T_{eff} cells. VLA-1 deficiency did not impact iNOS expression, the distribution of M-MDSC and G-MDSC subsets, and the suppressive capacity of MDSCs towards naïve and T_{eff} cells *in vitro*. In mice, VLA-1 had no effect on the homing capability of MDSCs to the spleen, which is a major reservoir for MDSCs. Since the splenic red pulp contains collagen IV and VLA-1 binds collagen IV with a high affinity, we found MDSCs and T_{eff} cells in this area as expected. We showed that T cell suppression in the spleen, indicated by reduced T cell recovery and proliferation as well as increased apoptosis and cell death, partially depended on VLA-1 expression by the MDSCs. In a mouse model of multiple sclerosis, MDSC injection prior to disease onset led to a decrease of the disease score, and this effect was significantly reduced when MDSCs were VLA-1 deficient. The expression of Sema7A by T_{eff} cells, a ligand for VLA-1 which is implicated in negative T cell regulation, resulted in a slightly stronger T_{eff} cell suppression by MDSCs compared to Sema7A deficient T cells. Live cell imaging and intravital 2-photon microscopy showed that the interaction time of MDSCs and T_{eff} cells was shorter when MDSCs lacked VLA-1 expression, however VLA-1 expression had no impact on MDSC mobility. Adding VLA-1 to the identification strategy of *in vitro* generated MDSCs resulted in a clearer separation of iNOS and Arg1 expressing cells from cells which lacked suppressor marker expression. In breast tumor-bearing mice and BCG-infected mice, which are established models for MDSC generation *in vivo*, VLA-1 was not upregulated by endogenous MDSCs, therefore VLA-1 may not be a suitable marker for MDSCs *in vivo*. We found CD16.2 (FcγRIV), which may be involved in MDSC-mediated immunosuppression, upregulated by M-MDSCs and G-MDSCs upon BCG infection, therefore CD16.2 may be a new potential MDSC marker *in vivo*. Analyzing published RNA sequencing and proteomics data of MDSCs yielded marker candidates which were upregulated by MDSCs, including VCAN and FCN1.

6 Zusammenfassung

MDSCs sind suppressive Immunzellen mit hoher Relevanz bei verschiedenen Krankheiten, einschließlich Krebs, Autoimmunerkrankungen und chronischen Infektionen. Die Expression der Oberflächenmarker von MDSCs ähnelt Monozyten und Neutrophilen, welche im Gegensatz zu MDSCs immunstimulatorische Funktionen haben. Daher es wichtig für die Forschung und die therapeutische Manipulation von MDSCs, spezifische Oberflächenmarker für MDSCs zu identifizieren. In dieser Studie haben wir analysiert, ob das Integrin VLA-1 das ein möglicher neuer MDSC-Marker ist.

Effektor-T-Zellen und M-MDSCs, aber nicht G-MDSCs exprimierten VLA-1. VLA-1-Defizienz hatte keinen Einfluss auf die iNOS-Expression, die Verteilung der M-MDSC- und G-MDSC-Subpopulationen und die suppressive Kapazität von MDSCs gegenüber naiven und Effektor-T-Zellen *in vitro*. In Mäusen hatte VLA-1 keinen Einfluss auf die Fähigkeit zur zielgerichteten Migration von MDSCs zur Milz, welche ein wichtiges Reservoir für MDSCs ist. Da die rote Pulpa der Milz Kollagen IV enthält und VLA-1 Kollagen IV mit hoher Affinität bindet, fanden wir wie erwartet MDSCs und Effektor-T-Zellen in diesem Bereich. Wir konnten zeigen, dass die T-Zell-Suppression in der Milz, indiziert durch verringerte T-Zell-Wiederfindung und -Proliferation sowie erhöhte Apoptose und Zelltod, teilweise von der VLA-1-Expression von MDSCs abhing. In einem Mausmodell für Multiple Sklerose führte die MDSC-Injektion vor Induktion der Krankheit zu einer Verringerung des Krankheits-Scores, und dieser Effekt war signifikant verringert, wenn MDSCs VLA-1-defizient waren. Die Expression von Sema7A durch Effektor-T-Zellen, ein Ligand für VLA-1, der mit negativer T-Zell-Regulierung assoziiert ist, führte zu einer etwas stärkeren Effektor-T-Zell-Suppression durch MDSCs im Vergleich zu Sema7A-defizienten T-Zellen. Live-Cell-Imaging und intravitale 2-Photonen-Mikroskopie zeigten eine kürzere Interaktionszeit von MDSCs und Effektor-T-Zellen bei VLA-1 defizienten MDSCs, jedoch hatte die VLA-1-Expression keinen Einfluss auf die MDSC-Mobilität. Die Verwendung von VLA-1 bei der Identifizierungsstrategie von *in vitro* generierten MDSCs führte zu einer reineren Trennung von $iNOS^+$ und $Arg1^+$ Zellen von Zellen ohne Expression von Suppressormarkern. In Brusttumor-tragenden Mäusen und BCG-infizierten Mäusen, welche etablierte Modelle für die MDSC-Generierung *in vivo* sind, wurde VLA-1 nicht von endogenen MDSCs hochreguliert, daher ist VLA-1 möglicherweise kein geeigneter MDSC Marker *in vivo*. In BCG-infizierten Mäusen fanden wir CD16.2 (FcγRIV), welcher möglicherweise an der MDSC-vermittelten Immunsuppression beteiligt ist, in M-MDSCs und G-MDSCs hochreguliert, daher könnte CD16.2 ein neuer potenzieller MDSC-Marker *in vivo* sein. Die Analyse veröffentlichter RNA-

Sequenzierungs- und Proteomikdaten von MDSCs ergab Markerkandidaten, die von MDSCs hochreguliert wurden, einschließlich VCAN und FCN1.

7 References

Agrati C, Sacchi A, Bordoni V, Cimini E, Notari S, et al. 2020. Expansion of myeloid-derived suppressor cells in patients with severe coronavirus disease (COVID-19). *Cell Death & Differentiation* 27: 3196-207

Alshetaiwi H, Pervolarakis N, McIntyre LL, Ma D, Nguyen Q, et al. 2020. Defining the emergence of myeloid-derived suppressor cells in breast cancer using single-cell transcriptomics. *Sci Immunol* 5

Alter G, Ottenhoff THM, Joosten SA. 2018a. Antibody glycosylation in inflammation, disease and vaccination. *Semin Immunol* 39: 102-10

Alter G, Ottenhoff THM, Joosten SA. 2018b. Antibody glycosylation in inflammation, disease and vaccination. *Seminars in immunology* 39: 102-10

Andrews JR, Noubary F, Walensky RP, Cerda R, Losina E, Horsburgh CR. 2012. Risk of progression to active tuberculosis following reinfection with Mycobacterium tuberculosis. *Clin Infect Dis* 54: 784-91

Ascherio A. 2013. Environmental factors in multiple sclerosis. *Expert Review of Neurotherapeutics* 13: 3-9

Aslam R, Burack WR, Segel GB, McVey M, Spence SA, Semple JW. 2018. Intravenous immunoglobulin treatment of spleen cells from patients with immune thrombocytopenia significantly increases the percentage of myeloid-derived suppressor cells. *Br J Haematol* 181: 262-64

Auffray C, Fogg D, Garfa M, Elain G, Join-Lambert O, et al. 2007. Monitoring of blood vessels and tissues by a population of monocytes with patrolling behavior. *Science* 317: 666-70

Baaten B, Tinoco R, Chen A, Bradley L. 2012. Regulation of Antigen-Experienced T Cells: Lessons from the Quintessential Memory Marker CD44. *Front Immunol* 3

Bajénoff M, Narni-Mancinelli E, Brau F, Lauvau G. 2010. Visualizing early splenic memory CD8+ T cells reactivation against intracellular bacteria in the mouse. *PLoS One* 5: e11524

Barczyk M, Carracedo S, Gullberg D. 2009. Integrins. *Cell and Tissue Research* 339: 269

Becker HM, Rullo J, Chen M, Ghazarian M, Bak S, et al. 2013. α1β1 Integrin-Mediated Adhesion Inhibits Macrophage Exit from a Peripheral Inflammatory Lesion. *The Journal of Immunology* 190: 4305-14

Bekiaris V, Timoshenko O, Hou TZ, Toellner K, Shakib S, et al. 2008. Ly49H+ NK cells migrate to and protect splenic white pulp stroma from murine cytomegalovirus infection. *J Immunol* 180: 6768-76

Ben-Horin S, Bank I. 2004. The role of very late antigen-1 in immune-mediated inflammation. *Clin Immunol* 113: 119-29

Bettelli E, Pagany M, Weiner HL, Linington C, Sobel RA, Kuchroo VK. 2003. Myelin oligodendrocyte glycoprotein-specific T cell receptor transgenic mice develop spontaneous autoimmune optic neuritis. *J Exp Med* 197: 1073-81

Bielekova B, Sung MH, Kadom N, Simon R, McFarland H, Martin R. 2004. Expansion and functional relevance of high-avidity myelin-specific CD4+ T cells in multiple sclerosis. *J Immunol* 172: 3893-904

Bingisser RM, Tilbrook PA, Holt PG, Kees UR. 1998. Macrophage-derived nitric oxide regulates T cell activation via reversible disruption of the Jak3/STAT5 signaling pathway. *J Immunol* 160: 5729-34

Blattner C, Fleming V, Weber R, Himmelhan B, Altevogt P, et al. 2018. CCR5(+) Myeloid-Derived Suppressor Cells Are Enriched and Activated in Melanoma Lesions. *Cancer Res* 78: 157-67

Boer MC, Prins C, Meijgaarden KEv, Dissel JTv, Ottenhoff THM, et al. 2015. Mycobacterium bovis BCG Vaccination Induces Divergent Proinflammatory or Regulatory T Cell Responses in Adults. *Clinical and Vaccine Immunology* 22: 778-88

Bradley LM, Atkins GG, Swain SL. 1992. Long-term CD4+ memory T cells from the spleen lack MEL-14, the lymph node homing receptor. *J Immunol* 148: 324-31

Briesewitz R, Epstein MR, Marcantonio EE. 1993. Expression of native and truncated forms of the human integrin alpha 1 subunit. *J Biol Chem* 268: 2989-96

Bronte V, Brandau S, Chen S-H, Colombo MP, Frey AB, et al. 2016. Recommendations for myeloid-derived suppressor cell nomenclature and characterization standards. *Nature Communications* 7: 12150

Bronte V, Pittet MJ. 2013. The spleen in local and systemic regulation of immunity. *Immunity* 39: 806-18

Bronte V, Zanovello P. 2005. Regulation of immune responses by L-arginine metabolism. *Nature Reviews Immunology* 5: 641-54

Burgess AW, Metcalf D. 1980. The nature and action of granulocyte-macrophage colony stimulating factors. *Blood* 56: 947-58

Cabezas-Wallscheid N, Klimmeck D, Hansson J, Lipka Daniel B, Reyes A, et al. 2014. Identification of Regulatory Networks in HSCs and Their Immediate Progeny via Integrated Proteome, Transcriptome, and DNA Methylome Analysis. *Cell Stem Cell* 15: 507-22

Capucetti A, Albano F, Bonecchi R. 2020. Multiple Roles for Chemokines in Neutrophil Biology. *Front Immunol* 11: 1259-59

Caramalho Í, Nunes-Cabaço H, Foxall RB, Sousa AE. 2015. Regulatory T-Cell Development in the Human Thymus. *Front Immunol* 6

Cassetta L, Bruderek K, Skrzeczynska-Moncznik J, Osiecka O, Hu X, et al. 2020. Differential expansion of circulating human MDSC subsets in patients with cancer, infection and inflammation. *Journal for ImmunoTherapy of Cancer* 8: e001223

Cha YJ, Koo JS. 2020. Role of Tumor-Associated Myeloid Cells in Breast Cancer. *Cells* 9

Chackerian AA, Behar SM. 2003. Susceptibility to Mycobacterium tuberculosis: lessons from inbred strains of mice. *Tuberculosis* 83: 279-85

Chang AL, Miska J, Wainwright DA, Dey M, Rivetta CV, et al. 2016. CCL2 Produced by the Glioma Microenvironment Is Essential for the Recruitment of Regulatory T Cells and Myeloid-Derived Suppressor Cells. *Cancer Res* 76: 5671-82

Chapman TJ, Topham DJ. 2010. Identification of a unique population of tissue-memory CD4+ T cells in the airways after influenza infection that is dependent on the integrin VLA-1. *J Immunol* 184: 3841-9

Chen L, Huq S, Gardner H, de Fougerolles AR, Barabino S, Dana MR. 2007. Very late antigen 1 blockade markedly promotes survival of corneal allografts. *Arch Ophthalmol* 125: 783-88

Cheng P, Corzo CA, Luetteke N, Yu B, Nagaraj S, et al. 2008. Inhibition of dendritic cell differentiation and accumulation of myeloid-derived suppressor cells in cancer is regulated by S100A9 protein. *J Exp Med* 205: 2235-49

Cheuk S, Schlums H, Gallais Sérézal I, Martini E, Chiang SC, et al. 2017. CD49a Expression Defines Tissue-Resident CD8(+) T Cells Poised for Cytotoxic Function in Human Skin. *Immunity* 46: 287-300

Chiu DK-C, Xu IM-J, Lai RK-H, Tse AP-W, Wei LL, et al. 2016. Hypoxia induces myeloid-derived suppressor cell recruitment to hepatocellular carcinoma through chemokine (C-C motif) ligand 26. *Hepatology* 64: 797-813

Chong SZ, Evrard M, Devi S, Chen J, Lim JY, et al. 2016. CXCR4 identifies transitional bone marrow premonocytes that replenish the mature monocyte pool for peripheral responses. *J Exp Med* 213: 2293-314

Chung JS, Tamura K, Akiyoshi H, Cruz PD, Jr., Ariizumi K. 2014. The DC-HIL/syndecan-4 pathway regulates autoimmune responses through myeloid-derived suppressor cells. *J Immunol* 192: 2576-84

Clements JD, Hogan Laura H, Markofski W, Bock A, Barger B, et al. 2001. Mycobacterium bovis BCG-Induced Granuloma Formation Depends on Gamma Interferon and CD40 Ligand but Does Not Require CD28. *Infection and Immunity* 69: 2596-603

Codarri L, Gyülvészi G, Tosevski V, Hesske L, Fontana A, et al. 2011. RORγt drives production of the cytokine GM-CSF in helper T cells, which is essential for the effector phase of autoimmune neuroinflammation. *Nat Immunol* 12: 560-7

Colegio OR, Chu N-Q, Szabo AL, Chu T, Rhebergen AM, et al. 2014. Functional polarization of tumour-associated macrophages by tumour-derived lactic acid. *Nature* 513: 559-63

Condamine T, Dominguez GA, Youn JI, Kossenkov AV, Mony S, et al. 2016. Lectin-type oxidized LDL receptor-1 distinguishes population of human polymorphonuclear myeloid-derived suppressor cells in cancer patients. *Sci Immunol* 1

Conrad C, Boyman O, Tonel G, Tun-Kyi A, Laggner U, et al. 2007. α1β1 integrin is crucial for accumulation of epidermal T cells and the development of psoriasis. *Nature Medicine* 13: 836-42

Cortez-Retamozo V, Etzrodt M, Newton A, Rauch PJ, Chudnovskiy A, et al. 2012. Origins of tumor-associated macrophages and neutrophils. *Proceedings of the National Academy of Sciences* 109: 2491

Cortez-Retamozo V, Etzrodt M, Newton A, Ryan R, Pucci F, et al. 2013. Angiotensin II Drives the Production of Tumor-Promoting Macrophages. *Immunity* 38: 296-308

Corzo CA, Condamine T, Lu L, Cotter MJ, Youn JI, et al. 2010. HIF-1α regulates function and differentiation of myeloid-derived suppressor cells in the tumor microenvironment. *J Exp Med* 207: 2439-53

Corzo CA, Cotter MJ, Cheng P, Cheng F, Kusmartsev S, et al. 2009. Mechanism regulating reactive oxygen species in tumor-induced myeloid-derived suppressor cells. *J Immunol* 182: 5693-701

Cuenca AG, Delano MJ, Kelly-Scumpia KM, Moreno C, Scumpia PO, et al. 2011. A paradoxical role for myeloid-derived suppressor cells in sepsis and trauma. *Molecular medicine (Cambridge, Mass.)* 17: 281-92

Czopik AK, Bynoe MS, Palm N, Raine CS, Medzhitov R. 2006. Semaphorin 7A Is a Negative Regulator of T Cell Responses. *Immunity* 24: 591-600

Däbritz J, Judd LM, Chalinor HV, Menheniott TR, Giraud AS. 2016. Altered gp130 signalling ameliorates experimental colitis via myeloid cell-specific STAT3 activation and myeloid-derived suppressor cells. *Sci Rep* 6: 20584

Darden DB, Bacher R, Brusko MA, Knight P, Hawkins RB, et al. 2020. Single Cell RNA-SEQ of Human Myeloid Derived Suppressor Cells in Late Sepsis Reveals Multiple Subsets with Unique Transcriptional Responses: A Pilot Study. *Shock* Online ahead of print.

Dekkers G, Bentlage AEH, Stegmann TC, Howie HL, Lissenberg-Thunnissen S, et al. 2017. Affinity of human IgG subclasses to mouse Fc gamma receptors. *MAbs* 9: 767-73

Delano MJ, Scumpia PO, Weinstein JS, Coco D, Nagaraj S, et al. 2007. MyD88-dependent expansion of an immature GR-1(+)CD11b(+) population induces T cell suppression and Th2 polarization in sepsis. *J Exp Med* 204: 1463-74

Dendrou CA, Fugger L, Friese MA. 2015. Immunopathology of multiple sclerosis. *Nature Reviews Immunology* 15: 545-58

Derkow K, Loddenkemper C, Mintern J, Kruse N, Klugewitz K, et al. 2007. Differential priming of CD8 and CD4 T-cells in animal models of autoimmune hepatitis and cholangitis. *Hepatology* 46: 1155-65

Desalegn G, Pabst O. 2019. Inflammation triggers immediate rather than progressive changes in monocyte differentiation in the small intestine. *Nature Communications* 10: 3229

Divangahi M, Aaby P, Khader SA, Barreiro LB, Bekkering S, et al. 2021. Trained immunity, tolerance, priming and differentiation: distinct immunological processes. *Nature Immunology* 22: 2-6

Dockrell HM, Smith SG. 2017. What Have We Learnt about BCG Vaccination in the Last 20 Years? *Front Immunol* 8: 1134-34

Dorhoi A, Du Plessis N. 2018. Monocytic Myeloid-Derived Suppressor Cells in Chronic Infections. *Front Immunol* 8

Driver ER, Ryan GJ, Hoff DR, Irwin SM, Basaraba RJ, et al. 2012. Evaluation of a mouse model of necrotic granuloma formation using C3HeB/FeJ mice for testing of drugs against Mycobacterium tuberculosis. *Antimicrob Agents Chemother* 56: 3181-95

du Plessis N, Loebenberg L, Kriel M, von Groote-Bidlingmaier F, Ribechini E, et al. 2013. Increased frequency of myeloid-derived suppressor cells during active tuberculosis and

after recent mycobacterium tuberculosis infection suppresses T-cell function. *Am J Respir Crit Care Med* 188: 724-32

Dugast AS, Haudebourg T, Coulon F, Heslan M, Haspot F, et al. 2008. Myeloid-derived suppressor cells accumulate in kidney allograft tolerance and specifically suppress effector T cell expansion. *J Immunol* 180: 7898-906

Dumartin L, Whiteman HJ, Weeks ME, Hariharan D, Dmitrovic B, et al. 2011. AGR2 is a novel surface antigen that promotes the dissemination of pancreatic cancer cells through regulation of cathepsins B and D. *Cancer research* 71: 7091-102

Dye C. 2013. Making wider use of the world's most widely used vaccine: Bacille Calmette-Guerin revaccination reconsidered. *J R Soc Interface* 10: 20130365-65

Eckert I, Ribechini E, Lutz MB. 2021a. In Vitro Generation of Murine Myeloid-Derived Suppressor Cells, Analysis of Markers, Developmental Commitment, and Function In *Myeloid-Derived Suppressor Cells*, ed. S Brandau, A Dorhoi, pp. 99-114. New York, NY: Springer US

Eckert IN, Ribechini E, Jarick KJ, Strozniak S, Potter SJ, et al. 2021b. VLA-1 Binding to Collagen IV Controls Effector T Cell Suppression by Myeloid-Derived Suppressor Cells in the Splenic Red Pulp. *Front Immunol* 11: 616531-31

Ehlers S, Schaible UE. 2013. The granuloma in tuberculosis: dynamics of a host-pathogen collusion. *Front Immunol* 3: 411-11

Ehrchen JM, Sunderkötter C, Foell D, Vogl T, Roth J. 2009. The endogenous Toll-like receptor 4 agonist S100A8/S100A9 (calprotectin) as innate amplifier of infection, autoimmunity, and cancer. *J Leukoc Biol* 86: 557-66

El Daker S, Sacchi A, Tempestilli M, Carducci C, Goletti D, et al. 2015. Granulocytic myeloid derived suppressor cells expansion during active pulmonary tuberculosis is associated with high nitric oxide plasma level. *PloS one* 10: e0123772-e72

Elain G, Jeanneau K, Rutkowska A, Mir AK, Dev KK. 2014. The selective anti-IL17A monoclonal antibody secukinumab (AIN457) attenuates IL17A-induced levels of IL6 in human astrocytes. *Glia* 62: 725-35

Eruslanov E, Daurkin I, Ortiz J, Vieweg J, Kusmartsev S. 2010. Pivotal Advance: Tumor-mediated induction of myeloid-derived suppressor cells and M2-polarized macrophages by altering intracellular PGE2 catabolism in myeloid cells. *Journal of Leukocyte Biology* 88: 839-48

Evans HG, Gullick NJ, Kelly S, Pitzalis C, Lord GM, et al. 2009. In vivo activated monocytes from the site of inflammation in humans specifically promote Th17 responses. *Proceedings of the National Academy of Sciences of the United States of America* 106: 6232-37

Farooqi N, Gran B, Constantinescu CS. 2010. Are current disease-modifying therapeutics in multiple sclerosis justified on the basis of studies in experimental autoimmune encephalomyelitis? *Journal of Neurochemistry* 115: 829-44

Fiorucci S, Mencarelli A, Palazzetti B, Sprague AG, Distrutti E, et al. 2002. Importance of Innate Immunity and Collagen Binding Integrin α1β1 in TNBS-Induced Colitis. *Immunity* 17: 769-80

Fleming V, Hu X, Weber R, Nagibin V, Groth C, et al. 2018. Targeting Myeloid-Derived Suppressor Cells to Bypass Tumor-Induced Immunosuppression. *Front Immunol* 9

Flores-Toro JA, Luo D, Gopinath A, Sarkisian MR, Campbell JJ, et al. 2020. CCR2 inhibition reduces tumor myeloid cells and unmasks a checkpoint inhibitor effect to slow progression of resistant murine gliomas. *Proceedings of the National Academy of Sciences* 117: 1129

Foster SL, Hargreaves DC, Medzhitov R. 2007. Gene-specific control of inflammation by TLR-induced chromatin modifications. *Nature* 447: 972-78

Frischer JM, Bramow S, Dal-Bianco A, Lucchinetti CF, Rauschka H, et al. 2009. The relation between inflammation and neurodegeneration in multiple sclerosis brains. *Brain* 132: 1175-89

Fujii W, Ashihara E, Hirai H, Nagahara H, Kajitani N, et al. 2013. Myeloid-Derived Suppressor Cells Play Crucial Roles in the Regulation of Mouse Collagen-Induced Arthritis. *The Journal of Immunology* 191: 1073

Fultang L, Panetti S, Ng M, Collins P, Graef S, et al. 2019. MDSC targeting with Gemtuzumab ozogamicin restores T cell immunity and immunotherapy against cancers. *EBioMedicine* 47: 235-46

Gabrilovich D, Ishida T, Oyama T, Ran S, Kravtsov V, et al. 1998. Vascular endothelial growth factor inhibits the development of dendritic cells and dramatically affects the differentiation of multiple hematopoietic lineages in vivo. *Blood* 92: 4150-66

Gabrilovich DI, Nagaraj S. 2009a. Myeloid-derived suppressor cells as regulators of the immune system. *Nature Reviews Immunology* 9: 162-74

Gabrilovich DI, Nagaraj S. 2009b. Myeloid-derived suppressor cells as regulators of the immune system. *Nat Rev Immunol* 9: 162-74

Gabrilovich DI, Ostrand-Rosenberg S, Bronte V. 2012. Coordinated regulation of myeloid cells by tumours. *Nature Reviews Immunology* 12: 253-68

Gallatin WM, Weissman IL, Butcher EC. 1983. A cell-surface molecule involved in organ-specific homing of lymphocytes. *Nature* 304: 30-34

Gao D, Joshi N, Choi H, Ryu S, Hahn M, et al. 2012. Myeloid Progenitor Cells in the Premetastatic Lung Promote Metastases by Inducing Mesenchymal to Epithelial Transition. *Cancer Research* 72: 1384-94

Gardner H, Kreidberg J, Koteliansky V, Jaenisch R. 1996. Deletion of integrin alpha 1 by homologous recombination permits normal murine development but gives rise to a specific deficit in cell adhesion. *Dev Biol* 175: 301-13

Germain RN. 2002. T-cell development and the CD4-CD8 lineage decision. *Nat Rev Immunol* 2: 309-22

Ghasemi N, Razavi S, Nikzad E. 2017. Multiple Sclerosis: Pathogenesis, Symptoms, Diagnoses and Cell-Based Therapy. *Cell J* 19: 1-10

Ghilas S, Valencia-Hernandez AM, Enders MH, Heath WR, Fernandez-Ruiz D. 2020. Resident Memory T Cells and Their Role within the Liver. *Int J Mol Sci* 21

Ginhoux F, Jung S. 2014. Monocytes and macrophages: developmental pathways and tissue homeostasis. *Nature Reviews Immunology* 14: 392-404

Goldenberg MM. 2012. Multiple sclerosis review. *P T* 37: 175-84

Goldmann O, Beineke A, Medina E. 2017. Identification of a Novel Subset of Myeloid-Derived Suppressor Cells During Chronic Staphylococcal Infection That Resembles Immature Eosinophils. *J Infect Dis* 216: 1444-51

Goldstein I, Ben-Horin S, Li J, Bank I, Jiang H, Chess L. 2003a. Expression of the alpha1beta1 integrin, VLA-1, marks a distinct subset of human CD4+ memory T cells. *The Journal of clinical investigation* 112: 1444-54

Goldstein I, Ben-Horin S, Li J, Bank I, Jiang H, Chess L. 2003b. Expression of the α1β1 integrin, VLA-1, marks a distinct subset of human CD4+ memory T cells. *J Clin Invest* 112: 1444-54

Gounaris E, Tung CH, Restaino C, Maehr R, Kohler R, et al. 2008. Live imaging of cysteine-cathepsin activity reveals dynamics of focal inflammation, angiogenesis, and polyp growth. *PLoS One* 3: e2916

Greifenberg V, Ribechini E, Rößner S, Lutz MB. 2009. Myeloid-derived suppressor cell activation by combined LPS and IFN-γ treatment impairs DC development. *European Journal of Immunology* 39: 2865-76

Grinenko T, Eugster A, Thielecke L, Ramasz B, Krüger A, et al. 2018. Hematopoietic stem cells can differentiate into restricted myeloid progenitors before cell division in mice. *Nature Communications* 9: 1898

Groth C, Hu X, Weber R, Fleming V, Altevogt P, et al. 2019. Immunosuppression mediated by myeloid-derived suppressor cells (MDSCs) during tumour progression. *Br J Cancer* 120: 16-25

Grzywa TM, Sosnowska A, Matryba P, Rydzynska Z, Jasinski M, et al. 2020. Myeloid Cell-Derived Arginase in Cancer Immune Response. *Front Immunol* 11

Gutcher I, Becher B. 2007. APC-derived cytokines and T cell polarization in autoimmune inflammation. *J Clin Invest* 117: 1119-27

Haddadi S, Thanthrige-Don N, Afkhami S, Khera A, Jeyanathan M, Xing Z. 2017. Expression and role of VLA-1 in resident memory CD8 T cell responses to respiratory mucosal viral-vectored immunization against tuberculosis. *Scientific Reports* 7: 9525

Halaby MJ, Hezaveh K, Lamorte S, Ciudad MT, Kloetgen A, et al. 2019. GCN2 drives macrophage and MDSC function and immunosuppression in the tumor microenvironment. *Sci Immunol* 4

Hammerich L, Tacke F. 2015. Emerging roles of myeloid derived suppressor cells in hepatic inflammation and fibrosis. *World Journal of Gastrointestinal Pathophysiology* 6: 43-50

Hanson EM, Clements VK, Sinha P, Ilkovitch D, Ostrand-Rosenberg S. 2009. Myeloid-derived suppressor cells down-regulate L-selectin expression on CD4+ and CD8+ T cells. *J Immunol* 183: 937-44

Harari O, Liao JK. 2004. Inhibition of MHC II gene transcription by nitric oxide and antioxidants. *Curr Pharm Des* 10: 893-98

Hartwig T, Montinaro A, von Karstedt S, Sevko A, Surinova S, et al. 2017. The TRAIL-Induced Cancer Secretome Promotes a Tumor-Supportive Immune Microenvironment via CCR2. *Mol Cell* 65: 730-42.e5

Heim CE, West SC, Ali H, Kielian T. 2018. Heterogeneity of Ly6G(+) Ly6C(+) Myeloid-Derived Suppressor Cell Infiltrates during Staphylococcus aureus Biofilm Infection. *Infection and immunity* 86: e00684-18

Heldwein KA, Liang MD, Andresen TK, Thomas KE, Marty AM, et al. 2003. TLR2 and TLR4 serve distinct roles in the host immune response against Mycobacterium bovis BCG. *J Leukoc Biol* 74: 277-86

Heppner GH, Miller FR, Shekhar PM. 2000. Nontransgenic models of breast cancer. *Breast Cancer Res* 2: 331-34

Heron M, Grutters JC, van Velzen-Blad H, Veltkamp M, Claessen AME, van den Bosch JMM. 2008. Increased Expression of CD16, CD69, and Very Late Antigen-1 on Blood Monocytes in Active Sarcoidosis. *CHEST* 134: 1001-08

Hettinger J, Richards DM, Hansson J, Barra MM, Joschko A-C, et al. 2013. Origin of monocytes and macrophages in a committed progenitor. *Nature Immunology* 14: 821-30

Hey Y-Y, Tan JKH, O'Neill HC. 2016. Redefining Myeloid Cell Subsets in Murine Spleen. *Front Immunol* 6

Hickey MJ, Sihota E, Amrani A, Santamaria P, Zbytnuik LD, et al. 2002. Inducible nitric oxide synthase (iNOS) in endotoxemia: chimeric mice reveal different cellular sources in various tissues. *The FASEB Journal* 16: 1141-43

Highfill SL, Cui Y, Giles AJ, Smith JP, Zhang H, et al. 2014. Disruption of CXCR2-mediated MDSC tumor trafficking enhances anti-PD1 efficacy. *Science translational medicine* 6: 237ra67-37ra67

Holmes S, Downs AM, Fosberry A, Hayes PD, Michalovich D, et al. 2002. Sema7A is a Potent Monocyte Stimulator. *Scandinavian Journal of Immunology* 56: 270-75

Hu CE, Gan J, Zhang RD, Cheng YR, Huang GJ. 2011. Up-regulated myeloid-derived suppressor cell contributes to hepatocellular carcinoma development by impairing dendritic cell function. *Scand J Gastroenterol* 46: 156-64

Huang B, Pan P-Y, Li Q, Sato AI, Levy DE, et al. 2006a. Gr-1⁺CD115⁺ Immature Myeloid Suppressor Cells Mediate the Development of Tumor-Induced T Regulatory Cells and T-Cell Anergy in Tumor-Bearing Host. *Cancer Research* 66: 1123

Huang B, Pan P-Y, Li Q, Sato AI, Levy DE, et al. 2006b. Gr-1+ CD115+ Immature Myeloid Suppressor Cells Mediate the Development of Tumor-Induced T Regulatory Cells and T-Cell Anergy in Tumor-Bearing Host. *Cancer Research* 66: 1123

Huang X, Cui S, Shu Y. 2016. Cisplatin selectively downregulated the frequency and immunoinhibitory function of myeloid-derived suppressor cells in a murine B16 melanoma model. *Immunol Res* 64: 160-70

Hynes RO. 2002. Integrins: Bidirectional, Allosteric Signaling Machines. *Cell* 110: 673-87

Hynes RO. 2004. The emergence of integrins: a personal and historical perspective. *Matrix Biol* 23: 333-40

Iacobaeus E, Douagi I, Jitschin R, Marcusson-Ståhl M, Andrén AT, et al. 2018. Phenotypic and functional alterations of myeloid-derived suppressor cells during the disease course of multiple sclerosis. *Immunol Cell Biol* 96: 820-30

Iclozan C, Antonia S, Chiappori A, Chen DT, Gabrilovich D. 2013. Therapeutic regulation of myeloid-derived suppressor cells and immune response to cancer vaccine in patients with extensive stage small cell lung cancer. *Cancer Immunol Immunother* 62: 909-18

Inamoto S, Itatani Y, Yamamoto T, Minamiguchi S, Hirai H, et al. 2016. Loss of SMAD4 Promotes Colorectal Cancer Progression by Accumulation of Myeloid-Derived Suppressor Cells through the CCL15-CCR1 Chemokine Axis. *Clin Cancer Res* 22: 492-501

Ioannou M, Alissafi T, Lazaridis I, Deraos G, Matsoukas J, et al. 2012. Crucial role of granulocytic myeloid-derived suppressor cells in the regulation of central nervous system autoimmune disease. *J Immunol* 188: 1136-46

Jakoš T, Pišlar A, Jewett A, Kos J. 2019. Cysteine Cathepsins in Tumor-Associated Immune Cells. *Front Immunol* 10: 2037

Janeway CJ, Travers P, Walport M, al. e. 2001. *Immunobiology: The Immune System in Health and Disease. General properties of armed effector T cells.*: Garland Science.

John V, Kotze LA, Ribechini E, Walzl G, Du Plessis N, Lutz MB. 2019a. Caveolin-1 Controls Vesicular TLR2 Expression, p38 Signaling and T Cell Suppression in BCG Infected Murine Monocytic Myeloid-Derived Suppressor Cells. *Front Immunol* 10

John V, Kotze LA, Ribechini E, Walzl G, Du Plessis N, Lutz MB. 2019b. Caveolin-1 Controls Vesicular TLR2 Expression, p38 Signaling and T Cell Suppression in BCG Infected Murine Monocytic Myeloid-Derived Suppressor Cells. *Front Immunol* 10

Jøntvedt Jørgensen M, Jenum S, Tonby K, Mortensen R, Walzl G, et al. 2021. Monocytic myeloid-derived suppressor cells reflect tuberculosis severity and are influenced by cyclooxygenase-2 inhibitors. *Journal of leukocyte biology* 110: 177-86

Joo Y-D, Lee S-M, Lee S-W, Lee W-S, Lee S-M, et al. 2009. Granulocyte colony-stimulating factor-induced immature myeloid cells inhibit acute graft-versus-host disease lethality through an indoleamine dioxygenase-independent mechanism. *Immunology* 128: e632-e40

Jordan KR, Kapoor P, Spongberg E, Tobin RP, Gao D, et al. 2017a. Immunosuppressive myeloid-derived suppressor cells are increased in splenocytes from cancer patients. *Cancer Immunol Immunother* 66: 503-13

Jordan KR, Kapoor P, Spongberg E, Tobin RP, Gao D, et al. 2017b. Immunosuppressive myeloid-derived suppressor cells are increased in splenocytes from cancer patients. *Cancer Immunology, Immunotherapy* 66: 503-13

Jung YW, Rutishauser RL, Joshi NS, Haberman AM, Kaech SM. 2010. Differential localization of effector and memory CD8 T cell subsets in lymphoid organs during acute viral infection. *Journal of immunology (Baltimore, Md. : 1950)* 185: 5315-25

Kaiser A, Donnadieu E, Abastado J-P, Trautmann A, Nardin A. 2005. CC Chemokine Ligand 19 Secreted by Mature Dendritic Cells Increases Naive T Cell Scanning Behavior and Their Response to Rare Cognate Antigen. *The Journal of Immunology* 175: 2349

Kaneko Y, Nimmerjahn F, Ravetch Jeffrey V. 2006. Anti-Inflammatory Activity of Immunoglobulin G Resulting from Fc Sialylation. *Science* 313: 670-73

Katoh H, Wang D, Daikoku T, Sun H, Dey SK, Dubois RN. 2013. CXCR2-expressing myeloid-derived suppressor cells are essential to promote colitis-associated tumorigenesis. *Cancer Cell* 24: 631-44

Katzenelenbogen Y, Sheban F, Yalin A, Yofe I, Svetlichnyy D, et al. 2020. Coupled scRNA-Seq and Intracellular Protein Activity Reveal an Immunosuppressive Role of TREM2 in Cancer. *Cell* 182: 872-85 e19

Kim N, Kim HK, Lee K, Hong Y, Cho JH, et al. 2020. Single-cell RNA sequencing demonstrates the molecular and cellular reprogramming of metastatic lung adenocarcinoma. *Nat Commun* 11: 2285

Kim Y-J, Chang S-Y, Ko H-J. 2015. Myeloid-Derived Suppressor Cells in Inflammatory Bowel Disease. *Intestinal Research* 13: 105-11

Knaul JK, Jörg S, Oberbeck-Mueller D, Heinemann E, Scheuermann L, et al. 2014. Lung-residing myeloid-derived suppressors display dual functionality in murine pulmonary tuberculosis. *Am J Respir Crit Care Med* 190: 1053-66

Knier B, Hiltensperger M, Sie C, Aly L, Lepennetier G, et al. 2018. Myeloid-derived suppressor cells control B cell accumulation in the central nervous system during autoimmunity. *Nat Immunol* 19: 1341-51

Kobayashi N, Hiraoka N, Yamagami W, Ojima H, Kanai Y, et al. 2007. FOXP3⁺ Regulatory T Cells Affect the Development and Progression of Hepatocarcinogenesis. *Clinical Cancer Research* 13: 902

Korn T, Bettelli E, Oukka M, Kuchroo VK. 2009. IL-17 and Th17 Cells. *Annu Rev Immunol* 27: 485-517

Kramnik I, Demant P, Bloom BB. 1998. Susceptibility to tuberculosis as a complex genetic trait: analysis using recombinant congenic strains of mice. *Novartis Found Symp* 217: 120-31; discussion 32-7

Krieglstein CF, Cerwinka WH, Sprague AG, Laroux FS, Grisham MB, et al. 2002. Collagen-binding integrin α1β1 regulates intestinal inflammation in experimental colitis. *J Clin Invest* 110: 1773-82

Kumar V, Patel S, Tcyganov E, Gabrilovich DI. 2016. The Nature of Myeloid-Derived Suppressor Cells in the Tumor Microenvironment. *Trends Immunol* 37: 208-20

Kunkl M, Frascolla S, Amormino C, Volpe E, Tuosto L. 2020. T Helper Cells: The Modulators of Inflammation in Multiple Sclerosis. *Cells* 9: 482

Kusmartsev S, Eruslanov E, Kübler H, Tseng T, Sakai Y, et al. 2008. Oxidative stress regulates expression of VEGFR1 in myeloid cells: link to tumor-induced immune suppression in renal cell carcinoma. *J Immunol* 181: 346-53

Kusmartsev S, Nefedova Y, Yoder D, Gabrilovich DI. 2004. Antigen-specific inhibition of CD8+ T cell response by immature myeloid cells in cancer is mediated by reactive oxygen species. *J Immunol* 172: 989-99

Kwak T, Wang F, Deng H, Condamine T, Kumar V, et al. 2020. Distinct Populations of Immune-Suppressive Macrophages Differentiate from Monocytic Myeloid-Derived Suppressor Cells in Cancer. *Cell Reports* 33: 108571

Labani-Motlagh A, Ashja-Mahdavi M, Loskog A. 2020. The Tumor Microenvironment: A Milieu Hindering and Obstructing Antitumor Immune Responses. *Front Immunol* 11

Laidlaw BJ, Craft JE, Kaech SM. 2016. The multifaceted role of CD4+ T cells in CD8+ T cell memory. *Nature Reviews Immunology* 16: 102-11

Lesokhin AM, Hohl TM, Kitano S, Cortez C, Hirschhorn-Cymerman D, et al. 2012. Monocytic CCR2(+) myeloid-derived suppressor cells promote immune escape by limiting activated CD8 T-cell infiltration into the tumor microenvironment. *Cancer Res* 72: 876-86

Li B, Zhang S, Huang N, Chen H, Wang P, et al. 2019. CCL9/CCR1 induces myeloid-derived suppressor cell recruitment to the spleen in a murine H22 orthotopic hepatoma model. *Oncol Rep* 41: 608-18

Liakka A, Karjalainen H, Virtanen I, Autio-Harmainen H. 1995. Immuno-electron-microscopic localization of types III pN-collagen and IV collagen, laminin and tenascin in developing and adult human spleen. *Cell Tissue Res* 282: 117-27

Liang H, Deng L, Hou Y, Meng X, Huang X, et al. 2017. Host STING-dependent MDSC mobilization drives extrinsic radiation resistance. *Nat Commun* 8: 1736

Libbey JE, Fujinami RS. 2011. Experimental autoimmune encephalomyelitis as a testing paradigm for adjuvants and vaccines. *Vaccine* 29: 3356-62

Lieu YK, Reddy EP. 2012. Impaired adult myeloid progenitor CMP and GMP cell function in conditional c-myb-knockout mice. *Cell Cycle* 11: 3504-12

Lim JK, Obara CJ, Rivollier A, Pletnev AG, Kelsall BL, Murphy PM. 2011. Chemokine Receptor Ccr2 Is Critical for Monocyte Accumulation and Survival in West Nile Virus Encephalitis. *The Journal of Immunology* 186: 471

Liu F, Li X, Lu C, Bai A, Bielawski J, et al. 2016. Ceramide activates lysosomal cathepsin B and cathepsin D to attenuate autophagy and induces ER stress to suppress myeloid-derived suppressor cells. *Oncotarget* 7: 83907-25

Liu Z, Gu Y, Chakarov S, Bleriot C, Kwok I, et al. 2019. Fate Mapping via Ms4a3-Expression History Traces Monocyte-Derived Cells. *Cell* 178: 1509-25.e19

Loeuillard E, Yang J, Buckarma E, Wang J, Liu Y, et al. 2020. Targeting tumor-associated macrophages and granulocytic myeloid-derived suppressor cells augments PD-1 blockade in cholangiocarcinoma. *J Clin Invest* 130: 5380-96

Lokmic Z, Lämmermann T, Sixt M, Cardell S, Hallmann R, Sorokin L. 2008. The extracellular matrix of the spleen as a potential organizer of immune cell compartments. *Semin Immunol* 20: 4-13

Lu C, Redd PS, Lee JR, Savage N, Liu K. 2016a. The expression profiles and regulation of PD-L1 in tumor-induced myeloid-derived suppressor cells. *Oncoimmunology* 5: e1247135-e35

Lu LL, Chung AW, Rosebrock TR, Ghebremichael M, Yu WH, et al. 2016b. A Functional Role for Antibodies in Tuberculosis. *Cell* 167: 433-43.e14

Lutz MB, Eckert IN. 2021. Comments on the ambiguity of selected surface markers, signaling pathways and omics profiles hampering the identification of myeloid-derived suppressor cells. *Cell Immunol* 364: 104347

Lutz MB, Kukutsch N, Ogilvie AL, Rössner S, Koch F, et al. 1999. An advanced culture method for generating large quantities of highly pure dendritic cells from mouse bone marrow. *J Immunol Methods* 223: 77-92

Magcwebeba T, Dorhoi A, du Plessis N. 2019. The Emerging Role of Myeloid-Derived Suppressor Cells in Tuberculosis. *Front Immunol* 10: 917-17

Makarenkova VP, Bansal V, Matta BM, Perez LA, Ochoa JB. 2006. CD11b⁺/Gr-1⁺ Myeloid Suppressor Cells Cause T Cell Dysfunction after Traumatic Stress. *The Journal of Immunology* 176: 2085

Mangtani P, Abubakar I, Ariti C, Beynon R, Pimpin L, et al. 2014. Protection by BCG Vaccine Against Tuberculosis: A Systematic Review of Randomized Controlled Trials. *Clinical Infectious Diseases* 58: 470-80

Mao C, Near R, Zhong X, Gao W. 2021. Cross-species higher sensitivities of FcγRIIIA/FcγRIV to afucosylated IgG for enhanced ADCC. *Antib Ther* 4: 159-70

Marigo I, Bosio E, Solito S, Mesa C, Fernandez A, et al. 2010. Tumor-Induced Tolerance and Immune Suppression Depend on the C/EBPβ Transcription Factor. *Immunity* 32: 790-802

Martino A, Badell E, Abadie V, Balloy V, Chignard M, et al. 2010. Mycobacterium bovis Bacillus Calmette-Guérin Vaccination Mobilizes Innate Myeloid-Derived Suppressor Cells Restraining In Vivo T Cell Priming via IL-1R–Dependent Nitric Oxide Production. *The Journal of Immunology* 184: 2038

Martrus G, Goebels H, Langeneckert AE, Kah J, Flomm F, et al. 2019. CD49a Expression Identifies a Subset of Intrahepatic Macrophages in Humans. *Front Immunol* 10

Marvel D, Gabrilovich DI. 2015. Myeloid-derived suppressor cells in the tumor microenvironment: expect the unexpected. *J Clin Invest* 125: 3356-64

McGinley AM, Sutton CE, Edwards SC, Leane CM, DeCourcey J, et al. 2020. Interleukin-17A Serves a Priming Role in Autoimmunity by Recruiting IL-1β-Producing Myeloid Cells that Promote Pathogenic T Cells. *Immunity* 52: 342-56.e6

McNally A, Hill GR, Sparwasser T, Thomas R, Steptoe RJ. 2011. CD4+CD25+ regulatory T cells control CD8+ T-cell effector differentiation by modulating IL-2 homeostasis. *Proceedings of the National Academy of Sciences of the United States of America* 108: 7529-34

Medina E, North RJ. 1998. Resistance ranking of some common inbred mouse strains to Mycobacterium tuberculosis and relationship to major histocompatibility complex haplotype and Nramp1 genotype. *Immunology* 93: 270-74

Melero-Jerez C, Suardíaz M, Lebrón-Galán R, Marín-Bañasco C, Oliver-Martos B, et al. 2019. The presence and suppressive activity of myeloid-derived suppressor cells are potentiated after interferon-β treatment in a murine model of multiple sclerosis. *Neurobiology of Disease* 127: 13-31

Menetrier-Caux C, Montmain G, Dieu MC, Bain C, Favrot MC, et al. 1998. Inhibition of the Differentiation of Dendritic Cells From CD34+ Progenitors by Tumor Cells: Role of Interleukin-6 and Macrophage Colony-Stimulating Factor. *Blood* 92: 4778-91

Metzger P, Kirchleitner SV, Kluge M, Koenig LM, Horth C, et al. 2019. Immunostimulatory RNA leads to functional reprogramming of myeloid-derived suppressor cells in pancreatic cancer. *J Immunother Cancer* 7: 288

Minns D, Smith KJ, Alessandrini V, Hardisty G, Melrose L, et al. 2021. The neutrophil antimicrobial peptide cathelicidin promotes Th17 differentiation. *Nature Communications* 12: 1285

Minton K. 2020. IL-17A brings new recruits to EAE. *Nature Reviews Immunology* 20: 137-37

Mirza N, Fishman M, Fricke I, Dunn M, Neuger AM, et al. 2006. All-trans-retinoic acid improves differentiation of myeloid cells and immune response in cancer patients. *Cancer Res* 66: 9299-307

Molgora M, Esaulova E, Vermi W, Hou J, Chen Y, et al. 2020. TREM2 Modulation Remodels the Tumor Myeloid Landscape Enhancing Anti-PD-1 Immunotherapy. *Cell* 182: 886-900 e17

Moliné-Velázquez V, Cuervo H, Vila-Del Sol V, Ortega MC, Clemente D, de Castro F. 2011. Myeloid-derived suppressor cells limit the inflammation by promoting T lymphocyte apoptosis in the spinal cord of a murine model of multiple sclerosis. *Brain Pathol* 21: 678-91

Molon B, Ugel S, Del Pozzo F, Soldani C, Zilio S, et al. 2011. Chemokine nitration prevents intratumoral infiltration of antigen-specific T cells. *J Exp Med* 208: 1949-62

Movahedi K, Guilliams M, Van den Bossche J, Van den Bergh R, Gysemans C, et al. 2008a. Identification of discrete tumor-induced myeloid-derived suppressor cell subpopulations with distinct T cell-suppressive activity. *Blood* 111: 4233-44

Movahedi K, Guilliams M, Van den Bossche J, Van den Bergh R, Gysemans C, et al. 2008b. Identification of discrete tumor-induced myeloid-derived suppressor cell subpopulations with distinct T cell–suppressive activity. *Blood* 111: 4233-44

Munthe-Fog L, Hummelshoj T, Honoré C, Moller ME, Skjoedt MO, et al. 2012. Variation in FCN1 affects biosynthesis of ficolin-1 and is associated with outcome of systemic inflammation. *Genes & Immunity* 13: 515-22

Murray PJ, Wynn TA. 2011. Protective and pathogenic functions of macrophage subsets. *Nature reviews. Immunology* 11: 723-37

Murray T, Fuertes Marraco SA, Baumgaertner P, Bordry N, Cagnon L, et al. 2016. Very Late Antigen-1 Marks Functional Tumor-Resident CD8 T Cells and Correlates with Survival of Melanoma Patients. *Front Immunol* 7: 573-73

Nagaraj S, Gupta K, Pisarev V, Kinarsky L, Sherman S, et al. 2007. Altered recognition of antigen is a mechanism of CD8+ T cell tolerance in cancer. *Nat Med* 13: 828-35

Najjar YG, Finke JH. 2013. Clinical perspectives on targeting of myeloid derived suppressor cells in the treatment of cancer. *Front Oncol* 3: 49-49

Netea MG, Schlitzer A, Placek K, Joosten LAB, Schultze JL. 2019. Innate and Adaptive Immune Memory: an Evolutionary Continuum in the Host’s Response to Pathogens. *Cell Host & Microbe* 25: 13-26

Nicolle D, Fremond C, Pichon X, Bouchot A, Maillet I, et al. 2004. Long-Term Control of Mycobacterium bovis BCG Infection in the Absence of Toll-Like Receptors (TLRs): Investigation of TLR2-, TLR6-, or TLR2-TLR4-Deficient Mice. *Infection and Immunity* 72: 6994-7004

Noster R, Riedel R, Mashreghi M-F, Radbruch H, Harms L, et al. 2014. IL-17 and GM-CSF Expression Are Antagonistically Regulated by Human T Helper Cells. *Science Translational Medicine* 6: 241ra80

Nykvist P, Tu H, Ivaska J, Käpylä J, Pihlajaniemi T, Heino J. 2000. Distinct recognition of collagen subtypes by alpha(1)beta(1) and alpha(2)beta(1) integrins. Alpha(1)beta(1) mediates cell adhesion to type XIII collagen. *J Biol Chem* 275: 8255-61

Obregón-Henao A, Henao-Tamayo M, Orme IM, Ordway DJ. 2013. Gr1(int)CD11b+ myeloid-derived suppressor cells in Mycobacterium tuberculosis infection. *PLoS One* 8: e80669

Ohl K, Tenbrock K. 2018. Reactive Oxygen Species as Regulators of MDSC-Mediated Immune Suppression. *Front Immunol* 9: 2499-99

Okuzaki D, Ota K, Takatsuki SI, Akiyoshi Y, Naoi K, et al. 2017. FCN1 (M-ficolin), which directly associates with immunoglobulin G1, is a molecular target of intravenous immunoglobulin therapy for Kawasaki disease. *Sci Rep* 7: 11334

Orme IM, Roberts AD. 2001. Animal models of mycobacteria infection. *Curr Protoc Immunol* Chapter 19: Unit-19.5

Ost M, Singh A, Peschel A, Mehling R, Rieber N, Hartl D. 2016. Myeloid-Derived Suppressor Cells in Bacterial Infections. *Frontiers in Cellular and Infection Microbiology* 6: 37

Ostrand-Rosenberg S, Sinha P. 2009. Myeloid-derived suppressor cells: linking inflammation and cancer. *Journal of immunology (Baltimore, Md. : 1950)* 182: 4499-506

Ouyang W, Löhning M, Gao Z, Assenmacher M, Ranganath S, et al. 2000. Stat6-independent GATA-3 autoactivation directs IL-4-independent Th2 development and commitment. *Immunity* 12: 27-37

Pai M, Behr MA, Dowdy D, Dheda K, Divangahi M, et al. 2016. Tuberculosis. *Nature Reviews Disease Primers* 2: 16076

Pan PY, Ma G, Weber KJ, Ozao-Choy J, Wang G, et al. 2010. Immune stimulatory receptor CD40 is required for T-cell suppression and T regulatory cell activation mediated by myeloid-derived suppressor cells in cancer. *Cancer Res* 70: 99-108

Pennock ND, White JT, Cross EW, Cheney EE, Tamburini BA, Kedl RM. 2013. T cell responses: naive to memory and everything in between. *Adv Physiol Educ* 37: 273-83

Periasamy S, Avram D, McCabe A, MacNamara KC, Sellati TJ, Harton JA. 2016. An Immature Myeloid/Myeloid-Suppressor Cell Response Associated with Necrotizing Inflammation Mediates Lethal Pulmonary Tularemia. *PLoS Pathog* 12: e1005517-e17

Piktel E, Niemirowicz K, Wnorowska U, Wątek M, Wollny T, et al. 2016. The Role of Cathelicidin LL-37 in Cancer Development. *Arch Immunol Ther Exp (Warsz)* 64: 33-46

Podolnikova NP, Kushchayeva YS, Wu Y, Faust J, Ugarova TP. 2016. The Role of Integrins αMβ2 (Mac-1, CD11b/CD18) and αDβ2 (CD11d/CD18) in Macrophage Fusion. *Am J Pathol* 186: 2105-16

Pulugulla SH, Packard TA, Galloway NLK, Grimmett ZW, Doitsh G, et al. 2018. Distinct mechanisms regulate IL1B gene transcription in lymphoid CD4 T cells and monocytes. *Cytokine* 111: 373-81

Raviglione M, Sulis G. 2016. Tuberculosis 2015: burden, challenges and strategy for control and elimination. *Infectious Disease Reports* 8

Rawat K, Syeda S, Shrivastava A. 2021. Neutrophil-derived granule cargoes: paving the way for tumor growth and progression. *Cancer and Metastasis Reviews* 40: 221-44

Ray SJ, Franki SN, Pierce RH, Dimitrova S, Koteliansky V, et al. 2004. The collagen binding alpha1beta1 integrin VLA-1 regulates CD8 T cell-mediated immune protection against heterologous influenza infection. *Immunity* 20: 167-79

Reilley MJ, McCoon P, Cook C, Lyne P, Kurzrock R, et al. 2018. STAT3 antisense oligonucleotide AZD9150 in a subset of patients with heavily pretreated lymphoma: results of a phase 1b trial. *Journal for immunotherapy of cancer* 6: 119-19

Reilly EC, Lambert Emo K, Buckley PM, Reilly NS, Smith I, et al. 2020. T(RM) integrins CD103 and CD49a differentially support adherence and motility after resolution of influenza virus infection. *Proceedings of the National Academy of Sciences of the United States of America* 117: 12306-14

Ren G, Zhao X, Wang Y, Zhang X, Chen X, et al. 2012. CCR2-Dependent Recruitment of Macrophages by Tumor-Educated Mesenchymal Stromal Cells Promotes Tumor Development and Is Mimicked by TNFα. *Cell Stem Cell* 11: 812-24

Rhodes JW, Tong O, Harman AN, Turville SG. 2019. Human Dendritic Cell Subsets, Ontogeny, and Impact on HIV Infection. *Front Immunol* 10

Ribechini E, Eckert I, Beilhack A, Du Plessis N, Walzl G, et al. 2019. Heat-killed Mycobacterium tuberculosis prime-boost vaccination induces myeloid-derived suppressor cells with spleen dendritic cell-killing capability. *JCI Insight* 5

Ribechini E, Greifenberg V, Sandwick S, Lutz MB. 2010. Subsets, expansion and activation of myeloid-derived suppressor cells. *Medical microbiology and immunology* 199: 273-81

Ribechini E, Hutchinson JA, Hergovits S, Heuer M, Lucas J, et al. 2017. Novel GM-CSF signals via IFN-γR/IRF-1 and AKT/mTOR license monocytes for suppressor function. *Blood Advances* 1: 947-60

Riikonen T, Vihinen P, Potila M, Rettig W, Heino J. 1995. Antibody against human alpha 1 beta 1 integrin inhibits HeLa cell adhesion to laminin and to type I, IV, and V collagens. *Biochem Biophys Res Commun* 209: 205-12

Rodriguez PC, Quiceno DG, Ochoa AC. 2007. L-arginine availability regulates T-lymphocyte cell-cycle progression. *Blood* 109: 1568-73

Rodriguez PC, Zea AH, Culotta KS, Zabaleta J, Ochoa JB, Ochoa AC. 2002. Regulation of T cell receptor CD3zeta chain expression by L-arginine. *J Biol Chem* 277: 21123-9

Rosales C. 2018. Neutrophil: A Cell with Many Roles in Inflammation or Several Cell Types? *Frontiers in Physiology* 9

Rose S, Misharin A, Perlman H. 2012. A novel Ly6C/Ly6G-based strategy to analyze the mouse splenic myeloid compartment. *Cytometry A* 81: 343-50

Rössner S, Voigtländer C, Wiethe C, Hänig J, Seifarth C, Lutz MB. 2005. Myeloid dendritic cell precursors generated from bone marrow suppress T cell responses via cell contact and nitric oxide production in vitro. *Eur J Immunol* 35: 3533-44

Roumenina LT, Daugan MV, Petitprez F, Sautès-Fridman C, Fridman WH. 2019. Context-dependent roles of complement in cancer. *Nat Rev Cancer* 19: 698-715

Rubio MA, Sotillos M, Jochems G, Alvarez V, Corbií AL. 1995. Monocyte activation: rapid induction of α1/β1 (VLA-1) integrin expression by lipopolysaccharide and interferon-γ. *European Journal of Immunology* 25: 2701-05

Sakaguchi S, Miyara M, Costantino CM, Hafler DA. 2010. FOXP3+ regulatory T cells in the human immune system. *Nature Reviews Immunology* 10: 490-500

Sallusto F, Geginat J, Lanzavecchia A. 2004. Central memory and effector memory T cell subsets: function, generation, and maintenance. *Annu Rev Immunol* 22: 745-63

Sallusto F, Lenig D, Förster R, Lipp M, Lanzavecchia A. 1999. Two subsets of memory T lymphocytes with distinct homing potentials and effector functions. *Nature* 401: 708-12

Saraiva M, O'Garra A. 2010. The regulation of IL-10 production by immune cells. *Nature Reviews Immunology* 10: 170-81

Sawanobori Y, Ueha S, Kurachi M, Shimaoka T, Talmadge JE, et al. 2008. Chemokine-mediated rapid turnover of myeloid-derived suppressor cells in tumor-bearing mice. *Blood* 111: 5457-66

Sawcer S, Hellenthal G, Pirinen M, Spencer CCA, Patsopoulos NA, et al. 2011. Genetic risk and a primary role for cell-mediated immune mechanisms in multiple sclerosis. *Nature* 476: 214-19

Schmidt A, Oberle N, Krammer PH. 2012. Molecular mechanisms of treg-mediated T cell suppression. *Front Immunol* 3: 51-51

Schmielau J, Finn OJ. 2001. Activated granulocytes and granulocyte-derived hydrogen peroxide are the underlying mechanism of suppression of t-cell function in advanced cancer patients. *Cancer Res* 61: 4756-60

Schulte-Schrepping J, Reusch N, Paclik D, Bassler K, Schlickeiser S, et al. 2020. Severe COVID-19 Is Marked by a Dysregulated Myeloid Cell Compartment. *Cell*

Serafini P, Meckel K, Kelso M, Noonan K, Califano J, et al. 2006. Phosphodiesterase-5 inhibition augments endogenous antitumor immunity by reducing myeloid-derived suppressor cell function. *J Exp Med* 203: 2691-702

Serafini P, Mgebroff S, Noonan K, Borrello I. 2008. Myeloid-derived suppressor cells promote cross-tolerance in B-cell lymphoma by expanding regulatory T cells. *Cancer Res* 68: 5439-49

Serbina NV, Pamer EG. 2006. Monocyte emigration from bone marrow during bacterial infection requires signals mediated by chemokine receptor CCR2. *Nat Immunol* 7: 311-17

Sharpe AH. 2009. Mechanisms of costimulation. *Immunol Rev* 229: 5-11

Shimoda K, van Deursen J, Sangster MY, Sarawar SR, Carson RT, et al. 1996. Lack of IL-4-induced Th2 response and IgE class switching in mice with disrupted Stat6 gene. *Nature* 380: 630-3

Shiow LR, Rosen DB, Brdičková N, Xu Y, An J, et al. 2006. CD69 acts downstream of interferon-α/β to inhibit S1P1 and lymphocyte egress from lymphoid organs. *Nature* 440: 540-44

Shive CL, Hofstetter H, Arredondo L, Shaw C, Forsthuber TG. 2000. The enhanced antigen-specific production of cytokines induced by pertussis toxin is due to clonal expansion of T cells and not to altered effector functions of long-term memory cells. *Eur J Immunol* 30: 2422-31

Singh B, Singh DK, Ganatra SR, Escobedo RA, Khader S, et al. 2021. Myeloid-Derived Suppressor Cells Mediate T Cell Dysfunction in Nonhuman Primate TB Granulomas. *mBio* 12: e0318921-e21

Sinha P, Clements VK, Bunt SK, Albelda SM, Ostrand-Rosenberg S. 2007. Cross-talk between myeloid-derived suppressor cells and macrophages subverts tumor immunity toward a type 2 response. *J Immunol* 179: 977-83

Sinha P, Okoro C, Foell D, Freeze HH, Ostrand-Rosenberg S, Srikrishna G. 2008a. Proinflammatory S100 proteins regulate the accumulation of myeloid-derived suppressor cells. *J Immunol* 181: 4666-75

Sinha P, Okoro C, Foell D, Freeze HH, Ostrand-Rosenberg S, Srikrishna G. 2008b. Proinflammatory S100 proteins regulate the accumulation of myeloid-derived suppressor cells. *Journal of immunology (Baltimore, Md. : 1950)* 181: 4666-75

Steele CW, Karim SA, Leach JDG, Bailey P, Upstill-Goddard R, et al. 2016. CXCR2 Inhibition Profoundly Suppresses Metastases and Augments Immunotherapy in Pancreatic Ductal Adenocarcinoma. *Cancer Cell* 29: 832-45

Stemme S, Holm J, Hansson GK. 1992. T lymphocytes in human atherosclerotic plaques are memory cells expressing CD45RO and the integrin VLA-1. *Arteriosclerosis and Thrombosis: A Journal of Vascular Biology* 12: 206-11

Suk Lee Y, Davila E, Zhang T, Milmoe HP, Vogel SN, et al. 2019. Myeloid-derived suppressor cells are bound and inhibited by anti-thymocyte globulin. *Innate Immun* 25: 46-59

Sung H, Ferlay J, Siegel RL, Laversanne M, Soerjomataram I, et al. 2021. Global Cancer Statistics 2020: GLOBOCAN Estimates of Incidence and Mortality Worldwide for 36 Cancers in 185 Countries. *CA: A Cancer Journal for Clinicians* 71: 209-49

Suzuki K, Okuno T, Yamamoto M, Pasterkamp RJ, Takegahara N, et al. 2007. Semaphorin 7A initiates T-cell-mediated inflammatory responses through α1β1 integrin. *Nature* 446: 680-84

Swirski FK, Nahrendorf M, Etzrodt M, Wildgruber M, Cortez-Retamozo V, et al. 2009a. Identification of Splenic Reservoir Monocytes and Their Deployment to Inflammatory Sites. *Science* 325: 612

Swirski FK, Nahrendorf M, Etzrodt M, Wildgruber M, Cortez-Retamozo V, et al. 2009b. Identification of splenic reservoir monocytes and their deployment to inflammatory sites. *Science* 325: 612-16

Szabo PA, Miron M, Farber DL. 2019. Location, location, location: Tissue resident memory T cells in mice and humans. *Science Immunology* 4: eaas9673

Tahmasebinia F, Pourgholaminejad A. 2017. The role of Th17 cells in auto-inflammatory neurological disorders. *Prog Neuropsychopharmacol Biol Psychiatry* 79: 408-16

Tan G-J, Peng Z-K, Lu J-P, Tang F-Q. 2013. Cathepsins mediate tumor metastasis. *World J Biol Chem* 4: 91-101

Tang Q, Adams JY, Tooley AJ, Bi M, Fife BT, et al. 2006. Visualizing regulatory T cell control of autoimmune responses in nonobese diabetic mice. *Nat Immunol* 7: 83-92

Tartour E, Pere H, Maillere B, Terme M, Merillon N, et al. 2011. Angiogenesis and immunity: a bidirectional link potentially relevant for the monitoring of antiangiogenic therapy and the development of novel therapeutic combination with immunotherapy. *Cancer and Metastasis Reviews* 30: 83-95

Tau GZ, von der Weid T, Lu B, Cowan S, Kvatyuk M, et al. 2000. Interferon gamma signaling alters the function of T helper type 1 cells. *The Journal of experimental medicine* 192: 977-86

Teng MW, Galon J, Fridman WH, Smyth MJ. 2015. From mice to humans: developments in cancer immunoediting. *J Clin Invest* 125: 3338-46

Toh B, Wang X, Keeble J, Sim WJ, Khoo K, et al. 2011. Mesenchymal transition and dissemination of cancer cells is driven by myeloid-derived suppressor cells infiltrating the primary tumor. *PLoS Biol* 9: e1001162-e62

Tsiganov EN, Verbina EM, Radaeva TV, Sosunov VV, Kosmiadi GA, et al. 2014. Gr-1dimCD11b+ immature myeloid-derived suppressor cells but not neutrophils are markers of lethal tuberculosis infection in mice. *Journal of immunology (Baltimore, Md. : 1950)* 192: 4718-27

Ugel S, Peranzoni E, Desantis G, Chioda M, Walter S, et al. 2012a. Immune Tolerance to Tumor Antigens Occurs in a Specialized Environment of the Spleen. *Cell Reports* 2: 628-39

Ugel S, Peranzoni E, Desantis G, Chioda M, Walter S, et al. 2012b. Immune tolerance to tumor antigens occurs in a specialized environment of the spleen. *Cell Rep* 2: 628-39

Umansky V, Blattner C, Gebhardt C, Utikal J. 2016. The Role of Myeloid-Derived Suppressor Cells (MDSC) in Cancer Progression. *Vaccines (Basel)* 4: 36

Unsoeld H, Voehringer D, Krautwald S, Pircher H. 2004. Constitutive Expression of CCR7 Directs Effector CD8 T Cells into the Splenic White Pulp and Impairs Functional Activity. *The Journal of Immunology* 173: 3013

Van Ginderachter JA, Beschin A, De Baetselier P, Raes G. 2010. Myeloid-derived suppressor cells in parasitic infections. *European Journal of Immunology* 40: 2976-85

van Krieken JH, te Velde J. 1988. Normal histology of the human spleen. *Am J Surg Pathol* 12: 777-85

Veglia F, Hashimoto A, Dweep H, Sanseviero E, De Leo A, et al. 2021a. Analysis of classical neutrophils and polymorphonuclear myeloid-derived suppressor cells in cancer patients and tumor-bearing mice. *J Exp Med* 218

Veglia F, Perego M, Gabrilovich D. 2018. Myeloid-derived suppressor cells coming of age. *Nat Immunol* 19: 108-19

Veglia F, Sanseviero E, Gabrilovich DI. 2021b. Myeloid-derived suppressor cells in the era of increasing myeloid cell diversity. *Nature Reviews Immunology*

Vorup-Jensen T, Chi L, Gjelstrup LC, Jensen UB, Jewett CA, et al. 2007. Binding between the integrin alphaXbeta2 (CD11c/CD18) and heparin. *The Journal of biological chemistry* 282: 30869-77

Vynnycky E, Fine PE. 1997. The natural history of tuberculosis: the implications of age-dependent risks of disease and the role of reinfection. *Epidemiol Infect* 119: 183-201

Waldman AD, Fritz JM, Lenardo MJ. 2020. A guide to cancer immunotherapy: from T cell basic science to clinical practice. *Nature Reviews Immunology* 20: 651-68

Weber R, Riester Z, Hüser L, Sticht C, Siebenmorgen A, et al. 2020. IL-6 regulates CCR5 expression and immunosuppressive capacity of MDSC in murine melanoma. *Journal for ImmunoTherapy of Cancer* 8: e000949

Wegner A, Verhagen J, Wraith DC. 2017. Myeloid-derived suppressor cells mediate tolerance induction in autoimmune disease. *Immunology* 151: 26-42

Wight TN, Kang I, Evanko SP, Harten IA, Chang MY, et al. 2020. Versican—A Critical Extracellular Matrix Regulator of Immunity and Inflammation. *Front Immunol* 11

Willenborg S, Lucas T, van Loo G, Knipper JA, Krieg T, et al. 2012. CCR2 recruits an inflammatory macrophage subpopulation critical for angiogenesis in tissue repair. *Blood* 120: 613-25

Workman CJ, Szymczak-Workman AL, Collison LW, Pillai MR, Vignali DAA. 2009. The development and function of regulatory T cells. *Cell Mol Life Sci* 66: 2603-22

Xu G, Qi F, Li H, Yang Q, Wang H, et al. 2020. The differential immune responses to COVID-19 in peripheral and lung revealed by single-cell RNA sequencing. *Cell Discov* 6: 73

Xue F, Yu M, Li L, Zhang W, Ma Y, et al. 2020. Elevated granulocytic myeloid-derived suppressor cells are closely related with elevation of Th17 cells in mice with experimental asthma. *Int J Biol Sci* 16: 2072-83

Yamauchi Y, Safi S, Blattner C, Rathinasamy A, Umansky L, et al. 2018. Circulating and Tumor Myeloid-derived Suppressor Cells in Resectable Non-Small Cell Lung Cancer. *Am J Respir Crit Care Med* 198: 777-87

Yan HH, Pickup M, Pang Y, Gorska AE, Li Z, et al. 2010. Gr-1+CD11b+ Myeloid Cells Tip the Balance of Immune Protection to Tumor Promotion in the Premetastatic Lung. *Cancer Research* 70: 6139

Yang AS, Lattime EC. 2003. Tumor-induced interleukin 10 suppresses the ability of splenic dendritic cells to stimulate CD4 and CD8 T-cell responses. *Cancer Res* 63: 2150-7

Yang B, Wang X, Jiang J, Zhai F, Cheng X. 2014. Identification of CD244-expressing myeloid-derived suppressor cells in patients with active tuberculosis. *Immunol Lett* 158: 66-72

Yang R, Cai Z, Zhang Y, Yutzy WHt, Roby KF, Roden RB. 2006. CD80 in immune suppression by mouse ovarian carcinoma-associated Gr-1+CD11b+ myeloid cells. *Cancer Res* 66: 6807-15

Yang S, Liu F, Wang QJ, Rosenberg SA, Morgan RA. 2011. The Shedding of CD62L (L-Selectin) Regulates the Acquisition of Lytic Activity in Human Tumor Reactive T Lymphocytes. *PLOS ONE* 6: e22560

Yang W-C, Ma G, Chen S-H, Pan P-Y. 2013. Polarization and reprogramming of myeloid-derived suppressor cells. *J Mol Cell Biol* 5: 207-09

Yin B, Ma G, Yen C-Y, Zhou Z, Wang GX, et al. 2010a. Myeloid-Derived Suppressor Cells Prevent Type 1 Diabetes in Murine Models. *The Journal of Immunology* 185: 5828

Yin B, Ma G, Yen CY, Zhou Z, Wang GX, et al. 2010b. Myeloid-derived suppressor cells prevent type 1 diabetes in murine models. *J Immunol* 185: 5828-34

Youn J-I, Collazo M, Shalova IN, Biswas SK, Gabrilovich DI. 2012. Characterization of the nature of granulocytic myeloid-derived suppressor cells in tumor-bearing mice. *J Leukoc Biol* 91: 167-81

Youn J-I, Nagaraj S, Collazo M, Gabrilovich DI. 2008a. Subsets of myeloid-derived suppressor cells in tumor-bearing mice. *Journal of immunology (Baltimore, Md. : 1950)* 181: 5791-802

Youn J-I, Nagaraj S, Collazo M, Gabrilovich DI. 2008b. Subsets of Myeloid-Derived Suppressor Cells in Tumor-Bearing Mice. *The Journal of Immunology* 181: 5791-802

Young MR, Wright MA, Young ME. 1991. Antibodies to colony-stimulating factors block Lewis lung carcinoma cell stimulation of immune-suppressive bone marrow cells. *Cancer Immunol Immunother* 33: 146-52

Yu F, Shi Y, Wang J, Li J, Fan D, Ai W. 2013. Deficiency of Kruppel-like factor KLF4 in mammary tumor cells inhibits tumor growth and pulmonary metastasis and is accompanied by compromised recruitment of myeloid-derived suppressor cells. *Int J Cancer* 133: 2872-83

Zhang C, Yang M, Ericsson AC. 2021a. Function of Macrophages in Disease: Current Understanding on Molecular Mechanisms. *Front Immunol* 12

Zhang J, Hodges A, Chen S-H, Pan P-Y. 2021b. Myeloid-derived suppressor cells as cellular immunotherapy in transplantation and autoimmune diseases. *Cellular Immunology* 362: 104300

Zhang L, Li Z, Skrzypczynska KM, Fang Q, Zhang W, et al. 2020. Single-Cell Analyses Inform Mechanisms of Myeloid-Targeted Therapies in Colon Cancer. *Cell* 181: 442-59 e29

Zhang W, Jiang M, Chen J, Zhang R, Ye Y, et al. 2018. SOCS3 Suppression Promoted the Recruitment of CD11b(+)Gr-1(-)F4/80(-)MHCII(-) Early-Stage Myeloid-Derived Suppressor Cells and Accelerated Interleukin-6-Related Tumor Invasion via Affecting Myeloid Differentiation in Breast Cancer. *Front Immunol* 9: 1699

Zhang X, Guo R, Kambara H, Ma F, Luo HR. 2019. The role of CXCR2 in acute inflammatory responses and its antagonists as anti-inflammatory therapeutics. *Curr Opin Hematol* 26: 28-33

Zhao F, Hoechst B, Duffy A, Gamrekelashvili J, Fioravanti S, et al. 2012. S100A9 a new marker for monocytic human myeloid-derived suppressor cells. *Immunology* 136: 176-83

Zhao W, Xu Y, Xu J, Wu D, Zhao B, et al. 2015. Subsets of myeloid-derived suppressor cells in hepatocellular carcinoma express chemokines and chemokine receptors differentially. *Int Immunopharmacol* 26: 314-21

Zhu B, Bando Y, Xiao S, Yang K, Anderson AC, et al. 2007. CD11b⁺Ly-6C^{hi} Suppressive Monocytes in Experimental Autoimmune Encephalomyelitis. *The Journal of Immunology* 179: 5228

Zhu YP, Thomas GD, Hedrick CC. 2016. 2014 Jeffrey M. Hoeg Award Lecture: Transcriptional Control of Monocyte Development. *Arterioscler Thromb Vasc Biol* 36: 1722-33

Zigmond E, Varol C, Farache J, Elmaliah E, Satpathy Ansuman T, et al. 2012. Ly6C^{hi} Monocytes in the Inflamed Colon Give Rise to Proinflammatory Effector Cells and Migratory Antigen-Presenting Cells. *Immunity* 37: 1076-90

Zitvogel L, Kroemer G. 2012. Targeting PD-1/PD-L1 interactions for cancer immunotherapy. *OncoImmunology* 1: 1223-25

8 List of Tables

9 List of Figures

10 Abbreviations

°C	degrees Celsius
ADAM17	a disintegrin and metalloproteinase domain 17
ADCC	antibody-dependent cellular cytotoxicity
A-MDSC	activated myeloid-derived suppressor cell
ANOVA	analysis of variance
Arg	arginase
APC	Allophycocyanin
B6	black 6
BCG	Bacillus Calmette-Guérin
BM	bone marrow
BM-MDSCs	bone marrow-derived myeloid-derived suppressor cells
BSA	bovine serum albumin
CAMP	cathelicidin antimicrobial peptide
CCR	C-C chemokine receptor
CCL	C-C chemokine ligand
CD	cluster of differentiation
CD62L	L-selectin
cDC	conventional dendritic cell
CFA	Complete Freund's adjuvant
CFSE	carboxyfluorescein diacetate succinimidyl ester
CO_2	carbon dioxide
CTLA4	cytotoxic T-lymphocyte-associated Protein 4
Cts	cathepsin
CyTOF	cytometry by time of flight
DC	dendritic cell
DMSO	dimethyl sulfoxide
DNase	deoxyribonuclease
EAE	experimental autoimmune encephalomyelitis
EDTA	ethylenediaminetetraacetic acid
ELISA	enzyme-linked immunosorbent assay
FACS	fluorescence-activated cell sorting
FCN1	ficolin-1
FCS	fetal calf serum
FITC	Fluorescein isothiocyanate
FoxP3	forkhead box P3
FSC	forward scatter
g	gram
G-MDSC	granulocytic myeloid-derived suppressor cell
GM-CSF	granulocyte-macrophage colony-stimulating factor
Gr-1	granulocyte receptor-1 antigen
h	hour
HIF-1α	hypoxia-inducible factor-1α
HLA	human leukocyte antigen
IFN-γ	interferon-γ
IDO	Indoleamine 2,3-dioxygenase

IL	interleukin
iNOS	inducible nitric oxide synthase
IVIG	intravenous gammaglobulin
JAK	janus kinase
LFA-1	lymphocyte function-associated antigen 1
LPS	lipopolysaccharides
Ly-6	lymphocyte antigen 6
MACS	magnetic-activated cell sorting
MDSC	myeloid-derived suppressor cell
MFI	mean fluorescence intensity
MHC	major histocompatibility complex
min	minute
ml	milliliter
M-MDSC	monocytic myeloid-derived suppressor cell
MFI	mean fluorescence intensity
MMP	matrix metalloproteinases
Mo-DC	monocytic dendritic cell
MOG	myelin oligodendrocyte glycoprotein
MPO	myeloperoxidase
M.tb	*Mycobacterium tuberculosis*
MS	multiple sclerosis
NADPH	nicotinamide adenine dinucleotide phosphate hydrogen
NK cells	natural killer
NO	nitric oxide
NOX	NADPH oxidase
OVA	ovalbumin
PE	Phycoerythrin
PBMCs	peripheral blood mononuclear cells
PBS	phosphate-buffered saline
PI3K	phosphatidylinositol 3-kinase
PD-1	programmed cell death 1
PD-L1	programmed cell death 1 ligand
R-MDSC	resting myeloid-derived suppressor cell
ROS	reactive oxygen species
rpm	revolutions per minute
RPMI	Roswell Park Memorial Institute
s	second
Sema7A	semaphorin 7A
SSC	side scatter
STAT	signal transducer and activator of transcription
TCR	T cell receptor
T_{eff} cells	effector T cells
TGF-β	transforming growth factor-β
Th cells	T helper cells
TLR	toll-like receptor
TMB	3,3’,5,5’-Tetramethylbenzidine
TNF-α	tumor necrosis factor-α
Treg	regulatory T cells
VCAN	versican
VEGF	vascular endothelial growth factor
VLA-1	very late antigen 1
WT	wildtype
µg	microgram
µl	microliter

11 Acknowledgement

I am extremely grateful to my supervisor Prof. Manfred Lutz for the exceptional support, guidance, encouragement and patience. His passion for immunology and his optimism when receiving contradictory data is very inspiring. His scientific teaching abilities were critical for this work. I am very lucky to have a supervisor who really cared about my work and who always answered my questions so quickly.

I would like to sincerely thank the members of my PhD committee Prof. Andreas Beilhack and Prof. Georg Gasteiger for their time and efforts during the annual meetings and for reading and evaluating this manuscript. The critical discussions of my data and their suggestions were very helpful.

I also would like to thank all members of AG Lutz for their continuous help and support but also for the familial atmosphere. Many thanks to Marion Heuer, Dr. Vini John and Dr. Diyaa Ashour and Dr. Emilia Vendelova for teaching me the experimental procedures and helping me with complicated experiments. Many thanks as well to Dr. Eliana Ribechini for working with me on my main project. I also would like to thank Arpa Aintablian, Laura Cyran, Sabrina Schneider, Andrea Fick for their support.

I am grateful to Dr. Sabine Kranz and the staff of the animal facility for helping me with breeding, crossing, and housing of the mice.

Many thanks also to Dr. Angela Riedel and Greta Mattavelli for the collaboration and the intriguing scientific discussions.

I would like to thank Dr. Irina Pleines-Meinhold, Dr. Gabriele Blum-Oehler and the GSLS team for offering very helpful courses and classes in the GSLS PhD study program and for nicely handling the administrative procedures. Many thanks to Heike Schrenk and Katharina Bötsch for helping me with submitting my thesis. Also I want to thank the organizers and speakers of the graduate program “Immunomodulation” for the weekly meetings and the annual retreats, which taught me a lot about immunology as well as networking.

I am deeply grateful to my partner, my parents and my brother who always support me. I could not make it without you. Also I want to thank my friends for their support.

12 Publication List

Eckert IN*, Ribechini E*, Jarick J, Strozniak S, Potter S, Jordán-Garrote AL, Beilhack S, Lutz MB. VLA-1 binding to collagen IV controls effector T cell suppression by myeloid-derived suppressor cells in the splenic red pulp. Front Immunol, 2021. *equal contribution

Eckert I, Ribechini E, Lutz MB. In vitro generation of murine myeloid-derived suppressor cells, analysis of markers, developmental commitment and function. In Myeloid-Derived Suppressor Cells, Methods and Protocols. S. Brandau, and A. Dorhoi, editors. Springer Nature, 2021.

Lutz MB, **Eckert IN.** Comments on the ambiguity of selected surface markers, signaling pathways and omics profiles hampering the identification of myeloid-derived suppressor cells. Cell Immunol, accepted 2021

Thomann AS, Schneider T, **Eckert I**, Kerstan A, Lutz MB. Conversion of anergic T cells into $Foxp3^{-}$ $IL\text{-}10^{+}$ regulatory T cells by a second antigen stimulus in vivo. Front Immunol, 2021.

Ribechini E, **Eckert I**, Beilhack A, Du Plessis N, Walzl G, Schleicher U, Ritter U, Lutz MB. Heat-killed Mycobacterium tuberculosis prime-boost vaccination induces myeloid- derived suppressor cells with spleen dendritic cell-killing capability. JCI insight, 2019.

Döhler A, Schneider T, **Eckert I**, Ribechini E, Andreas N, Riemann M, Reizis B, Weih F, Lutz MB. RelB+ Steady-State Migratory Dendritic Cells Control the Peripheral Pool of the Natural $Foxp3^{+}$ Regulatory T Cells. Front Immunol, 2017.

Affidavit

I hereby confirm that my thesis entitled ‘Molecular markers of myeloid-derived suppressor cells and their functional role for homing and in disease models in mice’ is the result of my own work. I did not receive any help or support from commercial consultants. All sources and / or materials applied are listed and specified in the thesis.

Furthermore, I confirm that this thesis has not yet been submitted as part of another examination process neither in identical nor in similar form.

Würzburg
Place, Date **Signature**

Eidesstattliche Erklärung

Hiermit erkläre ich an Eides statt, die Dissertation ‘Molekulare Marker von myeloiden Suppressorzellen und ihre funktionelle Rolle für deren zielgerichtete Migration und bei Krankheitsmodellen in Mäusen‘ eigenständig, d.h. insbesondere selbständig und ohne Hilfe eines kommerziellen Promotionsberaters, angefertigt und keine anderen als die von mir angegebenen Quellen und Hilfsmittel verwendet zu haben.

Ich erkläre außerdem, dass die Dissertation weder in gleicher noch in ähnlicher Form bereits in einem anderen Prüfungsverfahren vorgelegen hat. Würzburg,

Würzburg
Ort, Datum **Unterschrift**